HYBRID ELECTRIC POWER SYSTEMS IN REMOTE ARCTIC VILLAGES: ECONOMIC AND ENVIRONMENTAL ANALYSIS FOR MONITORING, OPTIMIZATION, AND CONTROL

A

THESIS

Presented to the Faculty

of the University of Alaska Fairbanks

in Partial Fulfillment of the Requirements

for the Degree of

DOCTOR OF PHILOSOPHY

By

Ashish N. Agrawal, M.S.

Fairbanks, Alaska

August 2006

HYBRID ELECTRIC POWER SYSTEMS IN REMOTE ARCTIC VILLAGES: ECONOMIC AND ENVIRONMENTAL ANALYSIS FOR MONITORING, OPTIMIZATION, AND CONTROL

By

Ashish N. Agrawal

RECOMMENDED:

Advisory Committee Chair

Chair, Department of Electrical and Computer Engineering

APPROVED:

Dean, College of Engineering and Mines

Dean of the Graduate School

August 8, 2006
Date

Abstract

The need for energy-efficient and reliable electric power in remote arctic communities of Alaska is a driving force for research in this work. Increasing oil prices, high transportation costs for fuels, and new environmental standards have forced many utilities to explore hybrid energy systems in an attempt to reduce the cost of electricity (COE). This research involves the development of a stand-alone hybrid power system model using MATLAB® Simulink® for synthesizing the power system data and performing the economic and environmental analysis of remote arctic power systems. The hybrid model consists of diesel electric generators (DEGs), a battery bank, a photovoltaic (PV) array, and wind turbine generators (WTGs). The economic part of the model is used to study the sensitivity analysis of fuel cost and the investment rate on the COE, the life cycle cost (LCC) of the system, and the payback time of the system. The environmental part of the model calculates the level of various pollutants including carbon dioxide (CO_2), nitrogen oxides (NOx), and the particulate matter (PM_{10}). The environmental analyses part of the model also calculates the avoided cost of various pollutants. The developed model was used to study the economics and environmental impacts of a stand-alone DEG system installed at the University of Alaska Fairbanks Energy Center, the wind-diesel-battery hybrid power system installed at Wales Village, Alaska, and the PV-diesel-battery hybrid power system installed at Lime Village, Alaska. The model was also used to predict the performance of a designed PV-wind-diesel-battery system for Kongiganak Village. The results obtained from the Simulink® model were in close agreement with those predicted by the Hybrid Optimization Model for Electric Renewables (HOMER) software developed at National Renewable Energy Laboratory (NREL).

Table of Contents

List of Figures

List of Tables

List of Appendices

List of Acronyms

DEG – Diesel Electric Generator

WTG – Wind Turbine Generator

PV – Photovoltaic

GHG – Green House Gases

COE – Cost of Electricity

NPV – Net Present Value

HARPSim – Hybrid Arctic Remote Power Simulator

HOMER – Hybrid Optimization Model for Electric Renewables

LCC – Life Cycle Cost

CO_2 – Carbon Dioxide

NOx – Nitrogen Oxides

PM_{10} – Particulate Matter with size of 10 microns

kWh – kilowatt hour

BTU – British Thermal Unit

List of Units and their Conversion

Quantity	Different units and their conversion
Fuel flow	liters (gallons) 1 gallon = 3.785 liters
Energy	Joules (BTU), kWh 1 kWh = 3413 BTU 1 BTU = 1055 Joules
Power	Horsepower (hp), Watts (W) 1 hp = 746 W
Mass	kg (pound), metric ton (US ton) 1 kg = 2.2 pound 1 metric ton = 1.1 US ton = 1000 kg
Pressure	Pascal (psi), atmosphere (atm) 1 psi = 6894.76 Pascal 1 atm = 101325 Pa
Speed	meters/sec (miles/hr) 1 meter/sec = 2.24 miles/hour
Temperature	°C (°F) °C = (°F – 32)*5/9
Area	square meters (square foot) 1 sq. m = 10.76 sq. ft.

Please note: The model developed in this dissertation is designed with the main focus on remote Alaskan communities. Therefore, English units are used in the development of the model. However, the results presented are both in SI units and English units, shown as XX SI Unit (XY English Unit).

Acknowledgements

I would like to express my sincere gratitude to Dr. Richard Wies who supervised this research and provided continuous support, both academically and personally, throughout my stay in Fairbanks.

My sincere appreciation goes to Dr. Ronald Johnson who provided great ideas, suggestions, and encouragement throughout the course of this project. He also contributed to a number of journal publications and conference proceedings.

I would like to thank my committee members Dr. Vikas Sonwalkar, Dr. John Aspnes, and Dr. Edward Bueler, for their contributions of new ideas throughout the project.

I would also like to thank the Arctic Energy Technology and Development Laboratory and the Graduate School at the University of Alaska Fairbanks for their financial support for this work.

Last but not least, I would like to thank my wife Ipshita Majhi, my parents, family and friends for their invaluable love, support, and encouragement throughout my life.

1 Introduction

Diesel electric generators (DEGs) are the main source of electricity for many remote communities in arctic regions. With the growing demand for energy, rising oil prices, depleting oil resources, and increasing concern for green house gases (GHG), governments and utility companies all over the world are making efforts to accelerate the growth of renewable energy programs.

It is necessary to study the performance of stand-alone hybrid power systems in remote Alaskan communities in order to optimize the cost, increase the efficiency, and decrease emissions of these systems. Some of the challenges in studying the performance of the systems installed in arctic regions are:

- Lack of data and poor quality of available data.
- Poor power quality.
- Lack of DEG optimization techniques.
- Remoteness of the site (grid extension not feasible).
- Harsh environmental conditions.
- Rising oil prices.
- High cost of transportation of diesel fuel.
- New environmental standards.

This research project is the extension of my master's thesis work performed on the development of a Simulink® model for hybrid power systems. The detailed model of the hybrid power system is described in my master's thesis [1]. The hybrid power system model consists of DEGs, wind turbine generators (WTGs), a photovoltaic (PV) array, and a battery bank as major components. The Simulink® model presented in my master's thesis calculates the fuel consumption for the PV-

diesel-battery (PVDB) system and the wind-diesel-battery (WDB) system for a period of 24-hours.

In this dissertation, the Simulink® model now called Hybrid Arctic Remote Power Simulator (HARPSim) is extended to optimize DEGs, study system performance in arctic regions, perform economic analyses, and calculate environmental pollutant levels that result from the use of hybrid power systems. The main objectives of HARPSim are to accomplish the following:

1) Improve the system efficiency.
2) Improve system economics.
3) Reduce the fuel consumption.
4) Reduce emissions.

In order to accomplish the above-mentioned tasks, HARPSim performs the following calculations:

1) It models the system performance in the arctic climate.
2) It optimizes the load on DEGs.
3) It calculates the annual fuel consumed for the given load profile.
4) It calculates and tracks the annual cost of fuel and other operational costs.
5) It performs a life cycle cost (LCC) analysis of the system.
6) It calculates the cost of electricity (COE) for the system.
7) It calculates the payback period of the system.
8) It performs the sensitivity analysis of fuel cost and investment rate on the COE, the LCC cost, and the payback period of the system.
9) It calculates various emission levels: carbon dioxide (CO_2), nitrogen oxides (NOx), and PM_{10} emissions.

10) It calculates the avoided cost of various emissions.

The results derived from HARPSim are compared with those derived from the Hybrid Optimization Model for Electric Renewables (HOMER) software developed at the National Renewable Energy Laboratory (NREL). TABLE 1-1 shows the important features of HARPSim and the HOMER software.

TABLE 1-1. Important features of HARPSim and HOMER

HARPSim	HOMER
The main focus of HARPSim is to study the performance of the hybrid power system in arctic regions by modeling system in arctic climates, optimizing the DEGs, and performing economic and environmental analysis of the system.	The main focus of HOMER is to study the long term performance and optimize the system component sizes based on the net present value (NPV) of the system.
HARPSim can study the analysis of a system with any data length and sampling rate. The low sampling rate used in HARPSim is to study the dynamic behavior of the system.	HOMER requires an hourly data set with data length of exactly one year.
In HARPSim, a non-linear model of the DEG combining the engine curve and the electrical efficiency curve as described in Section 2.1 is developed.	In HOMER, a DEG is modeled as a linear curve that gives the amount of fuel consumed based on the system load.
At present, HARPSim requires the entry of component sizes on a case by case basis and then optimizes for those conditions.	HOMER gives a flexibility to enter the range of component sizes and then optimizes all possible conditions.
The sensitivity analysis of increasing fuel cost on the net present value (NPV), the cost of electricity, and the payback period of the WTG and the PV array can be performed in HARPSim.	In HOMER the sensitivity analysis of increasing fuel cost on the NPV can be performed.

TABLE 1-2 shows the chronological developments in HARPSim and the HOMER software.

TABLE 1-2. Chronological developments in HARPSim and HOMER

Date	HARPSim	HOMER
1993	-	Development of HOMER as a linear programming model for residential renewable energy systems.
1997	-	Development of HOMER Windows application.
August 2003	Development of a Simulink® model to study the performance of the hybrid power system (calculated total fuel consumption and system efficiency).	• Ability to model the grid connected systems. • Ability to model AC loads, DC loads, thermal loads, and cogeneration. • Ability to model as many as three DEGs without optimization. • Added carbon tax.
August 2004	• Studied the system performance of remote arctic power system. • Incorporated different environmental emissions into the model • Incorporated life cycle cost calculations of the system into the model. • Developed the optimization technique for two generators [2].	-
November 2004	-	Incorporated different environmental emissions.
September 2005	Sensitivity analysis of increasing fuel cost and investment rates on the systems NPV, the COE, and the payback period [3].	-

TABLE 1-2 cont'd...

Date	HARPSim	HOMER
February 2006	• Changed the generator optimization technique to obtain maximum fuel efficiency. • Developed a Simulink® tool that can calculate the annual solar insolation of any place on the earth at the top of the atmosphere.	-
June 2006	-	Observed for the first time the optimization technique for multiple DEGs. The details for the multiple DEG optimization technique are not available in the HOMER help files.

The long-term goal of HARPSim is to incorporate into the hybrid power system various other energy technologies such as hydro-power, fuel cells, and geothermal. A comprehensive model will incorporate a control system strategy, a system dynamics module to study the power quality, and extensive computation of the system economy. The comprehensive model is intended to study the feasibility of installing different types of hybrid power systems in remote locations.

The government and utility companies are investing in research and development programs for renewable energy systems. The different renewable energy sources examined in the newly initiated programs include the possibilities of using wind, solar, biomass, geothermal, and small hydro-electric power to supply the energy demand in remote villages. The viability of a respective renewable energy program depends on the geographical location and varies from region to region. For example, Denver, CO is a viable region for the deployment of PV technology while Kotzebue, AK is a viable region for energy extraction via

WTGs. The investments in the renewable energy program and numerous tax benefits for using renewable energy sources [4] have given researchers opportunities to study the feasibility of integrating different energy sources. The integration of different energy sources to supply a system load is called a hybrid power system. It should be noted that fossil fuel may be used by one or more of the power sources in a hybrid system. The use of hybrid power systems in remote locations such as those found in Alaska and many other parts of the world have shown an improvement in overall system performance and efficiency. Hybrid power systems have also helped to save fossil fuel, thus improving the system economics and reducing GHG [5].

In remote villages, the cost of electricity (COE) and the efficiency of power systems are of great concern given the number of hybrid power systems installed in remote communities throughout the world. Mexico has 86,000 remote communities, each with a population of less than 1000. Some of these communities use PV-diesel-battery hybrid power systems for energy production [6]. In Asia, about 70% of all villages are considered remote [7]. There are many hybrid power systems installed throughout Asia. These hybrid power systems use WTGs, PV arrays, DEGs, hydro-power, and other available power sources for their energy production. Rural Alaska has more than 200 remote communities [8]. The State of Alaska incorporates WTGs [8], [9], [10], PV arrays [11], geothermal energy [12], and hydro-power [13] with DEGs to supply the energy needs for remote communities. DEGs are the main source of power for most of the remote communities in Alaska because they have been the most cost effective [8]. It is very difficult and uneconomical to extend the existing power transmission grid to such remote arctic communities.

A 2002 report by the Alaska Energy Authority (AEA) states that there are 198 rural communities that use DEGs to generate electricity [5]. The COE in rural Alaska averages 0.40 USD/kWh. However, for some extremely isolated

communities, the COE can be as high as 1.00 USD/kWh [8]. The rising cost of transportation and storage of the diesel fuel have augmented the COE in many remote communities of Alaska. Fortunately, for the residents of some of these rural Alaskan communities, the state government subsidizes much of the electric power through the power cost equalization (PCE) program. As of 2002, the residents of the 185 communities participating in the PCE program pay about 0.12 USD/kWh. The Alaska state government provides the additional funding that the rural power utilities need to pay for their extremely high COE [14]. Therefore, it is very important that DEGs operate efficiently.

1.1 Energy Scenario in the United States

According to the United States Department of Energy (USDOE), the total US energy consumption in the year 2003 was about 99 Q Btu (1 Q Btu = 10^{15} Btu and 1 Btu = 1055.056 Joules). The total energy consumption for the entire world for the same year was about 422 Q Btu [15]. Therefore, the US with about 5% of the world's population accounts for about 23.5% of the world's energy consumption. Fig. 1-1 shows the energy consumption in the US for the year 2004 from different sources. About 85% of the energy consumed in the US comes from fossil fuels; about 8% comes from nuclear resources; and about 7% comes from different renewable energy sources, including biomass, hydro, geothermal, solar, and wind power.

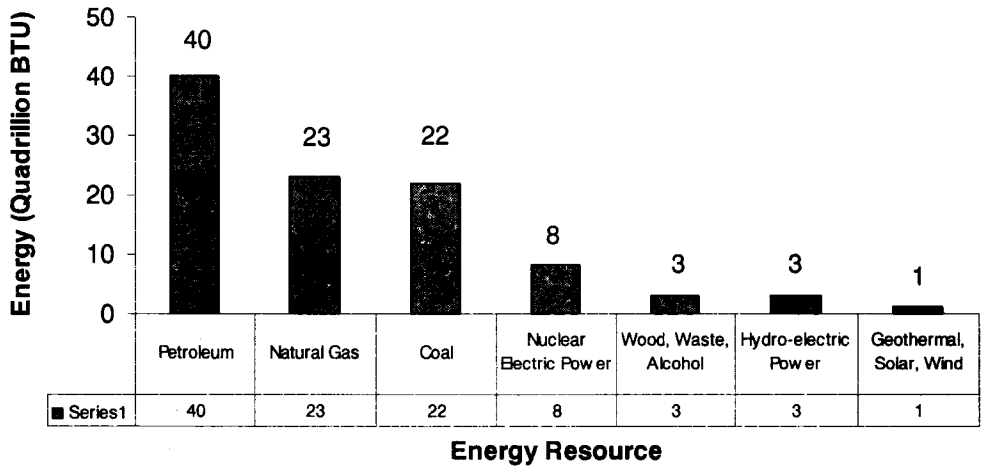

Fig. 1-1. Energy consumption in the US by different sources [15].

Fig. 1-2 shows a graph that juxtaposes energy consumption with energy production in the US.

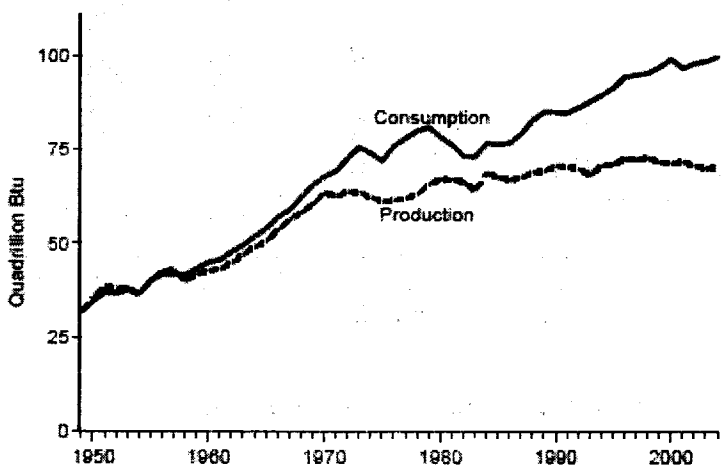

Fig. 1-2. Energy consumption versus energy production in the US [15].

Fig. 1-2 illustrates that the energy production has been almost constant in the last decade, while the demand for the energy has increased. The difference in

consumption and production accounts for the amount of energy imported into the US. This imported energy, in different forms, includes the direct import of oil from the Middle East and Canada and other countries, direct purchase of electricity from Canada, and the import of natural gas [16].

Fig. 1-3 includes the projected energy consumption in the world until the year 2025. In 2005, the USDOE, a department that operates under the US Federal Executive Branch, projected that the world will continue to use fossil fuel as the major source of energy in the coming decades. Thus, the consumption of fossil fuel will continue to surpass the consumption of renewable energy sources as well as nuclear energy sources.

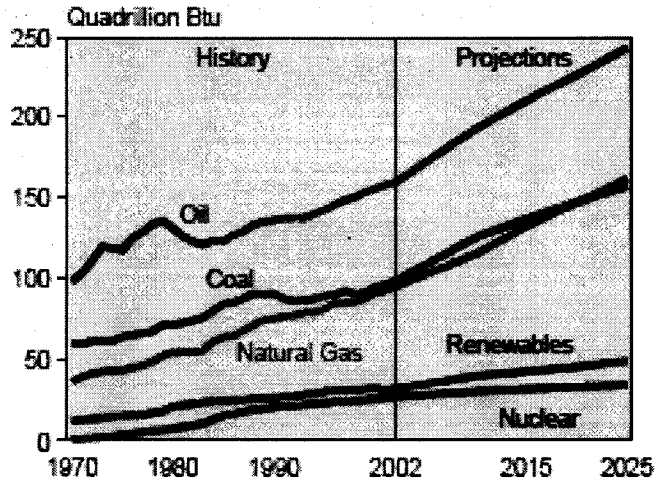

Fig. 1-3. Projected energy consumption in the world by energy source [17].

Fig. 1-4 shows a graph for the projected oil prices until the year 2025. This graph was formulated prior to today's high oil prices. In 2005, the USDOE, projected that there will be no significant change in the oil prices in the near future.

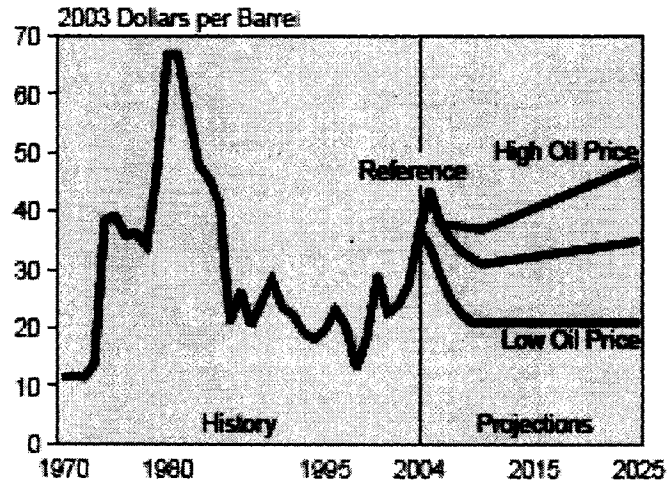

Fig. 1-4. Projected oil cost on the world market [17].

1.2 Renewable Energy Scenario in the US

Data obtained from Fig. 1-4 shows that, according to the USDOE, the maximum projected oil price in the year 2005 should have been around 38 USD per barrel. However, the oil prices in the year 2005 averaged around 50 USD per barrel which is 31.5% higher than the USDOE's projection and even exceeded 70 USD per barrel at times. This increase in the oil prices is due to the high demand and low supply of crude oil on the world market. If the trend of high oil prices continues, the oil prices could rise as high as 100 USD per barrel by the year 2025. In view of increasing oil prices, renewable energy sources such as wind, PV, geothermal, hydro-power, biomass, and ocean wave are now capturing the attention of governments around the world.

1.2.1 Wind Energy

At this point in time, wind power, due to its competitive COE compared to fossil fuel, is the fastest growing source of electricity in the remote areas around the

world. Some researchers have estimated that the wind could supply 12 percent of the world's electricity demand by 2020 [18]. Fig. 1-5 shows the pie chart for the top ten countries in the world using wind energy for their energy production as of the year 2004 [19]. It is observed that Germany is the world leader in the production of wind power, followed by Spain and the United States.

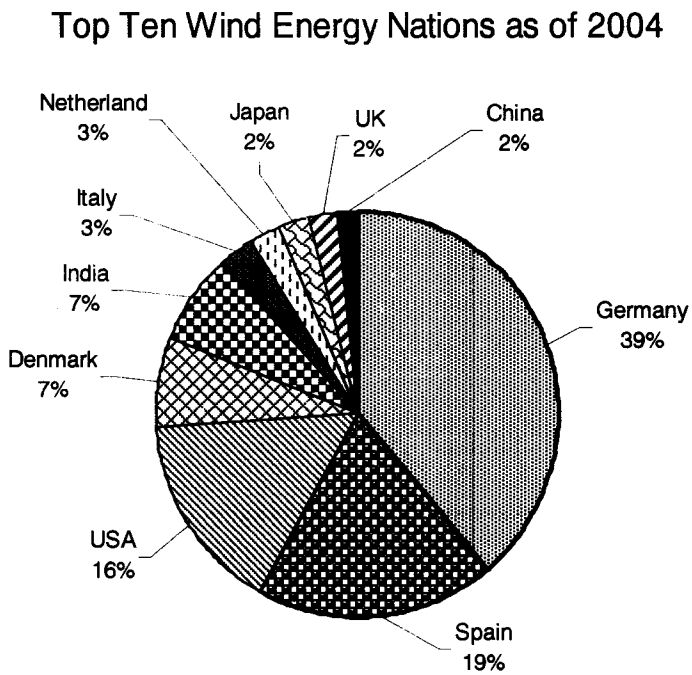

Fig. 1-5. Top ten wind energy producing nations as of 2004 [19].

As per the USDOE, the advances in wind turbines, including the special airfoils developed for wind turbine applications [20], [21], sophisticated control systems [22], innovative generator technology that operates at low and variable speeds [23], and new technology used in rotor construction [24], could bring down the COE using WTGs to 2.5 cents/kWh.

1.2.2 Solar Energy

Solar energy uses radiation from the sun to provide heat, light, hot water, electricity, cooling, and air conditioning for homes, offices, and factories. Although the COE for PV systems is higher than the COE for fossil fuel power plants and some other renewable energy sources, the solar energy technology is effective and can be economical in applications which include water heating, space heating, and solar cooking. The high COE in the PV system is tied to the high cost of the semiconductors used in the production of a PV array. However, the emerging technologies that use gallium arsenide, amorphous silicon, copper indium diselenide, and gallium indium phosphide in the production of high-efficiency multi-junction devices will eventually result in the drastic improvement of PV system efficiencies [25]. Mass production and technological improvements will reduce the COE for the PV system to a level that is competitive with other energy sources. Use of PV and other renewable technologies that utilize intermittent resources also are handicapped by the need to store the produced heat or electricity or utilize other energy sources when the resource is absent.

1.2.3 Geothermal

Geothermal technology uses the heat energy from the earth for domestic hot water, geothermal heat pumps, and for electric energy production. As per the USDOE, by the end of 2004, there were 43 power plants producing electricity with the help of geothermal resources [26]. Geothermal power plants in California, with an installed capacity of 2700 MW, produce about 40% of world's geothermal energy. About 33% of electric energy in Iceland is supplied using geothermal energy [27]. Alaska's first geothermal power plant is scheduled to come online in August 2006 at the Chena Hot Springs resort. The 200 kW organic Rankine cycle power plant will supply most of the electric demand for the system. Currently, the low temperature water at about 68 °C (155 °F) is used to supply most of the heating

load of the system. This water is also used to supply the cooling load of the ice museum at the Chena Hot Spring with the help of absorption chillers [28].

1.2.4 Hydropower

Hydropower uses the energy stored in water at an elevation. As per the USDOE, the US produces about 95 GW (1GW = 1000MW) of electricity using hydropower. This 95 GW of electric power supplies about 28 million households in the US, which is equivalent to 500 million barrels of oil annually. Hydropower is the highest ranked renewable energy resource in the US. The USDOE is in the process of developing new turbines in order to maximize the use of hydropower and to minimize its effects on the environment [29].

1.2.5 Biomass

Biomass technology converts energy from a renewable biomass into some useful form of energy including electricity, heat energy, and different types of solid, liquid, and gaseous fuels. In the US, biomass resources rank second as a primary renewable energy source and account for three percent of the total energy production in the US. Today, the US has about 10 GW of installed capacity for biomass energy production. Emerging technologies in energy extraction from biomass include the efficiency improvements via combined-cycle systems and fuel cell systems. Besides direct energy production, biomass is also used to make a variety of bio-fuels including the liquid fuels ethanol, methanol, bio-diesel, Fischer-Tropsch diesel, and gaseous fuels such as hydrogen and methane [30].

1.2.6 Ocean Energy

About 70% of the earth's surface is covered by water. The ocean is the largest absorber of solar energy. The energy from ocean water, in its various forms, include tidal energy, wave energy, and ocean thermal energy conversion (OTEC)

systems. Currently, there are no tidal power generation stations installed in the US, but research has shown that the tidal power generating stations are viable in the northwestern Pacific regions and the northeastern Atlantic regions of the US. Both the northeastern and northwestern coasts of the US have a high potential for energy extraction from wave power. OTEC systems convert thermal energy absorbed from the sun into electricity and can produce potable water. The National Energy Laboratory of Hawaii, no longer in operation, was one of the world's leading facilities where OTEC research was performed. Some of the drawbacks of the OTEC system are high installation costs, poor efficiency, and high maintenance costs [31].

1.3 Hybrid Power Systems

When two or more different sources of energy are operating together to supply a given load, the energy providing system is called a hybrid power system. The load on this hybrid power system can be a hybrid load consisting of A.C. loads, D.C. loads, and heating loads. The energy sources in a hybrid power system consist of two or more components, including a PV array, WTGs, DEGs, boilers, a battery bank, fuel cells, and other available power sources.

A general block diagram of a hybrid power system is shown in Fig. 1-6. The different power system components in this hybrid power system consist of a PV array, a DEG, a WTG, a battery bank and a boiler. The load in the system is a hybrid load consisting of an AC load, a DC load, and a heating load.

A PV array and a WTG are the renewable energy sources in the hybrid power system. They have the highest priority to supply the load. A PV array and a WTG supplies the DC load via a DC/DC converter and the AC load via a DC/AC inverter. If there is excess power available from the PV array and the WTG, the excess power can be used to charge the battery bank or to supply the heating load. However, the sun is not always shining and the wind is not always blowing.

Therefore, the DEG is generally the prime power source used in hybrid power systems for remote villages.

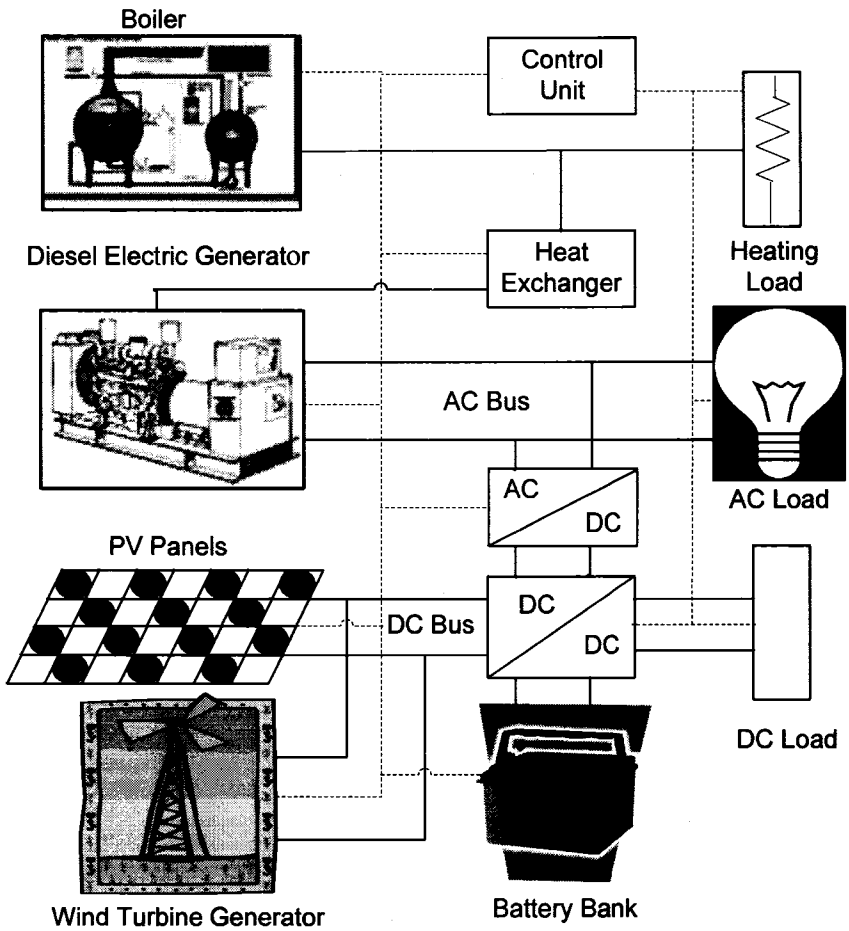

Fig. 1-6. General hybrid power system model.

A DEG is generally used as a backup generator to supply the electricity demand in a hybrid power system. In the absence of a battery bank, a DEG is generally kept spinning when the excess power available from the WTGs and the PV array is less than 20% of the load demand. The battery bank supplies the AC load if the power available from the PV array and the WTG is insufficient to supply

the AC load on the system. If the battery bank is discharged, the DEG supplies the AC load and charges the battery bank simultaneously. The heat exchanger recovers part of the heat energy present in the jacket water (cooling water) of the DEG and uses this heat energy to supply the heating load. In addition, a boiler is used in conjunction with the heat exchanger to supply the heating load. The control unit in a hybrid power system regulates the flow of energy between the different sources and loads.

1.4 Hybrid Power System Software Tools

There are a number of software tools available on the market to study hybrid power systems. The software tools that were discussed in my master's thesis are as follows:

- HOMER
- Hybrid2
- PVFORM

A few more software tools that were found during the literature search and the updates in the HOMER software are discussed in the following section.

1.4.1 HOMER

The word HOMER stands for Hybrid Optimization Model for Electric Renewables. HOMER is a computer program for modeling, optimizing, and studying the sensitivity analysis of hybrid power systems. HOMER can evaluate the economics of hybrid power systems comprised of PV arrays, WTGs, hydro-turbines, diesel electric generators, a battery bank, an AC-DC converter, an electrolyzer, and a hydrogen storage tank based on hourly data. For analysis purposes, HOMER requires a complete annual data set. The latest advancements in

HOMER include the calculation of environmental pollutant amounts including carbon dioxide, carbon monoxide, unburned hydrocarbons, sulfur dioxide, particulate matters, and nitrogen oxides. Besides calculating pollutant levels, the new version of HOMER also models the thermal/heating load, hydrogen load, and reformers. The new version also gives the flexibility to study the performance of the system for grid connection [32].

1.4.2 PV-DesignPro

PV-DesignPro is a Microsoft® Windows based software. This software is designed to simulate a PV energy system based on the climate and system design selected by the user. The program provides information on estimated power output from the PV system and the backup power required during system operation. The program also provides the user the capability of obtaining the maximum power via the installation of a Maximum Power Point Tracker (MPPT). The outputs from the model are the monthly data file which includes the energy contributed by the PV array, the battery state of charge, and the details of energy flow. The program also computes the annual energy profile, the life cycle cost analysis, the cost of energy, and the payback period [33].

1.4.3 PV*SOL®

PV*SOL® is a Microsoft® Windows based application. PV*SOL® is designed to optimize PV systems from economic and technical aspects for the stand-alone and grid connected systems. PV*SOL® accounts for the shading of the PV array, partial load on the PV array, the effect of MPPT on the system performance, emissions, and subsidies for using the PV array in computing the economic efficiency, replacement cost, and annual running cost calculations [34].

1.4.4 RETScreen®

RETScreen® software can be used to evaluate the energy production cost, life cycle cost, and GHG emission reductions for various types of renewable energy technologies (RET) that include: wind energy, small hydro-power plants, PV electric energy, biomass, solar air and water heating, ground source heat pump, and combined heat and power applications [35].

1.4.5 WindScreen3

WindScreen3 version 1.01 was coded using Microsoft Visual Basic 3.0 at the University of Massachusetts, Amherst. It was released on March 1st, 2000 and is available for downloading at http://www.ceere.org/rerl/projects/software/wind-screen3-overview.html. The computer model evaluates the performance of a hybrid wind-diesel system with and without energy storage. The model allows the use of more than one identical WTG and identical DEGs in the hybrid power system. In this model, synthetic load and wind data are generated using a Markov process, which results in a time series with a specified mean, standard deviation, autocorrelation and specified lag, and probability density. The WindScreen3 model is based on the principle of energy balance as follows [36]:

$$D = L - W + DP - U \tag{1-1}$$

where, 'D' is the power delivered from the diesel generator(s), 'L' is the power required by the load, 'W' is the power delivered from the wind turbine(s), 'DP' is the power dissipated in the dump load, and 'U' is the unmet load.

In WindScreen3 the WTG is modeled as a performance curve that describes wind speed versus wind power as obtained from the manufacturer. The DEG is modeled as a linear fuel curve describing the fuel consumed based on the load [36]. These performance curves are discussed in Chapter 2. The outputs from the

WindScreen3 model include the average values of available WTG power, DEG power, fuel used, power dissipated to the dump load, and the unmet load.

1.4.6 Windographer

Windographer is a data analysis tool used to analyze the wind speed data. Windographer supports a number of data files including .txt, .xls, at any sampling rate and gap filling for missing data. The gap filling in Windographer is carried out using the Markov algorithm that takes into account the diurnal pattern of the wind. Windographer can compute the power available in the wind, the Weibull parameters, and the autocorrelation coefficients. The turbulence analysis module in the Windographer computes the variation of turbulence intensity with wind speed, wind direction, and the time of year [37].

1.5 HARPSim with MATLAB® Simulink®

The HARPSim model developed in this dissertation uses MATLAB® Simulink® for designing and modeling hybrid electrical power systems for remote locations.

The main advantages of using Simulink® are:

1) Simulink® can model, analyze and simulate dynamic systems.
2) It supports linear and nonlinear systems, modeled in continuous time and/or discrete time.
3) Simulink® is a graphical user interface.
4) Capability of building new blocks with the use of s-functions or C MEX functions.
5) Use of Real Time Workshop can generate the codes automatically which guarantees faster execution.

6) Future incorporation of new components and a control/power management system.

Chapter 2 will describe a more detailed model of the different hybrid power system components built using MATLAB® Simulink®. The different power system component models include a DEG, a heat exchanger, a boiler, a battery bank, a WTG, and a PV array. The latter part of Chapter 2 will discuss the various economic and environmental parameters used in the study of the hybrid power system models.

2 Hybrid Power System Model Components Development

Chapter 1 described the various energy sources in the United States and the latest technologies in the development of the various renewable energy sources. While the latter part of Chapter 1 briefly described a hybrid power system and its operation, the current chapter will discuss the step-by-step procedure of the development of a hybrid power system model, using MATLAB® Simulink®.

In Simulink®, for clarity and ease of understanding, subsystems are generally developed for various components of the system. The different subsystems are placed in the library of Simulink® and can be accessed by the user to develop a hybrid power system. The work described in this chapter discusses the development of a Simulink® library for the various components of a hybrid power system.

A Simulink® model, called HARPSim, for evaluating the long term economic and environmental performance of stand-alone hybrid power systems in remote arctic villages is developed in this project. HARPSim incorporates the Simulink® model for various power system components including a DEG, a heat exchanger, a boiler, a WTG, a PV array, and a battery bank. Different system components are integrated to form a hybrid power system. Various control system strategies, including the optimization of the load on the DEGs to minimize the fuel consumption, power flow strategies between the energy sources and the load, and charge/discharge cycles for the battery bank are incorporated while integrating system components. The different hybrid power system components are described in the following sections.

2.1 DEG Model

The DEG consists of two parts: the electric generator and the diesel engine. The electric generator model consists of the efficiency curve that describes the relationship between the electrical efficiency and the electrical load on the generator. Fig. 2-1 shows a typical electrical efficiency curve for a 21 kW Marathon electric generator. The performance curve data were obtained from the manufacturer of the electric generator. The details of the 21 kW Marathon electric generator are given in Appendix 1.

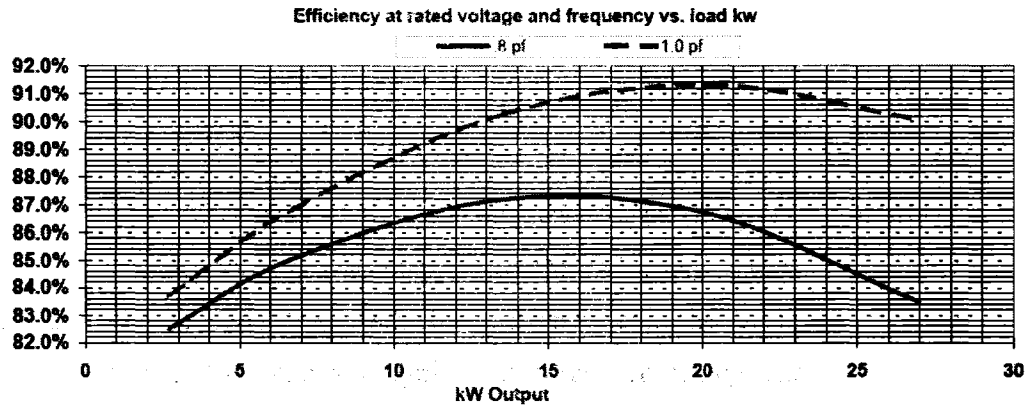

Fig. 2-1. Electrical efficiency for a 21 kW Marathon electric generator [Appendix 1].

A fourth order polynomial fit for the electrical efficiency curve at unity power factor and 0.8 power factor is given by Eq. 2-1 and Eq. 2-2, respectively,

$$\eta_{el1} = -6.953e-9*L^4 + 2.932e-7*L^3 - 9.858e-4*L^2 + 0.201*L + 81.372 \quad (2\text{-}1)$$

$$\eta_{el2} = 1.540e-7*L^4 - 4.424-5*L^3 + 2.996e-3*L^2 + 0.034*L + 81.652 \quad (2\text{-}2)$$

where 'L' is the load on the electric generator (%). The actual load on the electric generator is converted to its percentage value by dividing the actual load with the rating of the electric generator as given by Eq. (2-3),

$$\text{percentage load} = \frac{\text{actual load}}{\text{generator rating}} * 100 . \tag{2-3}$$

This operation is performed so that the same efficiency equations are independent of the rating of the electric generators. The values from Eq. (2-1) and Eq. (2-2) are used to obtain the value for the electrical efficiency of the generator for any given power factor 'pf' by means of linear interpolation as follows:

$$\eta_{el} = \eta_{el2} + \left(\frac{(\eta_{el1} - \eta_{el2})}{0.2} * (pf - 0.8) \right) \tag{2-4}$$

where η_{el} is the electrical efficiency of the generator for a given power factor 'pf'.

The load on the diesel engine (the input to the electric generator) is obtained from the system load (the output of the electric generator) and the electrical efficiency of the generator as follows:

$$L_{eng} = \frac{L_{gen}}{\eta_{el}} \tag{2-5}$$

where 'L_{eng}' is the load on the engine, 'L_{gen}' is the load on the generator, and 'η_{el}' is the electrical efficiency of the generator.

The block diagram representation of Eq. (2-1) through Eq. (2-5) as developed in Simulink® is shown in Fig. 2-2, and the subsystem for the electric

efficiency model for the generator is shown in Fig. 2-3. Inputs to the model are the percentage load on the DEG and the power factor data, while outputs from the model are the electrical efficiency (%) of the generator and the engine load (% of rated).

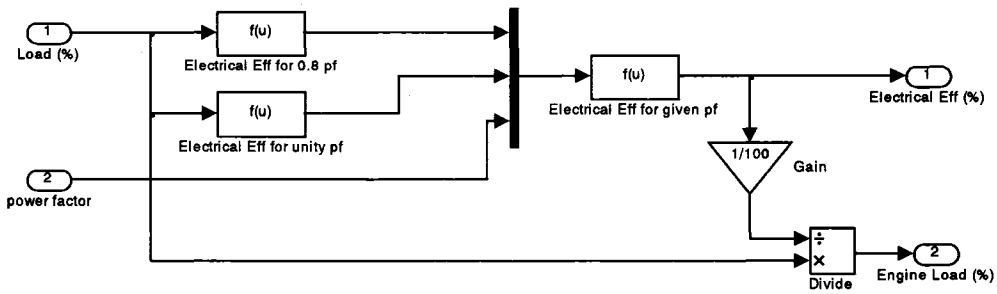

Fig. 2-2. Details of the electrical efficiency model block.

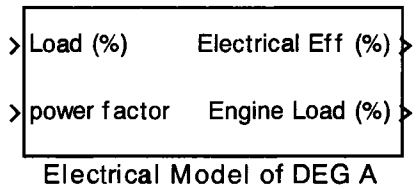

Fig. 2-3. Subsystem of the electrical efficiency model for the generator.

The fuel curve for a diesel engine describes the amount of fuel consumed depending on the engine load. A typical engine fuel curve is a linear plot of load versus fuel consumption as shown in Fig. 2-4. The data sheet for the 24 kW John Deere engine is given in Appendix 2.

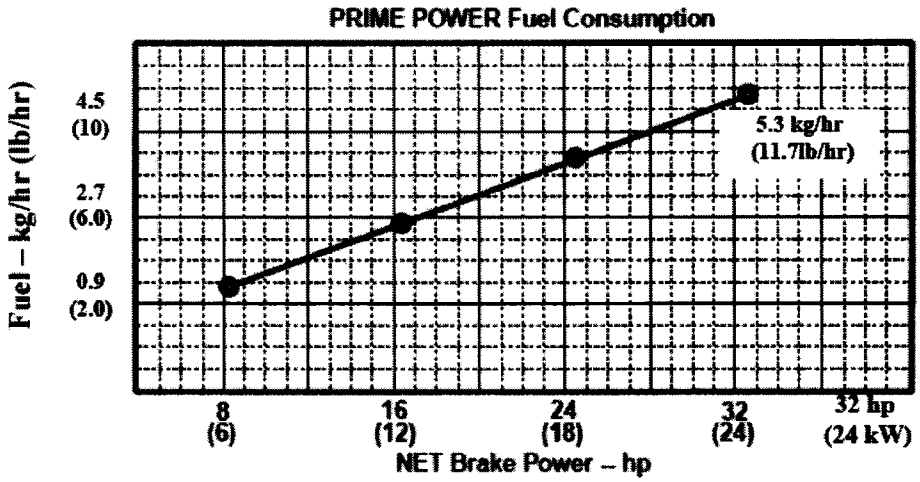

Fig. 2-4. Fuel consumption curve of a 24 kW John Deere engine [Appendix 2].

The linear curve fit for the John Deere's engine fuel curve is given as:

$$\dot{F}_c = 0.5 * (L_{eng} * \frac{kW\_A}{100}) - 0.44 \tag{2-6}$$

$$\text{Total } F_c = \int_0^T \dot{F}_c \, .dt \tag{2-7}$$

where '$\dot{F}_c$' is the fuel consumption rate in kg/hr (lbs/hr), 'L_{eng}' is the percentage load on the engine, 'kW_A' is the rating of the electric generator, 'F_c' is the total fuel consumed in kg (lbs), 'dt' is the simulation time-step, and 'T' is the simulation period. The fuel consumed in kg (lbs) is obtained by multiplying the fuel consumption rate of kg/hr (lbs/hr) by the simulation time-step 'dt' (given in hours), and the total fuel consumption in kg (lbs) is obtained by integrating the term '$\dot{F}_c \, .dt$' over the period of the simulation.

The block diagram representation and the subsystem for the engine model block are shown in Fig. 2-5 and Fig. 2-6, respectively.

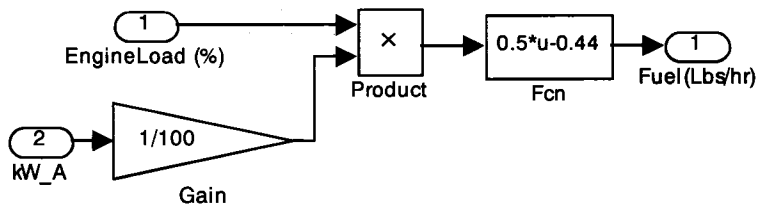

Fig. 2-5. Details of the engine model block.

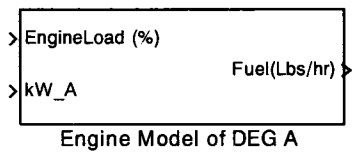

Fig. 2-6. Subsystem for the engine model.

2.1.1 Optimization of DEG Model

When there are two DEGs to supply the load, it is important that DEGs operate optimally. In the Simulink® model, the data are supplied in such a way that DEG 1 is more efficient than DEG 2. The following steps are performed to find the optimal point of operation for DEG 2.

1) The electrical generator performance curve (Fig. 2-1) and the diesel engine performance curve (Fig. 2-4) are combined to obtain the overall fuel consumption for the given load profile.
2) The load on the DEGs is varied from 0 to 100%.
3) The fuel consumption for each DEG is noted at different load points.

4) The point of intersection of the two curves is the optimal point of operation for DEG 2. Beyond this point DEG 1 is more efficient than DEG 2.
5) If the two curves do not intersect, the optimal point is taken as 0. This situation implies that DEG 1 is efficient throughout the operating range of the load.

Fig. 2-7 shows the overall fuel consumption curves for the two DEGs and the optimal point of operation for DEG 2. In order to avoid premature mechanical failures, it is important that DEGs operate above a particular load (generally 40% of rated). The long-term operation of DEGs on light loads leads to hydrocarbon built-up in the engine, resulting in high maintenance cost and reduced engine life [38]. In the Simulink® model, if the optimal point is less than 40% load, the optimal point is adjusted so that DEG 2 operates at or over 40% load.

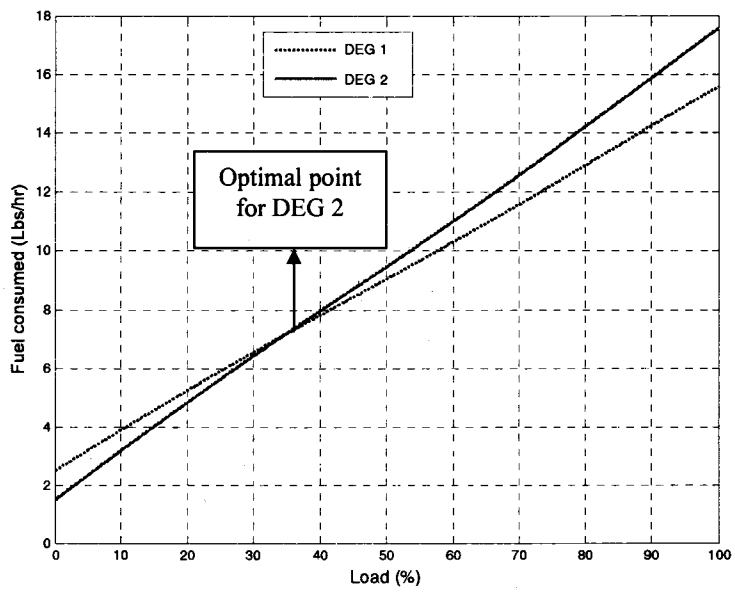

Fig. 2-7. Optimal point of operation for DEG 2.

The block diagram representation and the subsystem for the optimization model are shown in Fig. 2-8 and Fig. 2-9, respectively. The 'DEG_Load' in Fig. 2-8 is the s-function written in MATLAB® Simulink®. This s-function compares the load on two DEGs and divides the load based on the optimal point of operation.

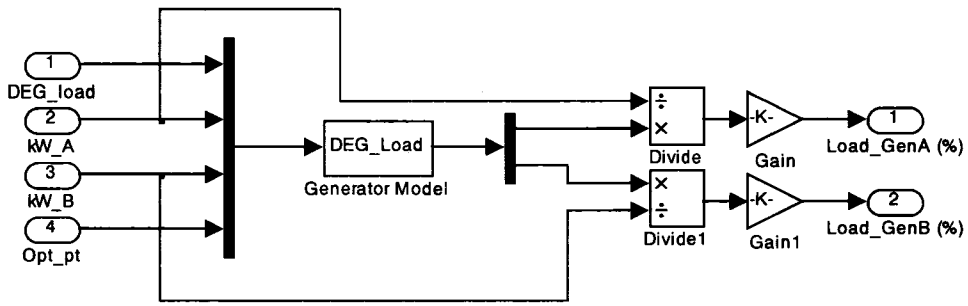

Fig. 2-8. Details of the optimization model block.

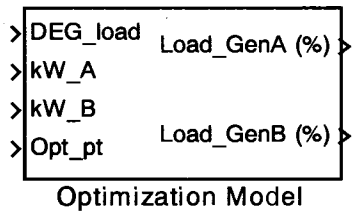

Fig. 2-9. Subsystem for the optimization model

2.2 Heat Exchanger Model

The heat flux recovered from the jacket water of a DEG using a heat exchanger is calculated as follows [39]:

$$\dot{Q} = \eta_{HE} * \dot{m} * Cp * \Delta T \qquad (2\text{-}8)$$

where '$\dot{Q}$' is the rate at which heat is transferred in Joules/sec (BTU/sec), 'η_{HE}' (eta_HE in Fig. 2-10 and) is the efficiency of the heat exchanger, '$\dot{m}$' is the mass flow rate of the coolant in kg/sec (lbs/sec), 'Cp' is the specific heat of the coolant in Joules/(kg °K) (BTU/(lb °F)), and 'ΔT' is the temperature difference in °K (°F) of the coolant in and out of the jacket. The total heat recovered 'Q' (kWh) is calculated by integrating the heat recovery rate over the entire time of the simulation and is calculated as follows:

$$Q = \int_0^T \dot{Q}.dt. \tag{2-9}$$

In addition to the total heat recovered, the heat exchanger model also calculates the total avoided pollutants including CO_2, PM_{10}, and NOx. The method used to calculate the avoided pollutants is discussed in Section 2.8.

The subsystem and the block diagram representation for a heat exchanger model block are shown in Fig. 2-10 and Fig. 2-11, respectively.

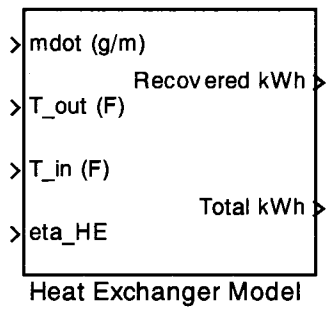

Fig. 2-10. Subsystem for the heat exchanger model.

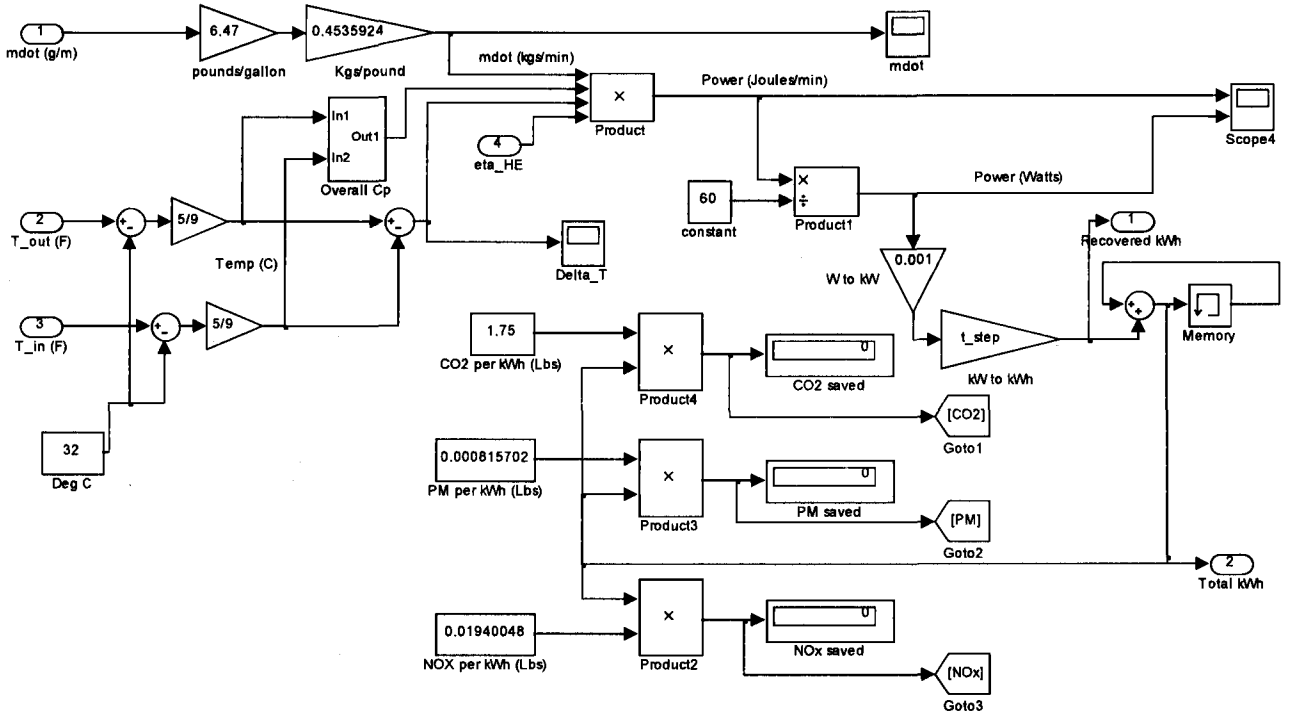

Fig. 2-11. Details of the heat exchanger model block.

2.3 Boiler Model

The boiler model block calculates the fuel saved if the total heat recovered from the heat exchanger, given by Eq. (2-9), is supplied using a boiler. The total fuel saved is obtained using the following equation:

$$Fs = \frac{Q}{HV * \eta_b} \tag{2-10}$$

where 'Fs' in liters (gallons) is the total fuel saved due to the heat recovery, 'Q' is the total heat energy recovered (kWh), 'HV' is the heating value of the boiler fuel in kWh/liter (kWh/gallon), and 'η_b' (eta_boiler in Fig. 2-12 and Fig. 2-13) is the efficiency of the boiler.

The block diagram representation and the subsystem for the boiler model block are shown in Fig. 2-12 and Fig. 2-13, respectively.

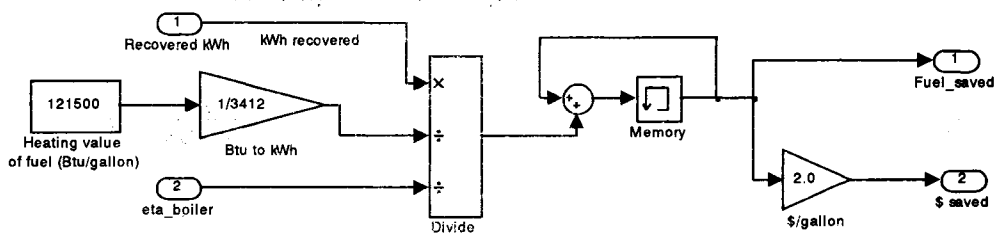

Fig. 2-12. Details of the boiler model block.

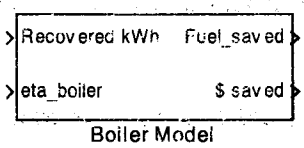

Fig. 2-13. Subsystem for the boiler model.

2.4 WTG Model

The wind model block calculates the total power available from the wind turbines based on the power curve. The power curve gives the value of the electrical power based on the wind speed. Fig. 2-14 shows the power curve for the 15/50 Atlantic Oriental Corporation (AOC) wind turbine generator [40]. The details of the AOC wind turbine generator are available in Appendix 3.

The fifth order polynomial for the power curve is given as follows:

$$P_{WTG} = -4.12e-6*S^5 + 7.58e-4*S^4 - 5.22e-2*S^3 + 1.59*S^2 - 17.8*S + 63.12 \quad (2\text{-}11)$$

$$E_{WTG} = \int_0^T P_{WTG}\,dt \quad (2\text{-}12)$$

where 'P_{WTG}' is the power output (kW) from the WTG, 'S' is the wind speed in m/s (miles/hour), 'E_{WTG}' is the energy obtained from the WTG (kWh), 'T' is the simulation time (hours), and 'dt' is the simulation time-step (hours).

The wind model block also calculates the second law efficiency of the WTG. The second law efficiency of the WTG is given as follows:

$$\eta_{second\_law} = \frac{actual\_power}{max\_possible\_power} \quad (2\text{-}13)$$

where 'η_{second_law}' is the second law efficiency of the WTG, 'actual_power' is the actual power output from the WTG and 'max_possible_power' is the maximum possible power output from the WTG.

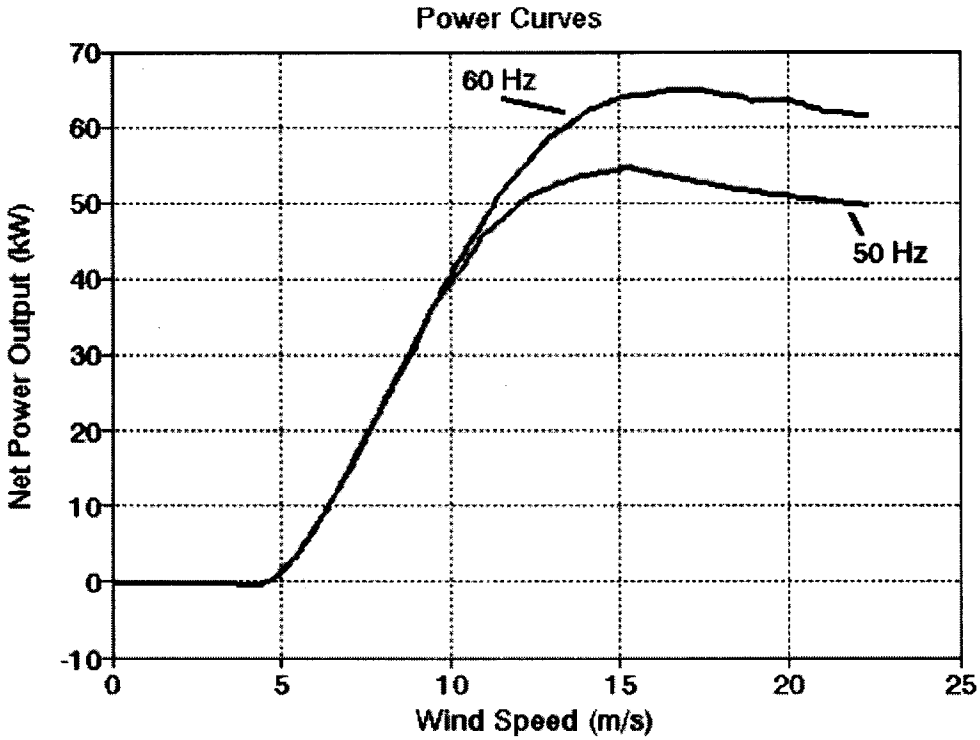

Fig. 2-14. Power curve for 15/50 Atlantic Oriental Corporation WTG [40].

The actual power of the wind turbine is obtained from the manufacturer's power curve given by Eq. (2-11) and the maximum possible power is obtained from the Betz formula described in [41] and given as follows:

$$P_{max} = \frac{1}{2}\rho.A.V^3.0.59 \qquad (2\text{-}14)$$

where 'P_{max}' is the maximum possible power, 'ρ' is the density of air taken as 1.225 kg/m^3 (0.076 lb/ft^3) at sea level, 1 atmospheric pressure i.e. 101.325 kPa (14.7 psi), and a temperature of 15.55°C (60°F), 'A' is the rotor swept area in m^2 (ft^2), 'V' is the velocity of wind in m/s (miles/hour), and the factor '0.59' is the

theoretical maximum value of power coefficient of the rotor (Cp) or theoretical maximum rotor efficiency which is the fraction of the upstream wind power that is captured by the rotor blade.

The air density 'ρ' can be corrected for the site specific temperature and pressure in accordance with the gas law and is given as follows:

$$\rho = \frac{p}{RT} \tag{2-15}$$

where 'ρ' is the density of air, 'p' is the air pressure, 'R' is the gas constant, and 'T' is the temperature.

It should be noted from Eq. (2-14) that the wind power varies with the cube of the air velocity. Therefore, a slight change in wind speed results in a large change in the wind power.

The block diagram representation and the subsystem for the wind model are shown in Fig. 2-15 and Fig. 2-16, respectively.

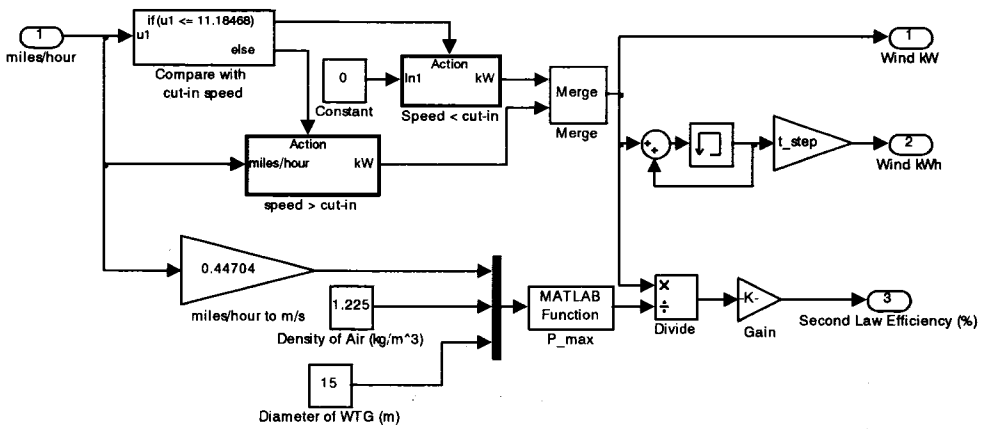

Fig. 2-15. Details of the wind model block.

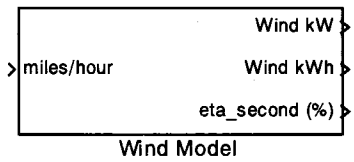

Fig. 2-16. Subsystem for the wind model.

2.5 PV Model

The PV model block calculates the PV power (kW) and the total PV energy (kWh) supplied by the PV array using the following equations:

$$P_{PV} = \eta_{pv} * ins * A * PV \tag{2-16}$$

$$E_{PV} = \int_0^T P_{PV}.dt \tag{2-17}$$

where 'P_{PV}' is the power obtained from the PV array (kW), 'η_{pv}' is the efficiency of the solar collector, 'ins' is the solar insolation (kWh/m^2/day), 'A' is the area of the solar collector/kW, 'PV' is the rating of the PV array (kW), and E_{PV} is the total energy obtained from the PV array.

The efficiency of the solar collector is obtained from the manufacturer. The data sheets for the solar panels manufactured by Siemens and BP are available in Appendix 4. The solar insolation values are available from the site data or can be obtained by using the solar maps from the National Renewable Energy Laboratory website [42]. The area of the solar collector depends on the number of PV modules and the dimensions of each module. The number of PV modules depends on the installed capacity of the PV array and the dimensions of each PV module are obtained from the manufacturer's data sheet.

The block diagram representation and the subsystem for the PV model block are shown in Fig. 2-17 and Fig. 2-18, respectively.

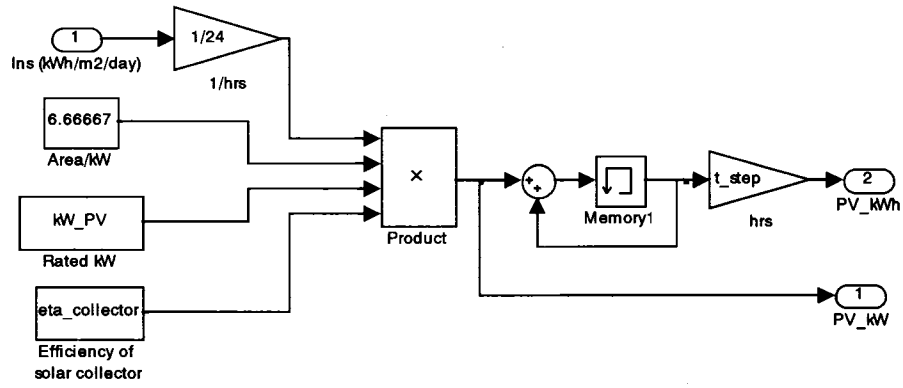

Fig. 2-17. Details of the PV model block.

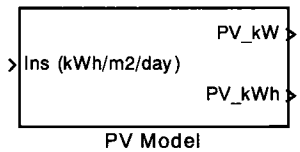

Fig. 2-18. Subsystem for the PV model.

2.6 Battery Model

In the Simulink® model, the battery-bank is modeled so that the battery-bank acts as a source of power, rather than back-up power. The battery model block controls the flow of power to and from the battery bank. A roundtrip efficiency of 90% is assumed for the battery charge and discharge cycle. The battery model incorporates the effect of ambient temperature as described in [43] into the hybrid power system model. Therefore, the model can be used for cold region applications. The manufacturer's data sheet for the battery-bank is available in Appendix 5. The details of the battery model block are shown in Fig. 2-19.

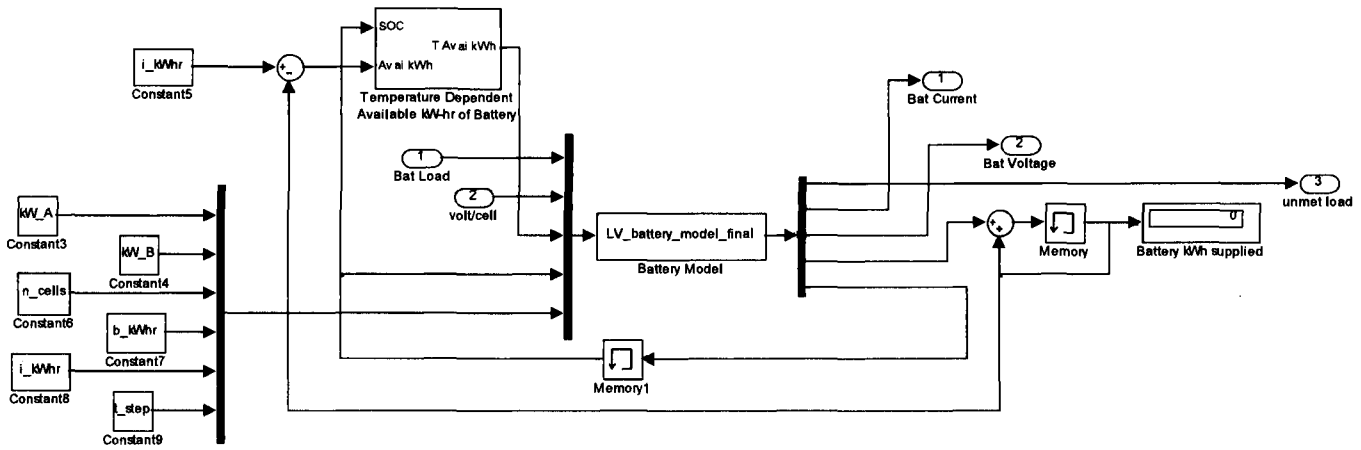

Fig. 2-19. Details of the battery model block.

The details of the temperature dependent available battery energy model are shown in Fig. 2-20 and the subsystem for the battery model is shown in Fig. 2-21.

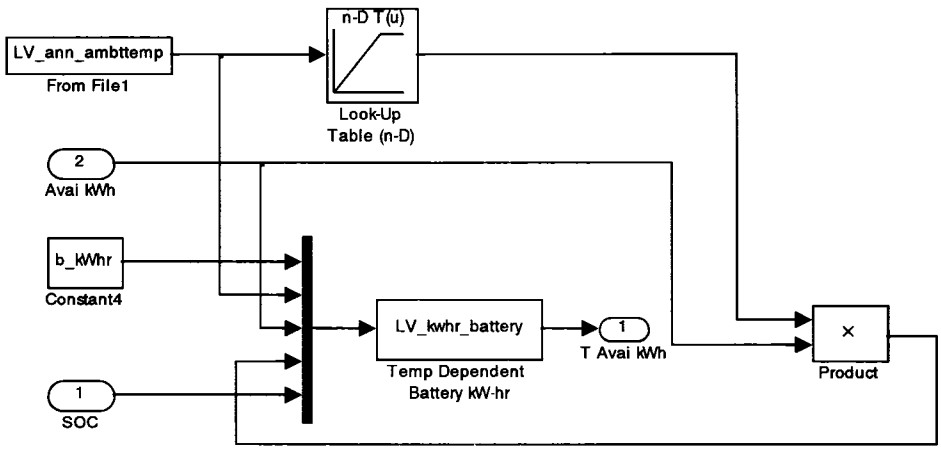

Fig. 2-20. Details of the temperature dependent available battery energy model.

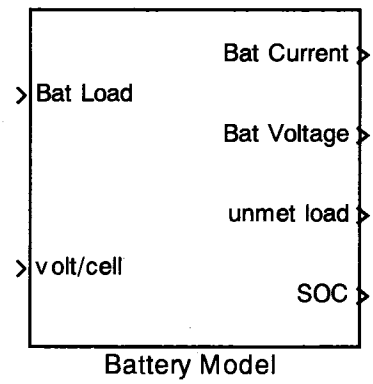

Fig. 2-21. Subsystem for the battery model.

The life of the battery bank depends on the depth of discharge and the number of charge discharge cycles. In the Simulink® model the battery-bank is modeled so that it acts as a source of power rather than back-up power. Therefore,

the depth of discharge of the battery-bank is assumed between 95% and 20% of the rated capacity. This higher depth of discharge reduces the number of battery operating cycles for the same energy output. It should be noted that the number of battery cycles plays a more significant role in the life of the battery-bank.

2.7 Economic Parameters Used in the Model

It is very important for the system designer to get acquainted with different economic parameters used in the modeling process of hybrid power systems. Economic parameters are used to calculate the COE, the payback period, and the life cycle cost of the system. The various economic parameters used in the hybrid power system model are discussed in the following sections [44].

2.7.1 Investment Rate, Inflation Rate, and Discount Rate

The investment rate is the percentage rate at which the value of money increases every year.

Inflation rate is the tendency of prices to rise over time. Inflation rate takes into account the future price rise in the project commodities including fuel and different power system components.

Discount rate is the difference between the investment rate and the inflation rate. Discount rate is generally used in life cycle cost analysis calculations.

$$\text{Discount rate} = \text{Investment rate} - \text{Inflation rate}. \tag{2-18}$$

2.7.2 Life Cycle

The life cycle is the life-time of the project. It is the time at the end of which the system components require replacement.

2.7.3 Net Present Value

The net present value (NPV) is the money that will be spent in the future discounted to today's money. The NPV plays an important role in deciding the type of the system to be installed. The NPV of a system is used to calculate the total spending on the installation, maintenance, replacement, and fuel cost for the type of system over the life-cycle of the project. Knowing the NPV of different systems, the user can install a system with minimum NPV. The different equations used in the calculation of NPVs are given as follows:

$$P = \frac{F}{(1+I)^N} \tag{2-19}$$

$$P = \frac{A[1-(1+I)^{-N}]}{I} \tag{2-20}$$

where 'P' is the present worth, 'F' is the money that will be spent in the future, 'I' is the discount rate, 'N' is the year in which the money will be spent, and 'A' is the annual sum of money.

2.7.4 Life Cycle Cost

The life cycle cost (LCC) is the total cost of the system over the period of its life cycle including the cost of installation, operation, maintenance, replacement, and the fuel cost. The life cycle cost also includes the interest paid on the money borrowed from the bank or other financial institutes to start the project. The life cycle cost of the project can be calculated as follows:

$$LCC = C + M + E + R - S \tag{2-21}$$

where 'LCC' is the life cycle cost, 'C' is the installation cost (capital cost), 'M' is the overhead and maintenance cost, 'E' is the energy cost (fuel cost), 'R' is the replacement and repair costs, and 'S' is the salvage value of the project.

2.7.5 Payback Period

Payback period is the time in which the total extra money invested in a project is recovered and is given as,

$$\text{Payback Period} = \frac{\text{Extra Investment}}{\text{Rate of Return}}. \tag{2-22}$$

Payback period is the major deciding factor for the feasibility of the project. If the payback period of the system is less than the life cycle of the system, the project is economically feasible.

2.8 Environmental Parameters in the Model

Researchers believe that with the industrial revolution, humans have altered the climate and the environment by releasing large amounts of different gases into the atmosphere. The different environmental parameters in the analysis of the Simulink® model include carbon dioxide (CO_2), nitrogen oxide (NOx), and particulate matter (PM_{10}). The environmental parameters are discussed in detail in the following sections.

2.8.1 Carbon Dioxide (CO_2)

CO_2 is released in the atmosphere due to the combustion of fossil fuels including coal, oil, natural gas, wood, and biomass. CO_2 is believed to be one of the major GHGs responsible for causing global warming [45]. However, there is a group of researchers who believe that increased CO_2 and other gases are not

responsible for the global warming [46]. In the Simulink® model the total CO_2 was calculated based on the equation for the combustion of diesel fuel. For example, one empirical formula for light diesel $C_nH_{1.8n}$ is given in [47]. For this empirical formula, with 0 % excess air the combustion reaction is given as follows:

$$C_nH_{1.8n} + (1.45n)(O_2 + 3.76N_2) = nCO_2 + 0.9nH_2O + (1.45N_2)(3.76N_2). \quad (2\text{-}23)$$

For any n, the mass in kg (lb) of CO_2 per unit mass in kg (lb) of fuel = 44/(12 + 1.8) = 3.19. So, to get the emissions per unit electrical energy output, the above is combined with an engine efficiency of 3.17 kWh/liter (12 kWh/gallon) and a fuel density of 0.804 kg/liter (6.7 lb/gallon). Doing this results in specific CO_2 emissions of 3.1*(0.804/3.17) = 0.786 kg (1.73 lb) of CO_2 per kWh of electricity. This figure of 0.786 kg/kWh (1.73 lb/kWh) agrees closely with the data obtained from the manufacturer 0.794 kg/kWh (1.75 lb/kWh). The annual CO_2 amount was calculated from the lb CO_2/kWh and the annual kWh produced and is given as follows:

$$\text{Total pollutant in kg (lb)} = \frac{\text{pollutant}}{\text{kWh}} * \text{kWh}_{\text{Gen}} \quad (2\text{-}24)$$

where kWh_{Gen} is the total kWh supplied by the diesel generator during the simulation period.

2.8.2 Nitrogen Oxide

Nitrogen oxide (NOx) is one pollutant responsible for acid rain. Besides global warming, NOx is the major source for the formation of ground ozone. Ozone has severe health impacts including asthma, emphysema, and bronchitis. Acute

exposure to ozone may result in premature death. The U.S. Environmental Protection Agency (EPA) has initiated several programs to reduce the formation of ozone by reducing NOx and volatile organic compounds from the atmosphere [48]. In the Simulink® model, the total NOx emitted is calculated based on the value of 0.0088 kg (0.0194 lb) of NOx per kWh of electricity produced, as obtained from the manufacturer. The annual NOx was calculated using Eq. (2-24).

2.8.3 Particulate Matter

Particulate matter (PM) is the complex mixture of extremely small particles and liquid droplets. During the combustion of diesel fuel, PM may contain carbon particles and unburned hydrocarbons. Particulate matter smaller than 10 micrometers can cause severe health problems including lung cancer, aggravated asthma, irregular heart beats, and nonfatal heart attacks [49]. In the Simulink® model, the total PM was calculated based on the value of 0.00037 kg (0.00082 lb) of PM_{10} per kWh of electricity produced as obtained from the manufacturer. The annual PM_{10} was calculated using Eq. (2-24).

2.8.4 Avoided Cost of Pollutants

Generally, a power plant incorporating renewable energy is more expensive than a non-renewable energy plant because of the high installation cost associated with the renewable energy systems. The avoided cost of pollutants is the extra cost associated with the low emissions power plant (the plant incorporating renewable energy sources) due to the use of renewable energy. The avoided cost of pollutants is given as follows [50]:

$$AC = \frac{COE_L - COE_H}{E_H - E_L} \tag{2-25}$$

where 'AC' is the avoided cost of pollutants in USD/metric ton (USD/US ton), 'COE_L' is the COE from the low emissions plant, 'COE_H' is the COE from the high emissions plant, 'E_H' is the amount of emissions from the high emissions plant in metric ton (US ton), and 'E_L' is the amount of emissions from the low emissions plant in metric ton (US ton).

In this chapter the algorithm for modeling the various hybrid power system components of the Simulink® model is implemented using s-functions in Simulink®. S-functions are not secured and can be modified easily. Therefore, for security reasons and to avoid accidental changes in the algorithm, it is suggested that the algorithm for modeling the various hybrid power system components be implemented using C MEX functions. C MEX functions are written in C and compiled using the MEX command in MATLAB®. The output of the compilation process results in a .dll file. These .dll files assure the security of the algorithm as they cannot be used to modify the algorithm. The .dll files can be generated for different model components, and then distributed to users for use with the hybrid power system model.

Chapter 3 will describe the development of various hybrid power systems used in this project. The power system components developed in Chapter 2 are used to develop various hybrid power system models. The latter part of Chapter 3 will describe the graphical user interface (GUI) developed in MATLAB® to assess various hybrid power systems. The GUI model is named the Hybrid Arctic Remote Power Simulator (HARPSim). HARPSim can be used to study the performance of remote hybrid power systems in different parts of the world.

3 Hybrid Power System Models

Chapter 2 described various hybrid power system components developed using MATLAB® Simulink® as well as various economic and environmental parameters that are used in the study of hybrid power systems. In this chapter, various system components will be connected to form a hybrid power system. The latter part of this chapter will describe the development of the GUI model (HARPSim). HARPSim was developed to study the performance of hybrid power systems in remote arctic villages and can be used to study similar systems in other parts of the world.

3.1 Diesel-Battery Model

Fig. 3-1 shows the Simulink® model for the diesel-battery hybrid power system. The diesel-battery hybrid power system model consists of a battery bank and one or more DEGs as sources of energy. If there are two generators in the hybrid power system, an optimization model block is used to minimize the fuel used in supplying the load.

In a diesel-battery hybrid power system model, the battery bank has a higher priority to supply the load. If the battery bank is in the charging stage, the DEGs supply the load and charge the battery bank simultaneously. Various output parameters from the diesel-battery hybrid power system model include: total fuel consumed in liters (gallons), total cost of fuel (USD), the system efficiency in kWh/liter (kWh/gallon), total CO_2 emitted in metric tons (US tons), total NOx emitted in kg (pounds), and total PM_{10} emitted in kg (pounds). These output parameters are used to perform the economic analysis and assess the environmental impacts of the system.

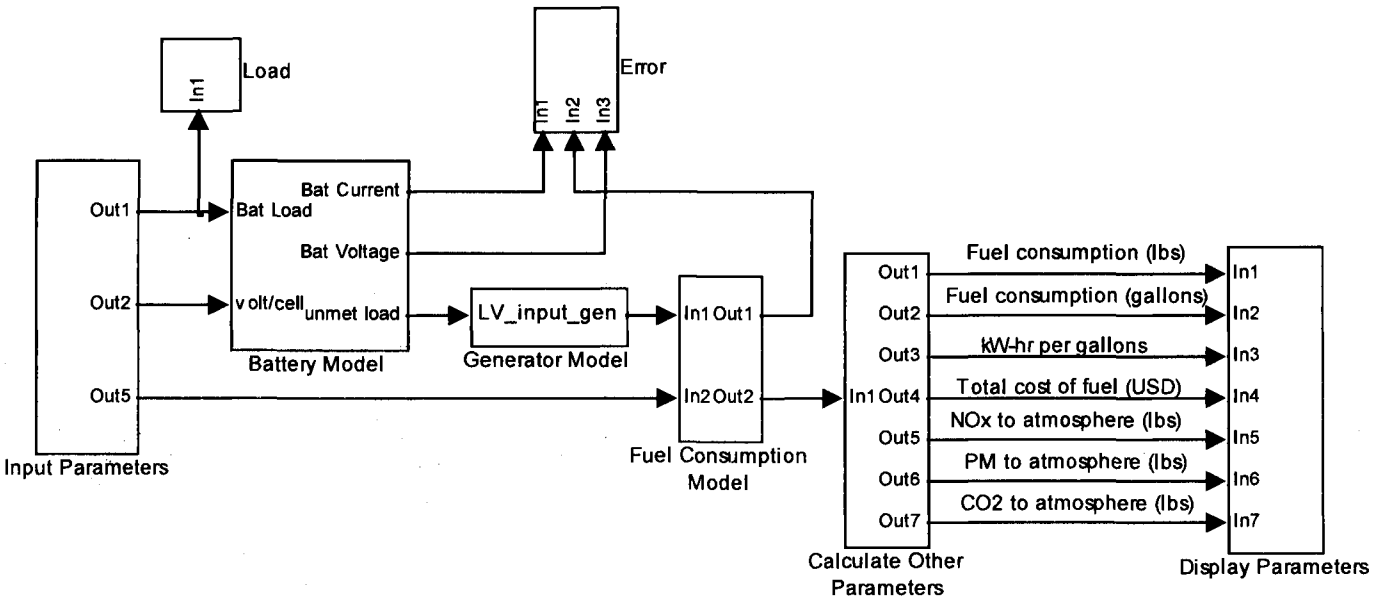

Fig. 3-1. Diesel-battery hybrid power system model.

Fig. 3-2 shows the flow-chart algorithm for the diesel-battery hybrid power system.

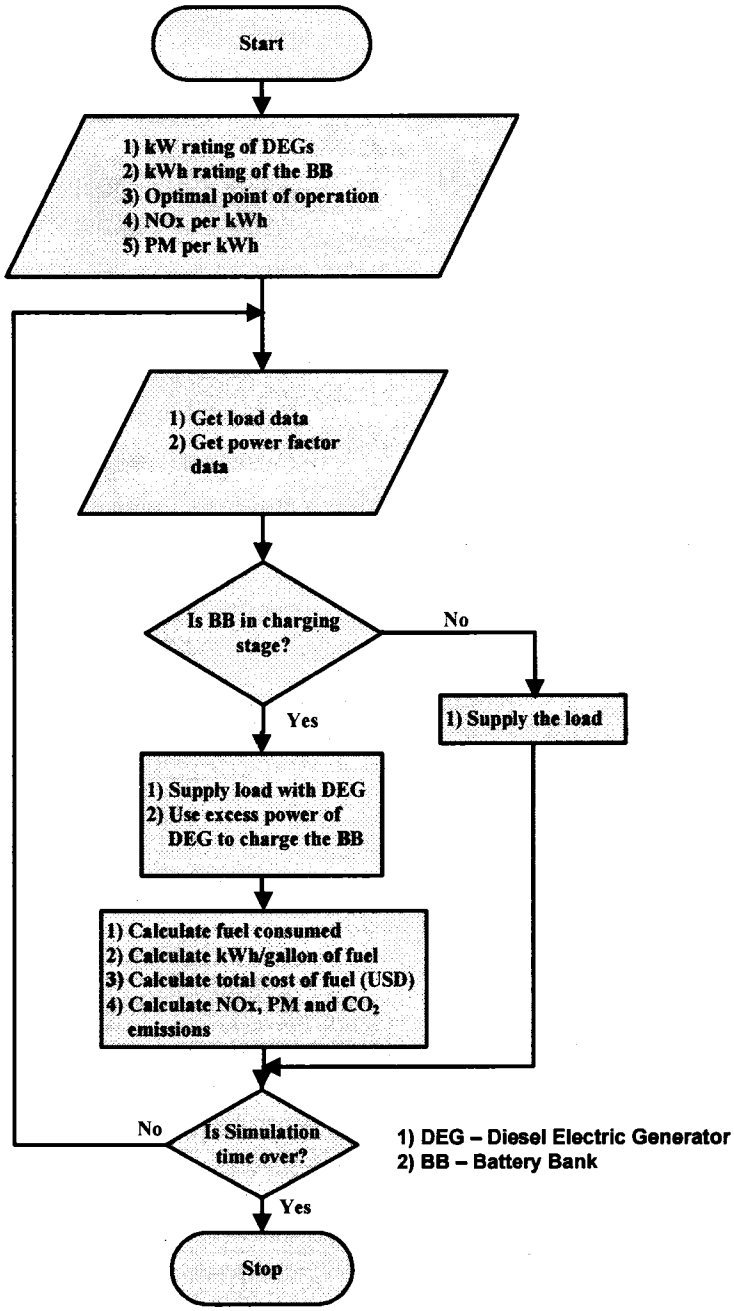

Fig. 3-2. Flow-chart algorithm for the diesel-battery hybrid power system model.

3.2 PV-Diesel-Battery Model

Fig. 3-3 shows the Simulink® model for the PV-diesel-battery hybrid power system. The PV-diesel-battery hybrid power system consists of a PV array, a battery bank, and one or more DEGs as sources of energy.

In a PV-diesel-battery hybrid power system, the PV array has the highest priority to supply the load. If the system load is more than the PV array power, the unmet load is sent to the battery bank. If the battery bank is discharged, DEGs supply the unmet load and charge the battery bank simultaneously. Outputs from the PV-diesel-battery hybrid power system include: the power obtained from the PV array (kW), total fuel consumed in liters (gallons), total cost of fuel (USD), the system efficiency in kWh/liter (kWh/gallon), total CO_2 emitted in metric tons (US tons), total NOx emitted in kg (pounds), and total PM_{10} emitted in kg (pounds). These output parameters are used to calculate the economic and environmental parameters of the system. Economic parameters include the life cycle cost analysis, the COE , the PV array pay pack time, and the sensitivity analysis of fuel cost and investment rate on the life cycle cost and the PV array pay back period. The environmental parameters include the avoided cost of different pollutants including CO_2, NOx and PM_{10}.

Fig. 3-4 shows the flow-chart algorithm for the PV-diesel-battery hybrid power system model.

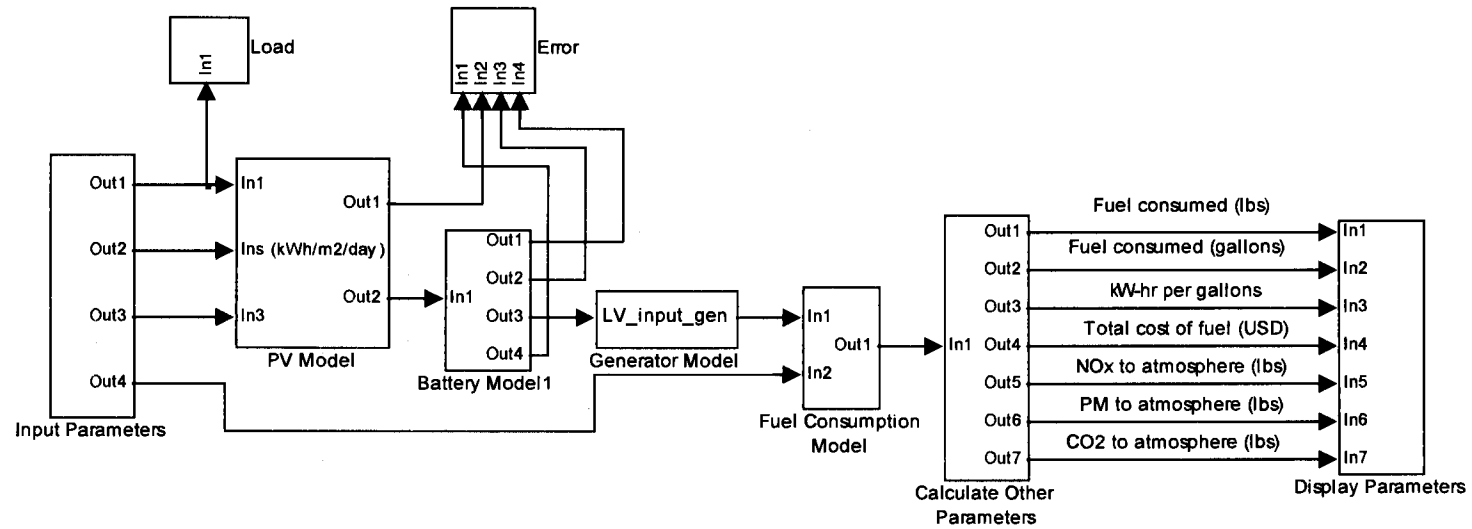

Fig. 3-3. PV-diesel-battery hybrid power system model.

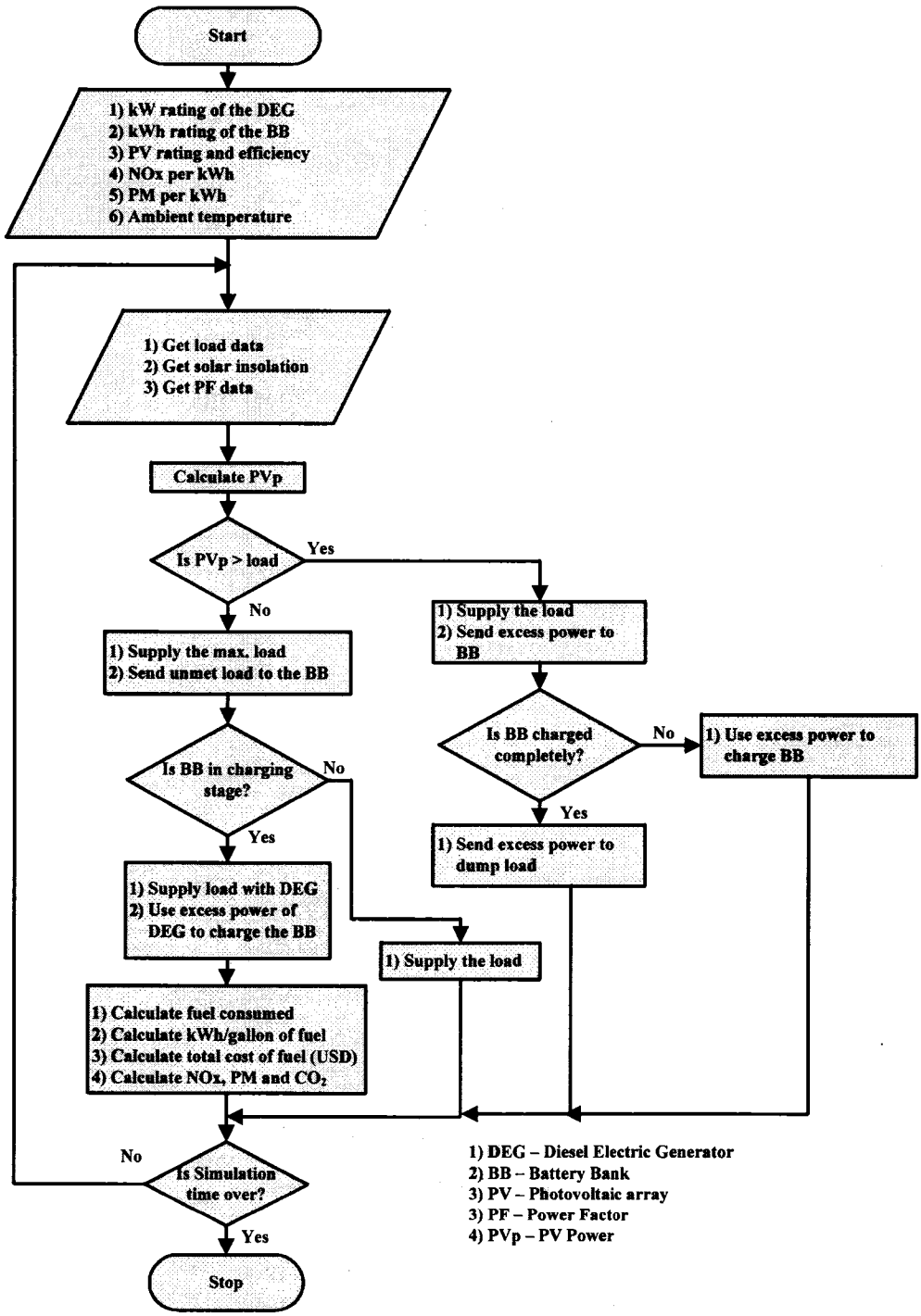

Fig. 3-4. Flow-chart algorithm for the PV-diesel-battery hybrid power system.

3.3 Wind-Diesel Model

Fig. 3-5 shows the Simulink® model for the wind-diesel hybrid power system. The wind-diesel hybrid power system model consists of WTGs and DEGs as sources of electrical energy.

In a wind-diesel hybrid power system, the WTGs have the higher priority to supply the load. If the system load is more than the power obtained from the WTGs, the unmet load is supplied using DEGs. If there is excess power available from the WTGs, the excess power is used to supply a heating load. Various output parameters from the wind-diesel hybrid power system model include: the power available from WTGs (kW), total fuel consumed in liters (gallons), total cost of fuel (USD), total CO_2 emitted in metric tons (US tons), total NOx emitted in kg (pounds), and total PM_{10} emitted in kg (pounds). These output parameters are used to calculate the COE, the pay back period of the WTGs, the life cycle cost of the system, and the avoided cost of various pollutants.

Fig. 3-6 shows the flow-chart algorithm of the wind-diesel hybrid power system model.

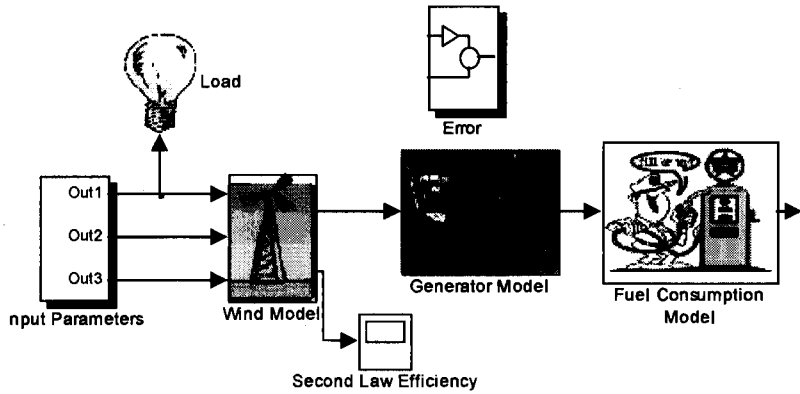

Fig. 3-5. Wind-diesel hybrid power system model.

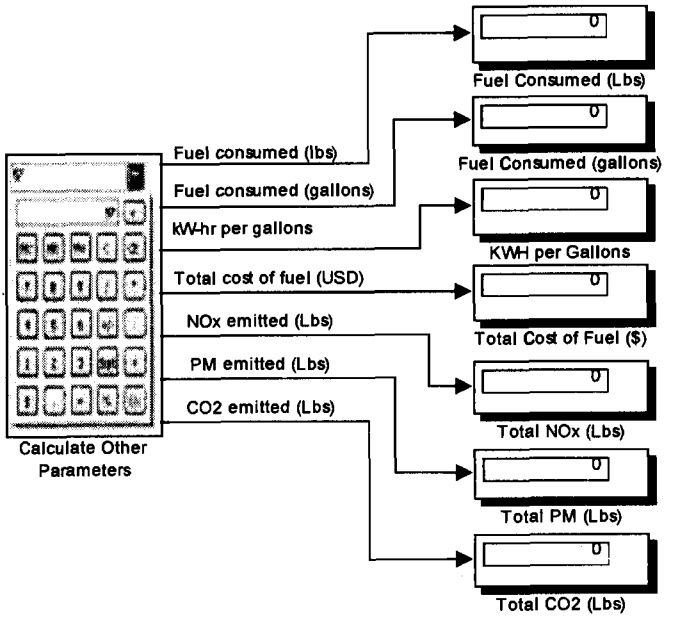
Fuel consumed (lbs)
Fuel consumed (gallons)
kW-hr per gallons
Total cost of fuel (USD)
NOx emitted (Lbs)
PM emitted (Lbs)
CO2 emitted (Lbs)
Calculate Other Parameters
0
Fuel Consumed (Lbs)
0
Fuel Consumed (gallons)
0
KWH per Gallons
0
Total Cost of Fuel ($)
0
Total NOx (Lbs)
0
Total PM (Lbs)
0
Total CO2 (Lbs)

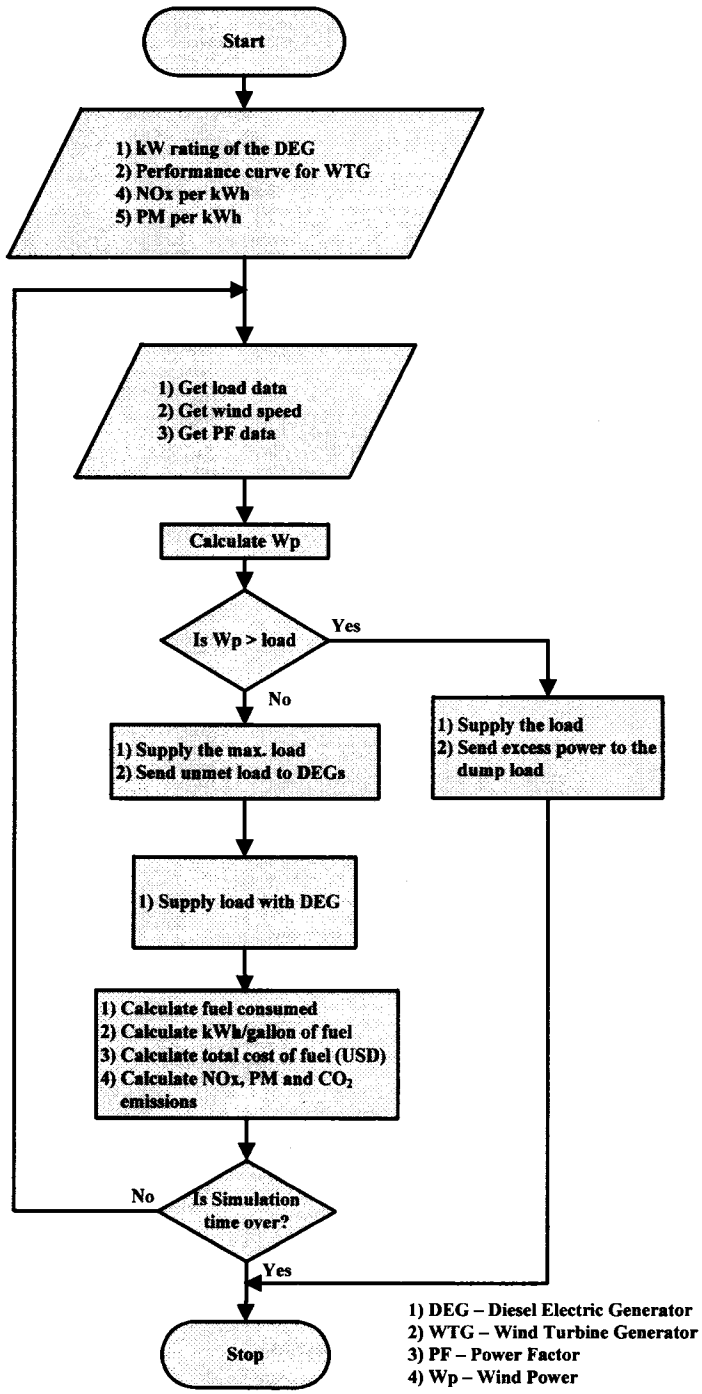

Fig. 3-6. Flow-chart algorithm for the wind-diesel hybrid power system.

3.4 Wind-Diesel-Battery Model

Fig. 3-7 shows the Simulink® model for the wind-diesel-battery hybrid power system model. The model consists of WTGs, a battery bank, and DEGs as sources of electrical energy.

In a wind-diesel-battery hybrid power system, the WTGs have the highest priority to supply the load. If the load is not met using power from the WTGs, the unmet load is supplied by the battery bank. When the battery bank is discharged, DEGs supply the unmet load and charge the battery bank simultaneously. Various output parameters from the wind-diesel-battery hybrid power system include: the power obtained from the WTGs (kW), total fuel consumed in liters (gallons), total cost of fuel (USD), total CO_2 emitted (metric tons), total NOx emitted in kg (pounds), and total PM_{10} emitted in kg (pounds). These output parameters can be used to calculate the life cycle cost, the COE, the pay back period of the WTGs, and the avoided cost of pollutants for the system.

Fig. 3-8 shows the flow chart algorithm for the wind-diesel-battery hybrid power system.

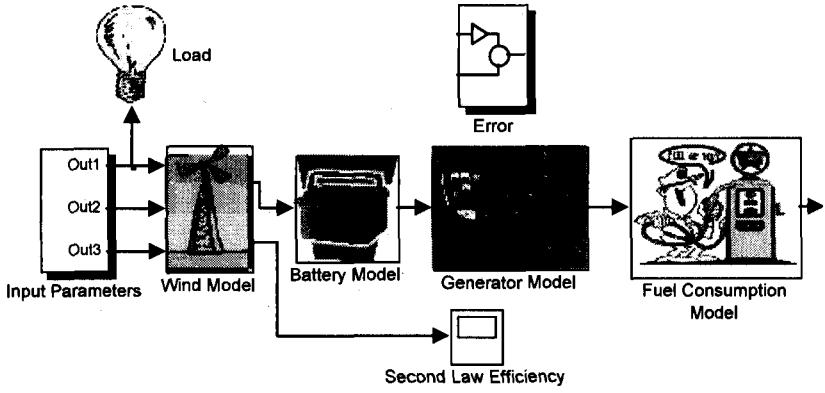

Fig. 3-7. Wind-diesel-battery hybrid power system model.

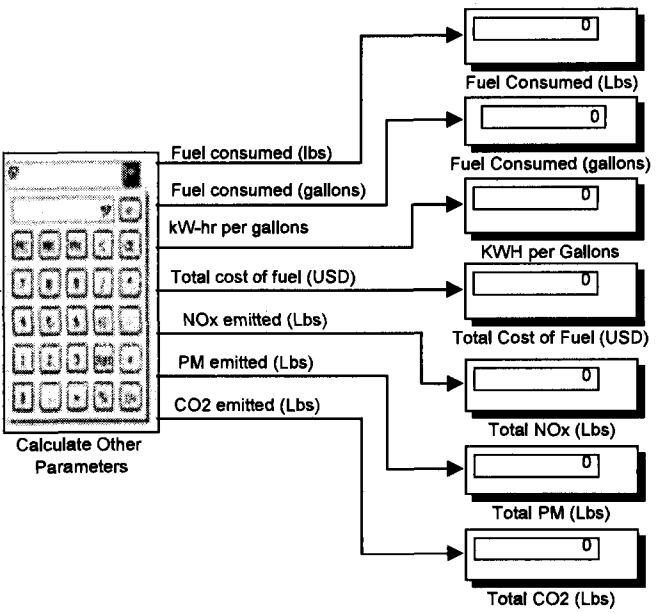
Fuel consumed (lbs)
Fuel consumed (gallons)
kW-hr per gallons
Total cost of fuel (USD)
NOx emitted (Lbs)
PM emitted (Lbs)
CO2 emitted (Lbs)
Calculate Other Parameters
0
Fuel Consumed (Lbs)
0
Fuel Consumed (gallons)
0
KWH per Gallons
0
Total Cost of Fuel (USD)
0
Total NOx (Lbs)
0
Total PM (Lbs)
0
Total CO2 (Lbs)

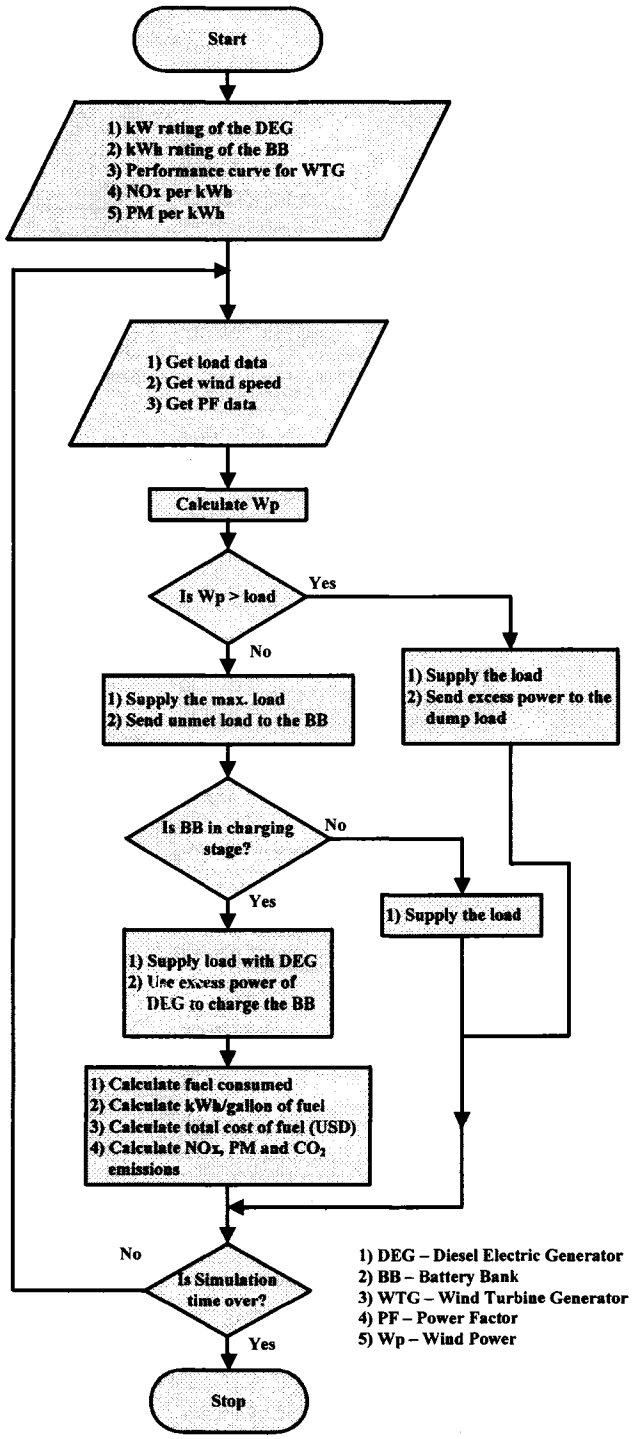

Fig. 3-8. Flow-chart algorithm for the wind-diesel-battery hybrid power system.

3.5 PV-Wind-Diesel-Battery Model

Fig. 3-9 shows the Simulink® model for the PV-wind-diesel-battery hybrid power system. The electrical energy sources in the model include a PV array, WTGs, a battery bank, and DEGs.

In a PV-wind-diesel-battery system, the PV array and the WTGs have the highest priority to supply the load. If there is extra power available from the PV array and the WTGs, the extra power is sent to the resistive/dump load. If the load is not met entirely by the PV array and WTGs, the unmet load is fed by the battery bank. When the battery bank is discharged, DEGs supply the unmet load and charge the battery bank simultaneously. Various output parameters from the model include: the second law efficiency of the WTGs (%), the power supplied by the WTGs (kW), the power supplied by the PV array (kW), total fuel consumed in liters (gallons), total fuel cost (USD), total CO_2 emitted (metric tons), total NOx emitted in kg (pounds), and total PM_{10} emitted in kg (pounds). These output parameters are used to calculate the life cycle cost, the COE, the payback period for the PV array and the WTGs, and the avoided cost of pollutants.

Fig. 3-10 shows the flow-chart algorithm for the PV-wind-diesel-battery hybrid power system.

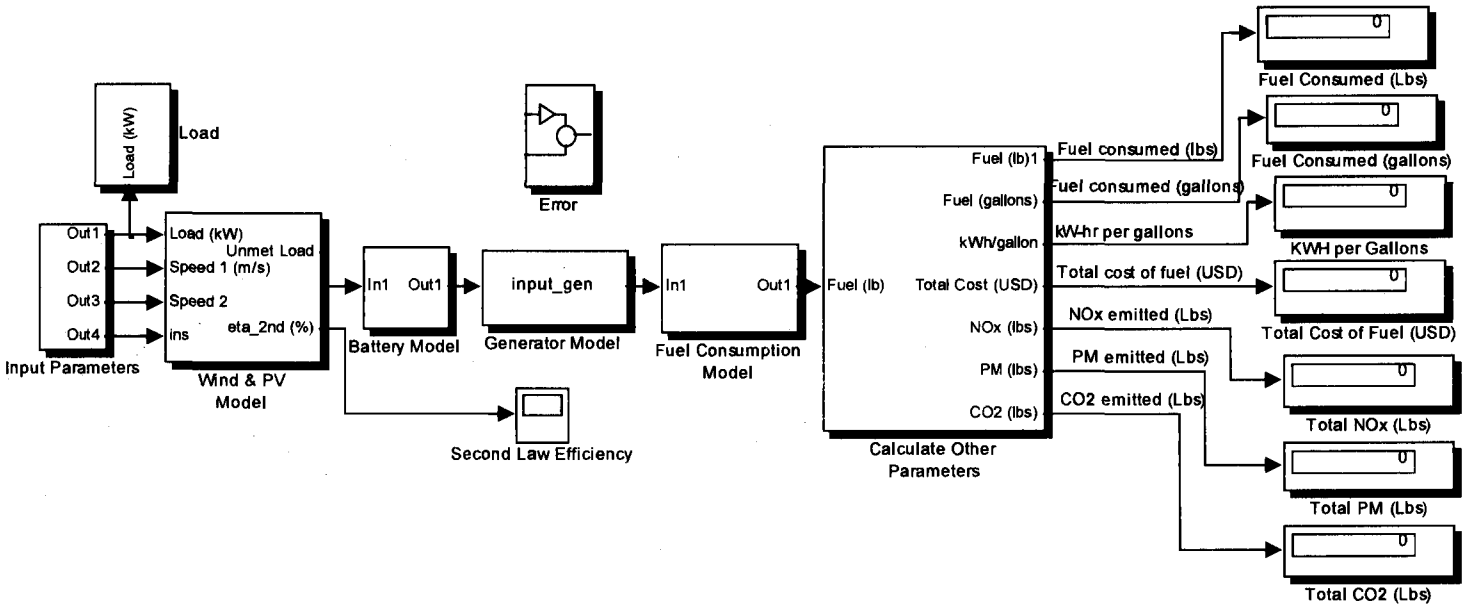

Fig. 3-9. PV-wind-diesel-battery hybrid power system model.

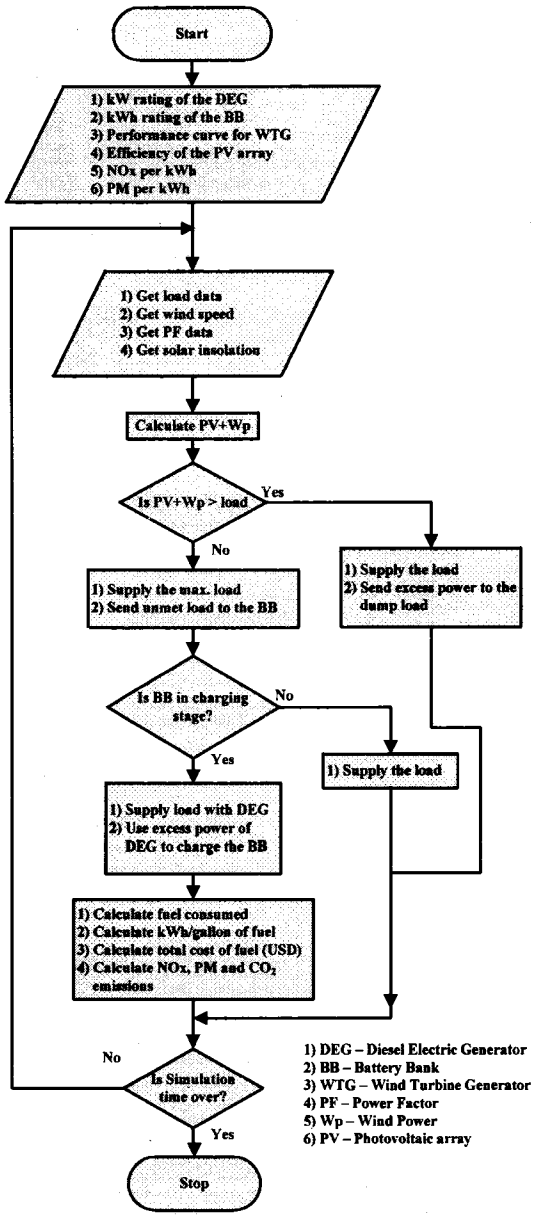

Fig. 3-10. Flow-chart algorithm for the PV-wind-diesel-battery hybrid power system.

3.6 Graphical User Interface of Hybrid Power System

A graphical user interface (GUI) called Hybrid Arctic Remote Power Simulator (HARPSim) was developed for various hybrid power system models using MATLAB® Simulink®. The front-end of the HARPSim GUI is shown in Fig. 3-11.

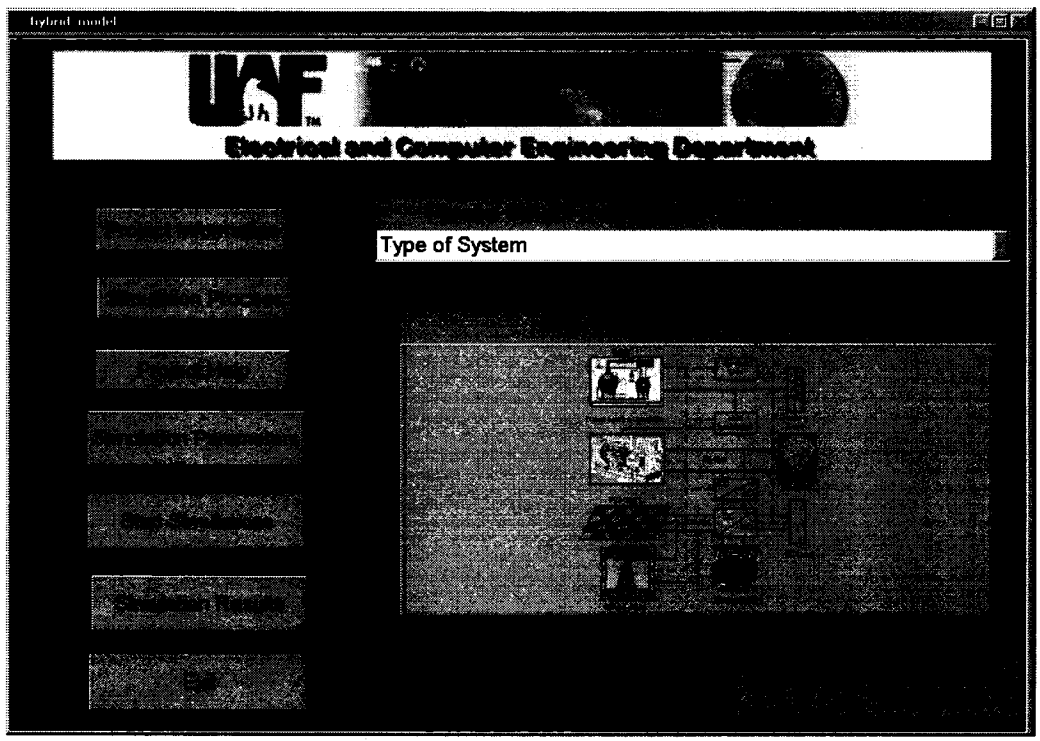

Fig. 3-11. Front-end of the HARPSim model.

Currently, HARPSim incorporates three case studies in the drop down menu labeled as 'Type of System': (1) Diesel-only system with heat recovery (UAF Energy Center), (2) PV-diesel-battery system (Lime Village, Alaska), and (3) Wind-diesel-battery system (Wales Village, Alaska). The users also have a choice to design and study any other system, consisting of one or more combinations of a DEG, a battery bank, a PV array, and a WTG. The functions of different push-buttons on the front-end of HARPSim are explained as follows:

(a) Project Information:

The 'Project Information' button is used to direct the user to the project webpage from where the user can find the detailed information about the project. If the user does not have access to the internet, the program will automatically divert to the project information page saved in the current folder.

(b) Simulation Process:

The 'Simulation Process' button describes the detailed procedure to be followed to perform the simulation. The user can obtain information about how to change simulation parameters to the advanced level. In the advanced level, the user can change the performance curves of the DEGs and the WTGs, change fuel parameters, change the optimal point of operation for the DEGs, and the simulation time period.

(c) Project Help:

The 'Project Help' button is used to answer the 'frequently asked questions' (FAQs) about the HARPSim model. The user can get help on various topics from the FAQs section. Examples of help files include: the default value of fuel density, the fuel price, environmental pollutants, and the different equations involved in the calculation process. The user can also get information on how to change the above parameters.

(d) Simulation Parameters:

The 'Simulation Parameters' button gives the user control of the simulation parameters. From here the user can change various parameters like the rating of a DEG and the battery-bank, the efficiency of the PV array, the simulation time-step, and the power factor. Fig. 3-12 shows the screenshot of the 'Simulation Parameters' window for the DEG system installed at the UAF Energy Center,

discussed in Section 4.2. The user can study the effect of varying these parameters and thus can optimize the system.

(e) Start Simulation:

The 'Start Simulation' button is used to start the simulation. Once the button is pressed, the Simulink® model of the selected system is opened and the simulation begins. At the end of the simulation, a window showing the real time required for the simulation appears.

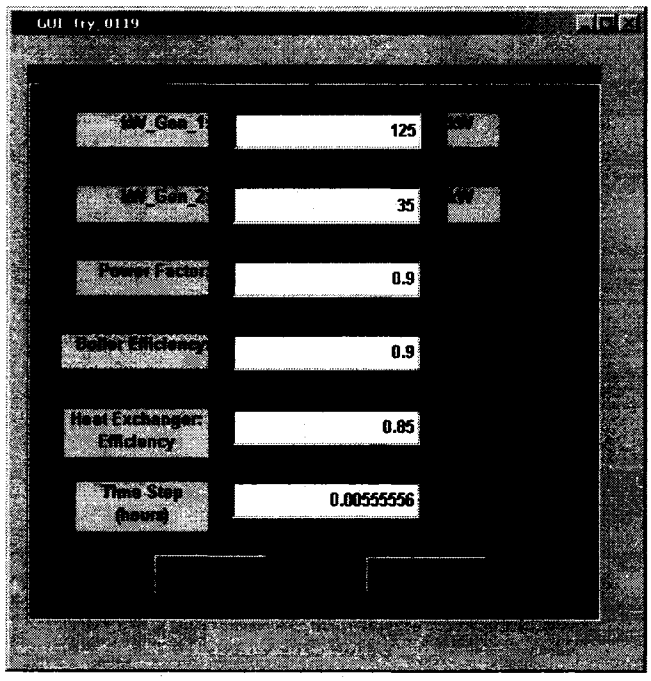

Fig. 3-12. Screenshot for the 'Simulation Parameters' for the DEG system of UAF Energy Center

(f) Simulation Results:

The 'Simulation Results' button is used to view the simulation results. The user has the option to view results as plots or export results to an EXCEL file. Fig. 3-13 shows the screenshot of the 'Simulation Results' window.

Fig. 3-13. Screenshot for the 'Simulation Results' for DEG system of UAF Energy Center

While this chapter described the development of various hybrid power system models, Chapter 4 will validate various components of a hybrid power system. In order to validate a hybrid power system component, the component model will be tested using the HOMER software. The results obtained from the HARPSim model will be compared with those obtained from the HOMER software for the simulated load profile.

4 Validation of Hybrid Power System Model Components

Chapter 3 described the development of various hybrid power system models. It is important to validate the hybrid power system components before they can be used to study the performance of the actual system. In this chapter, the different hybrid power system components of HARPSim are validated. These components include a DEG model, a WTG model, and a PV model.

The validation process for the DEG model involves the comparison of results obtained from HARPSim with those obtained from the HOMER software. The validation process for the WTG model and the PV model involves the development of component models using the HOMER software and comparing the results obtained from HARPSim with those obtained from the HOMER software.

4.1 Data Collection and Pre-processing

The load profile used to validate the DEG model is synthetic data obtained using an EXCEL based simulator called 'Alaska Village Electric Load Calculator'. The 'Alaska Village Electric Load Calculator' was developed by the National Renewable Energy Laboratories (NREL) in 2004 [51]. Lack of electric load data availability for Alaskan Villages motivated the development of the 'Alaska Village Electric Load Calculator'. The data used in the development of the electric load calculator is the actual data collected from 50 remote Alaskan communities. These 50 communities are operated and maintained by a non-profit utility company named Alaska Village Electric Cooperative (AVEC).

The electric load analyses in the development of the 'Alaska Village Electric Load Calculator' involves the following steps:

1) The electric load of the 50 communities was divided into the following sectors: residential sector, schools, commercial sector, public water system, city/government buildings, communications facilities, and health clinic.
2) The electric use pattern of each sector was analyzed in detail based on the electric utility records.
3) The consumption pattern in various sectors was incorporated into the 'Alaska Village Electric Load Calculator'.
4) The energy consumption from each sector was normalized by the population of the community.
5) The 'Alaska Village Electric Load Calculator' adds up the load data from various sectors to generate the overall load profile.

The detailed analyses of each sector are available in an NREL report [51]. The report is available for downloading at http://www.nrel.gov/docs/fy05osti/36824.pdf.

Fig. 4-1 shows a 24-hour simulated load profile, with samples every 1-hour, obtained using the 'Alaska Village Electric Load Calculator'. This load profile was developed for a fictitious Alaskan village. The village population was then adjusted to give a maximum load of about 125 kW. The value of 125 kW for the maximum load was selected because the load profile was programmed into the controller which supplied the load on a 125 kW DEG, as described later in Section 4.2. It was observed that, with the village population of 170 people, the maximum load during the 24-hour period was 124.7 kW with the average load of about 80 kW.

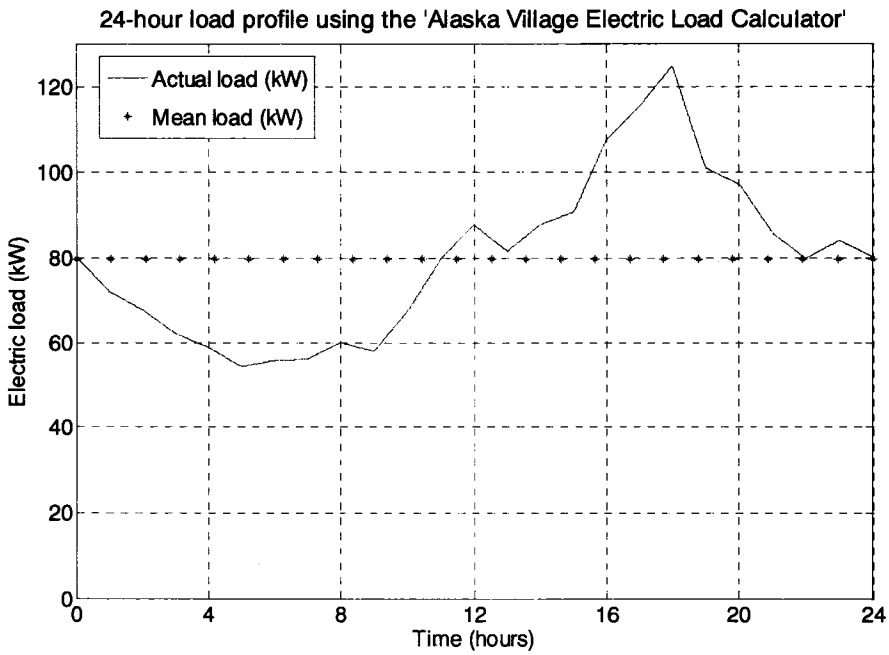

Fig. 4-1. 24-hour simulated load profile generated using 'Alaska Village Electric Load Calculator'.

The load profile and wind speed profile used to validate the wind turbine model was obtained from the data acquisition system installed at Wales Village, Alaska [8]. The data was collected at 15-minute intervals. In the Simulink® model, simulations are performed every minute. Therefore, in order to get data samples every minute, Simulink® performs the linear interpolation of the load data and the wind speed data. The linear interpolation is performed using the MATLAB® function 'linspace' as follows:

$$A = \text{linspace}(x1, x2, n) \tag{4-1}$$

where 'A' is the vector of length 'n' (each element representing the load data or wind speed at a given minute), 'x1' is the starting value, and 'x2' is the end value of the vector.

An example for 1 minute linear interpolation of 15 minute sampling for wind speeds of 10 m/s and 12 m/s is graphically shown in Fig. 4-2.

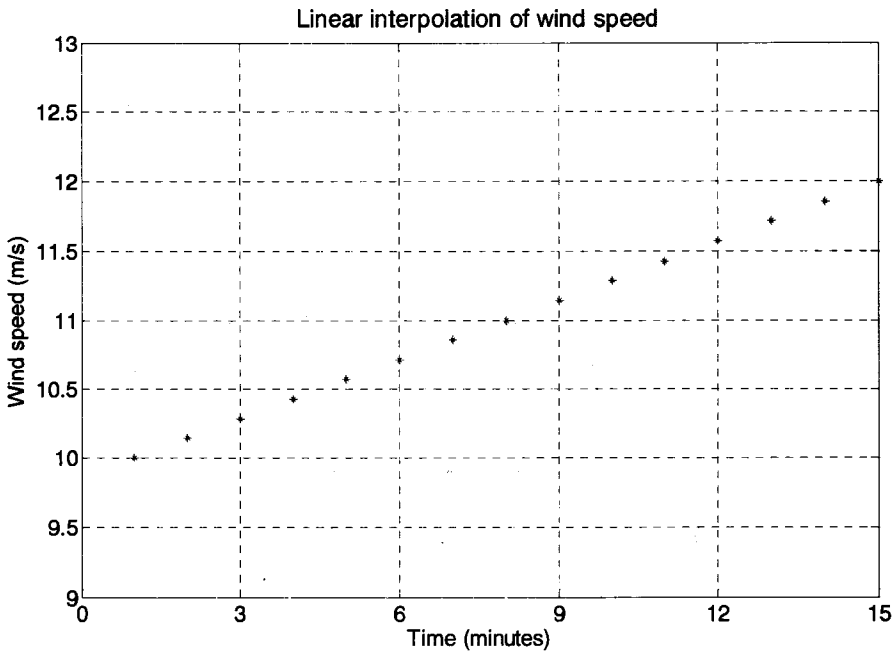

Fig. 4-2. Linear interpolation technique using MATLAB®.

The load profile and PV profile used to validate the PV model was obtained from the data acquisition system installed in the power system of Lime Village, Alaska. The load data available from Lime Village consists of a 24-hour summer load profile and a 24-hour winter load profile as shown in Fig. 4-3.

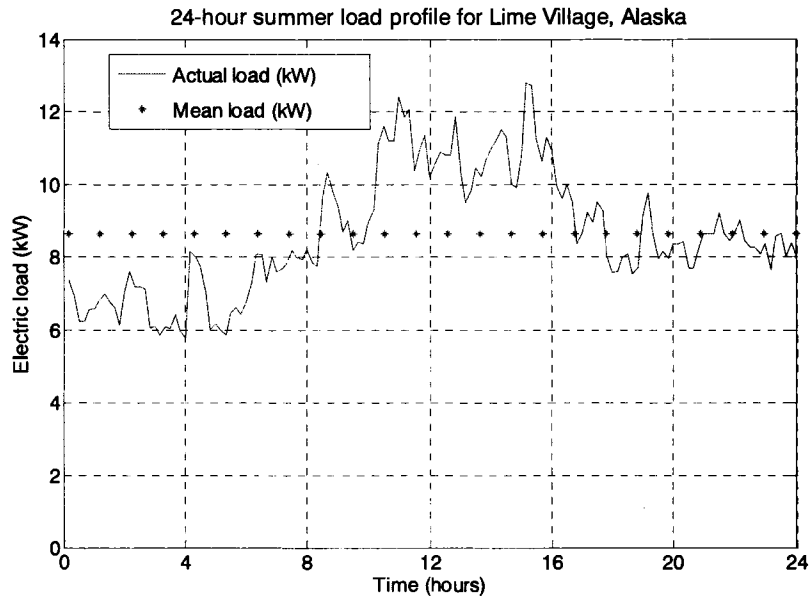

(a)

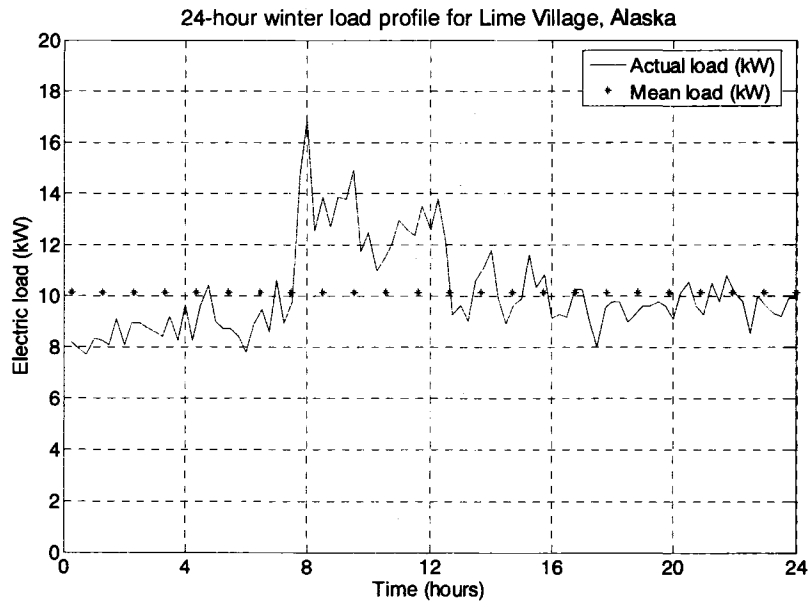

(b)

Fig. 4-3. 24-hour (a) summer load profile and (b) winter load profile for Lime Village, Alaska.

The 24-hour summer load data was collected from 06:38 am of July 11th, 2000 to 06:23 am of July 12th, 2000 with a sampling rate of 10 minutes and the 24-hour winter load data was collected from midnight of November 2nd, 2000 to the midnight of November 3rd, 2000 with a sampling period of 15 minutes. The 10 minute samples of the summer load profile and the 15 minute samples of the winter load profile are converted to 1 minute samples by means of linear interpolation using Simulink® as discussed earlier in this section. After obtaining the 1 minute samples for the summer load profile and the winter load profile, linear interpolation was performed to obtain the load data over the period of one year with samples every minute. In order to obtain the annual load profile it is assumed that the electric load is maximum on December 21st, the winter solstice, and minimum on June 21st, the summer solstice. The annual load profile and the second order polynomial fit to the load profile are shown in Fig. 4-4. The average daily data points are plotted in the figure.

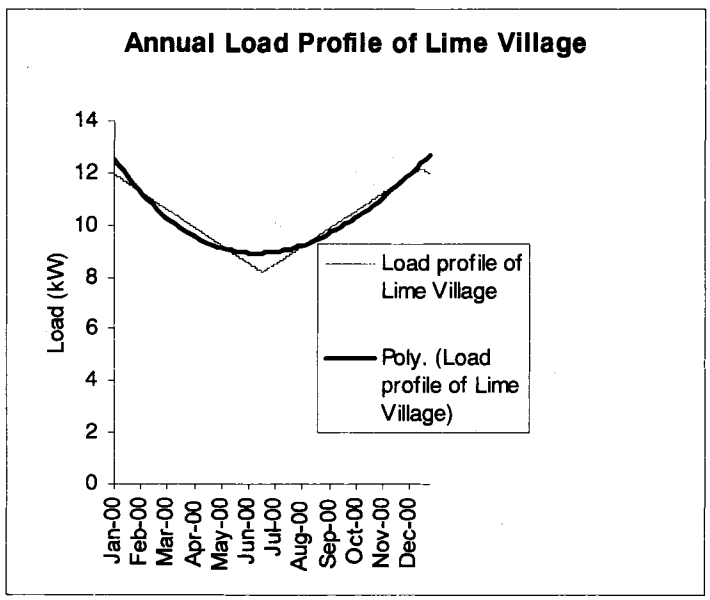

Fig. 4-4. Annual load profile for Lime Village, Alaska.

4.1.1 Synthetic Load Profile for Arctic Regions

If the annual minimum and the annual maximum load of the arctic community are known, a synthetic annual load profile can be generated for modeling purposes. The following steps are used to generate the annual synthetic load profile:

1. A typical arctic load profile consists of high load during winter months and low load during summer months. Therefore, the annual daily average load can be approximated by using a shifted sine wave.
2. Given the annual minimum and the annual maximum, the synthetic load profile can be generated by dividing the sine wave into 365 points (each point corresponding to the daily average load). The amplitude and the shift (both in x and y direction) of the sine wave are adjusted so that the maximum point of the sine wave occurs on December 21st (winter solstice) with the maximum load and the minimum point occurs on June 21st (summer solstice) with the minimum load.
3. A noise of suitable magnitude is added to this sine wave to represent the actual load profile.
4. The daily load profile of a typical village shows a shifted negative half of a sine wave from midnight to 8:00 am and a shifted positive half of a sine wave from 8:00 am to midnight the following day with a magnitude approximately equal to two times that of the shifted negative half of a sine wave.
5. The hourly noise is added to the daily load profile and the average value of the overall sine wave is adjusted so that it is the average daily load. A similar procedure is followed for the rest of the days.

Fig. 4-5 shows an annual hourly synthetic load profile for a typical arctic village. The maximum load of this village is 155 kW, the minimum load is 45 kW, the daily noise is 10 kW, and the hourly noise is 2 kW.

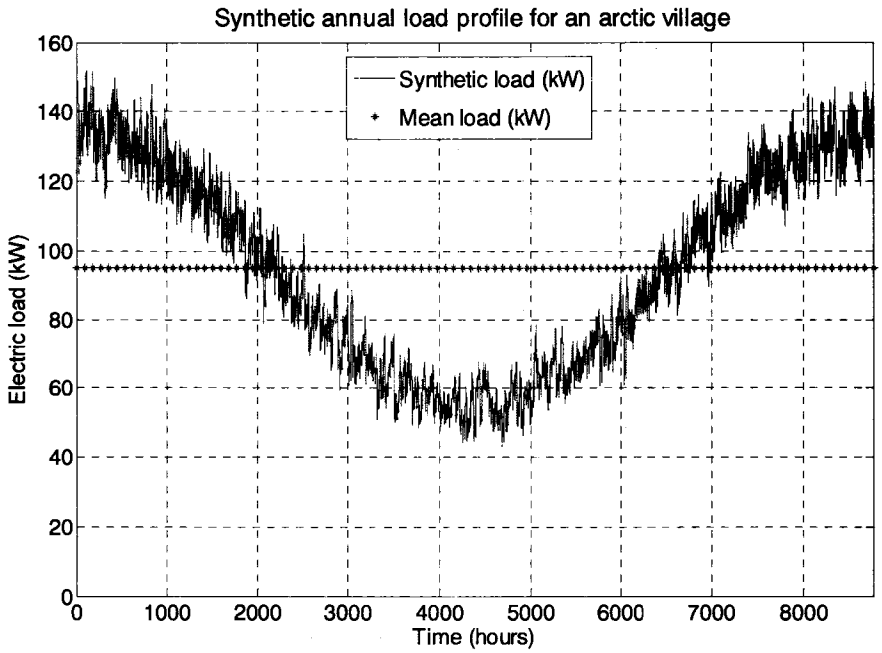

Fig. 4-5. Annual synthetic load profile for a typical arctic village.

4.1.2 Synthetic Wind Speed Profile for Arctic Regions

The annual hourly synthetic wind speed profile for an arctic community can be generated using the average annual wind speed and the exponential Gaussian noise as shown in the flowchart of Fig. 4-6. Fig. 4-7 shows the annual wind speed profile generated for an arctic village.

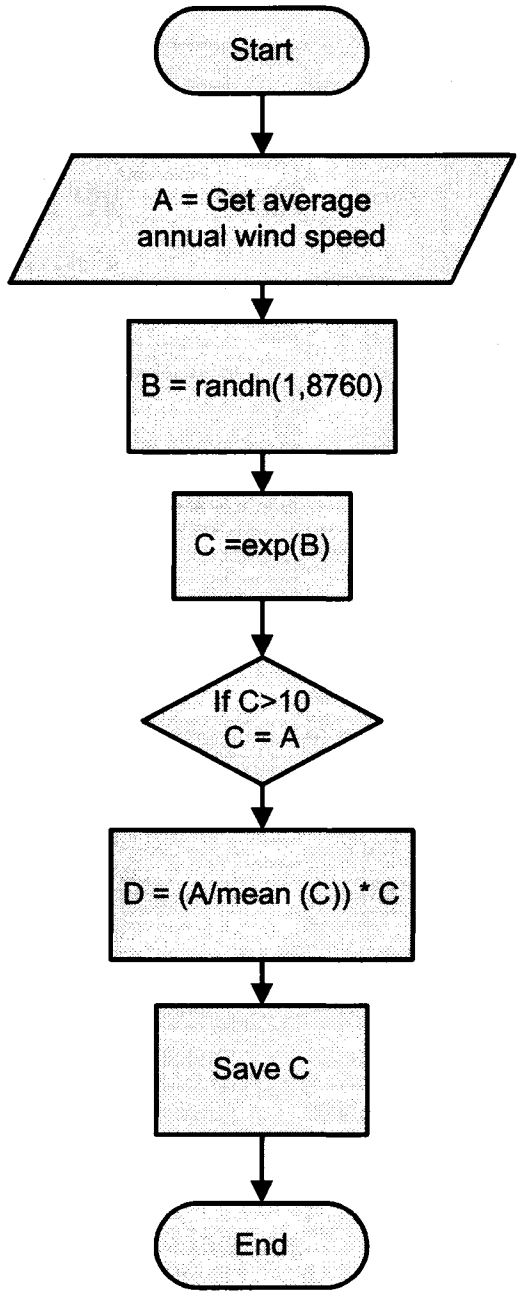

Fig. 4-6. Flowchart algorithm for annual wind speed.

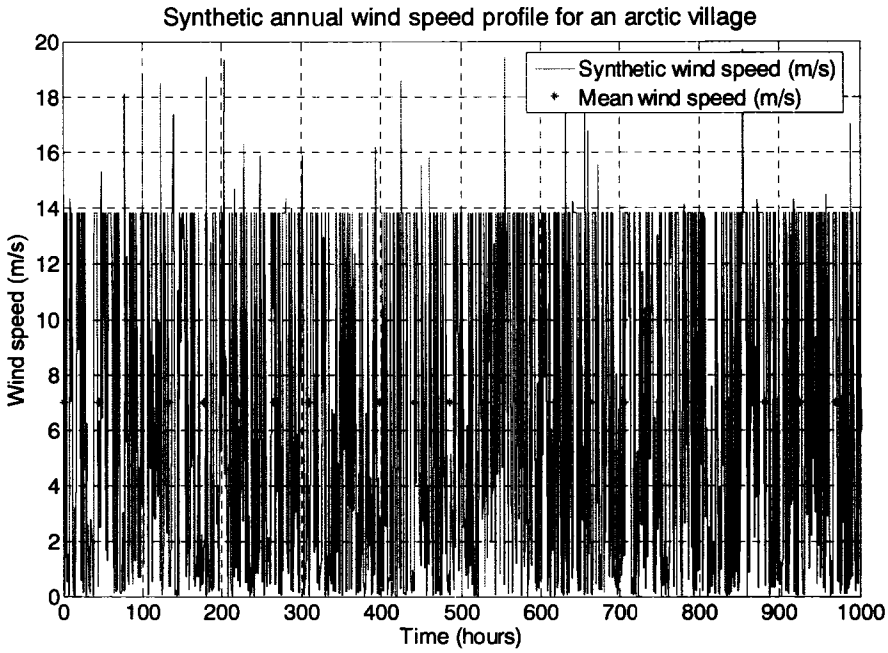

Fig. 4-7. Synthetic annual wind speed profile for an arctic village.

4.1.3 Synthetic Solar Flux for Arctic Regions

The annual hourly solar flux for any location on the earth on the top of the atmosphere can be obtained as described in [52] as follows:

$$Q = S_0 \left(\frac{\bar{d}}{d} \right)^2 \cos\theta_s \tag{4-2}$$

where 'Q' is the hourly solar flux, S_0 is the maximum solar flux on the earth and taken as 1367 W/m^2 , 'd_bar' is the mean distance for which the flux is measured, 'd' is the actual distance from the sun, and θ_s is the solar zenith angle that depends on the latitude of the place, the hour of the day and the time of the year. The solar zenith angle is given as follows:

$$\cos\theta_s = \sin\varphi \sin\delta + \cos\varphi \cos\delta \cos h \qquad (4\text{-}3)$$

where 'φ' is the latitude of the location, 'δ' is the declination angle which depends on the day of the year, and 'h' is the hour of the day.

An annual hourly solar flux profile for an arctic village is shown in Fig. 4-8.

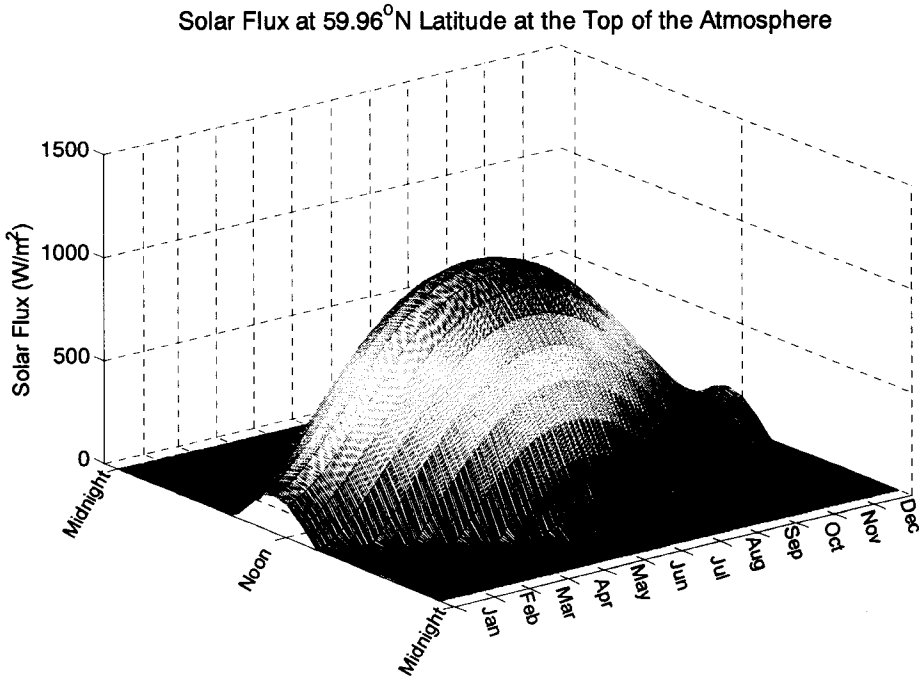

Fig. 4-8. Annual solar flux for a arctic village.

The actual solar flux available on the earth's surface can by obtained by multiplying the above solar flux by the clearness index. The clearness index is the ratio of the amount of sunlight reaching the earth's surface to the amount of sunlight available on the top of the atmosphere. The various factors affecting the clearness index are clouds, aerosols, and the moisture content of the air. The values of clearness index can by obtained from the solar maps developed at NREL.

4.2 Validation of the Diesel Electric Generator Model

In order to validate the DEG model in HARPSim, the results obtained from the actual DEG system installed at the UAF Energy Center were compared with the results obtained from HARPSim and the HOMER software. The main objective of the DEG system installed at the UAF Energy Center is to study the feasibility of using alternate fuels like bio-diesel, syntroleum fuel, and fish oil with DEGs installed in remote Alaskan communities. The DEG system installed at the UAF Energy Center consists of a 125 kW Detroit Series 50 DEG, a 125 kW resistive load bank, various flow meters, a number of sensors, a Nexus 1252 remote terminal unit (RTU), a bulk fuel storage tank, a day fuel storage tank, a generator housing, and various control equipment. The details of the DEG system installed at UAF Energy Center are available in [53].

A 24-hour simulated load profile was supplied to the DEG system installed at the UAF Energy Center with the help of a controller. Fig. 4-9 shows a 24-hour simulated load profile with a 10 second sampling time supplied to the DEG system.

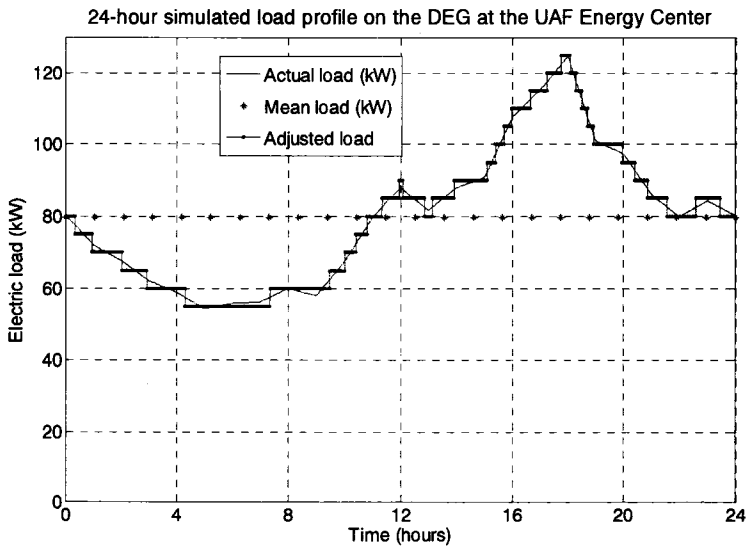

Fig. 4-9. 24-hour simulated load profile on the DEG at the UAF Energy Center.

The control unit which feeds the load to the DEG is designed with load steps of 5 kW. Therefore, the actual load profile was adjusted to obtain a load profile with a step size of 5 kW. The fuel used for the DEG system is syntroleum fuel with a heating value of 9.408 kWh/liter (121,500 BTUs/gallon) (1 kWh = 3412 BTUs).

Fig. 4-10 shows the HOMER model for the 125 kW DEG installed at UAF Energy Center. The HOMER model consists of a DEG and a primary load.

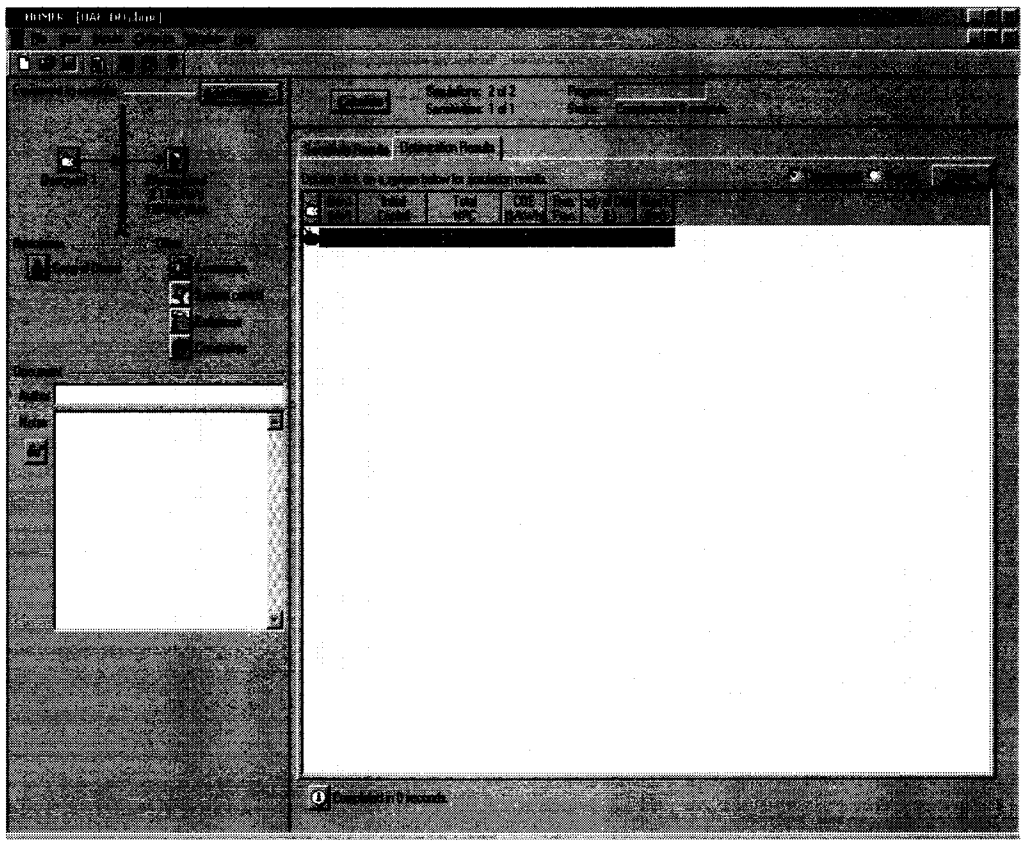

Fig. 4-10. HOMER model for the 125 kW DEG installed at UAF Energy Center.

Simulations were performed using HARPSim for the DEG system using the 24-hour adjusted load profile shown in Fig. 4-9. TABLE 4-1 shows the comparison of results obtained from the Nexus RTU, HARPSim, and the HOMER model.

TABLE 4-1. Simulation results from HARPSim model

Parameter	**Results from RTU**	**Results from HOMER**	**Results from HARPSim**	
			Results (η_{el} = 92.2%)	**Results (η_{el} = 89.5%)**
Load energy (kWh)	2123	2123	2123	2123
Fuel consumed in liters (gallons)	631.26 (167)	627.93 (166.12)	624.83 (165.3)	638.82 (169)
Efficiency of engine (kWh/gallon)	3.36 (12.71)	3.38 (12.788)	3.40 (12.84)	3.33 (12.57)
Total cost of fuel (USD)	334	332.24	330.7	338
NOx emitted in kg (lbs)	18.47 (40.71)	-	18.28 (40.30)	18.69 (41.2)
PM_{10} emitted in kg (lbs)	0.78 (1.716)	-	0.77 (1.694)	0.79 (1.732)
CO_2 emitted in kg (lbs)	1665.59 (3672)	1615.36 (3561.25)	1648.65 (3634.64)	1685.55 (3716)
Heat energy recovered (kWh)	401.9	-	401.9	401.9
Boiler fuel saved liters (gallons)	47.4 (12.54)	-	47.4 (12.54)	47.4 (12.54)
Cost of boiler fuel saved (USD)	25.07	-	25.07	25.07
NOx avoided in kg (lbs)	3.54 (7.796)	-	3.54 (7.796)	3.54 (7.796)
PM_{10} avoided in kg (lbs)	0.1487 (0.3278)	-	0.1487 (0.3278)	0.1487 (0.3278)
CO_2 avoided in kg (lbs)	318.97 (703.2)	-	318.97 (703.2)	318.97 (703.2)
% of fuel energy converted to electricity*	35.69%	32.6%	36.06%	35.27%
% of fuel energy recovered from jacket**	6.83%	-	6.83%	6.83%

*For syntroleum fuel with heating value of 9.408 kWh/liter (121,500 BTUs/gallon)
**Based on 85% heat exchanger efficiency

Data obtained from the Nexus RTU showed that the total fuel consumed was about 632 liters (167 gallons) for the 24-hour load profile. The fuel consumed using HARPSim was about 1.2% more at 639 liters (169 gallons) if the electrical efficiency values are used from the available performance curve for a 35 kW generator. The average electrical efficiency obtained is about 89.5%. With the increase in the size of the generator, the electrical efficiency of the generator increases. Therefore, for a 125 kW generator the electrical efficiency will be more than that for a 35 kW generator. If this increase in efficiency is accounted for in HARPSim, the fuel consumption by the DEG system using HARPSim will decrease. It was observed that an improvement of 3% in the electrical efficiency (92.2%) reduced the fuel consumption to 625 liters (165 gallons) from 639 liters (169 gallons) which is about 1% less than that obtained from the Nexus RTU. The actual electrical efficiency data for a 125 kW generator could not be obtained from the manufacturer.

Further analysis was carried out on this work to obtain a simple payback period for the heat exchanger. In order to calculate the total cost of the heat exchanger, the cost of different heat exchanger components was obtained from [54] and inflated to reflect today's prices. The actual price for a shell and tube type heat exchanger was obtained from [55]. The costs of the various heat exchanger components are shown in TABLE 4-2.

The simple payback period for the heat exchanger is calculated as follows:

$$PBP = \frac{P}{S} \tag{4-4}$$

where 'PBP' is the payback period for the heat exchanger, 'P' is the extra spending in the installation of the heat exchanger, and 'S' is the rate of saving (USD) due to the saving in fuel from the recovered heat.

$$\therefore \text{PBP} = \frac{17{,}284 \text{ USD}}{25.07 \text{ USD/day}} = 689.4 \text{ days} = 1.89 \text{ years}.$$

TABLE 4-2. Component cost of heat exchanger

Heat Exchanger Component	Cost (USD)
(Shell & tube type)* (250,000 BTU/hr)	642 USD
Unit Heaters	600 USD
Expansion Tank	100 USD
Pumps	300 USD
Control Valves	2,000 USD
Piping	2,500 USD
Shipping	2,500 USD
Net	8,642 USD
Installation & Labor	8,642 USD
Gross Total	17,284 USD

The results obtained from the HARPSim model were is close agreement with the results obtained from the Nexus RTU and the HOMER software. Therefore, the DEG model developed in HARPSim can be used to study the performance of other systems.

4.3 Validation of the Wind Model

In order to validate the wind model in HARPSim, the total wind power obtained from HARPSim, based on a given wind speed profile over the period of one year, was compared with the total wind power obtained using the HOMER software, for the same wind profile. Fig. 4-11 shows the wind profile used for the simulation to validate the wind model block. These wind speed data are the actual wind speed values recorded at Wales Village from August 1st, 1993 to July 31st, 1994. The average wind speed over the one year period was observed as 8.45 m/s.

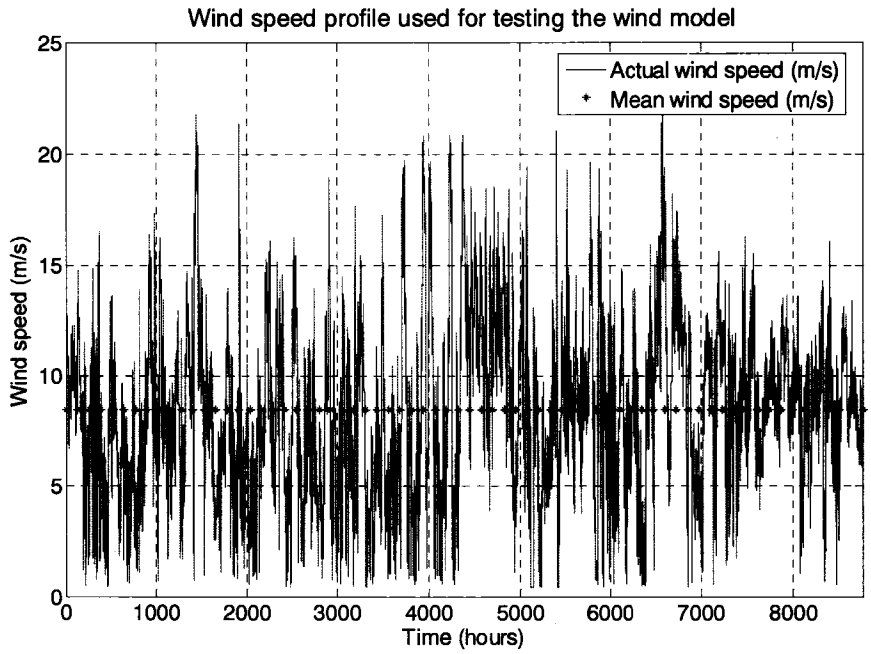

Fig. 4-11. Annual wind speed profile used to validate the wind model.

Fig. 4-12 shows the Simulink® model for validating the wind model block. The total electrical energy produced for the given wind speed profile over the one year period using the Simulink® model was observed as 235,219 kWh.

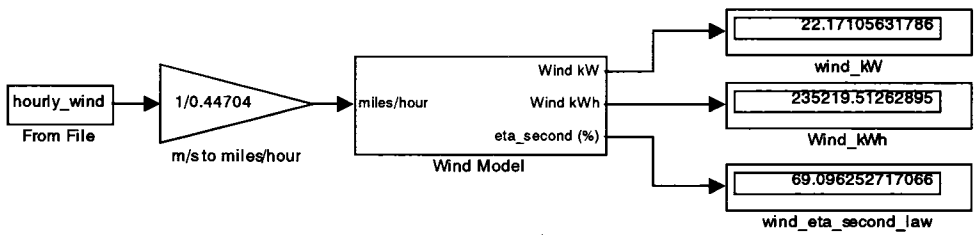

Fig. 4-12. Simulink® model for validating the wind model block.

Fig. 4-13 shows the HOMER model developed for validating the wind model block.

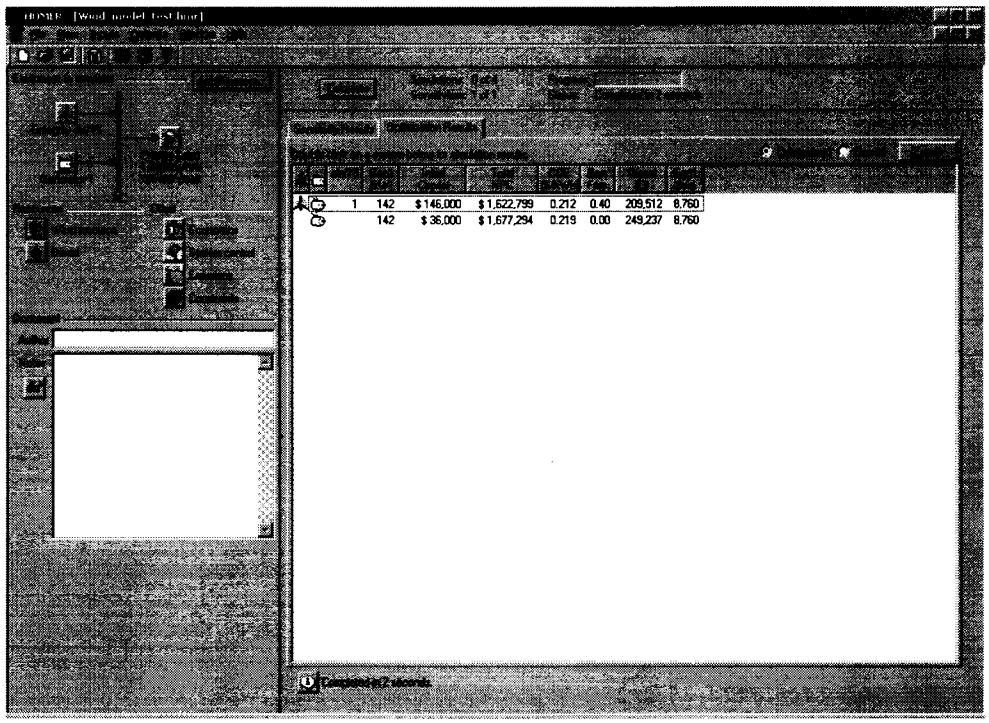

Fig. 4-13. Screenshot of the HOMER model for validating the wind model block.

HOMER does not calculate the power available from the WTG unless the electric load is connected. Therefore, a hybrid power system model consisting of a WTG, a DEG, and an electric load is used in HOMER. It should be noted that the hybrid power system in HOMER is used only to check the total power available from the WTG. Therefore, a DEG or any other source of electricity in conjunction with the WTG is used to supply the load. To validate the wind model block, the power obtained from the WTG using HOMER is compared with the power obtained using HARPSim.

The total electrical energy produced for the annual wind speed profile using the HOMER model was 295,699 kWh. It was observed that the total electrical energy produced for the annual wind profile using the HOMER model was about 20% more than that obtained from HARPSim. The wind power in HOMER is partly based on the look-up table that gives the electrical power output depending on the wind speed data. In order to find the energy output over the period of one year in the HOMER model, a second Simulink® model was developed for the WTG based on the look-up table data. The look-up table data for power output from the WTG obtained from HOMER is given in TABLE 4-3.

The second Simulink® model for the WTG uses the look-up table versus the fifth order polynomial given by Eq. (2-11) to calculate the total electrical energy. The second Simulink® model for the WTG, based on the look-up table data, is shown in Fig. 4-14.

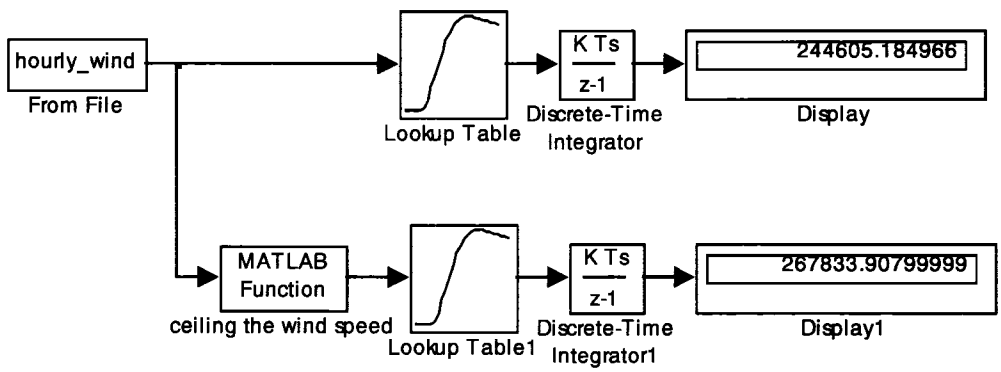

Fig. 4-14. Simulink® model for the WTG to validate the HOMER model.

TABLE 4-3. Look-up table for power output in HOMER

Wind speed (m/s)	Power output (kW)
0	0
1	0
2	0
3	0
4	0
5	1.8
6	7.8
7	15.9
8	24.0
9	32.4
10	41.3
11	48.1
12	53.8
13	58.9
14	62.1
15	64.1
16	64.5
17	65.1
18	64.4
19	63.9
20	63.6
21	62.7
22	61.8
23	60.9
24	60.0
25	59.1

The total annual electrical energy obtained from the WTG using the look-up table in the Simulink® model for the annual wind profile was 244,605 kWh. This value is about 3.8% more than that obtained using the fifth order polynomial fit in the Simulink® model. The results from the second Simulink® model for the WTG show that there are some other parameters in HOMER, besides the look-up table, on which the electrical power output from the WTG depends. These parameters include: the hub height, the altitude of the location, the anemometer height, the Weibull distribution factor, the autocorrelation factor, the diurnal strength of wind, and the hour of peak wind speed. In HOMER the wind speeds are entered as average monthly values. HOMER uses this average monthly wind speeds and the Weibull distribution to predict the hourly wind speed. The Weibull distribution factor describes the variation of wind speed depending on two characteristics, the shape parameter and the scale parameter, of the annual wind speed curve [41].

4.4 Validation of the PV Model

In order to validate the PV model, the total power obtained from the PV model block in HARPSim was compared with the total power obtained from the PV model developed using the HOMER software for the same solar insolation values. The solar insolation values were selected for Wales Village, Alaska located at 65.60917° north latitude and 168.0875° west longitude. The solar insolation values were imported in the HOMER model from the Surface Meteorology and Solar Energy (SSE) model developed by NASA [56]. Fig. 4-15 shows the simulated annual solar insolation values from January 1st to December 31st for Wales Village as obtained from the SSE model.

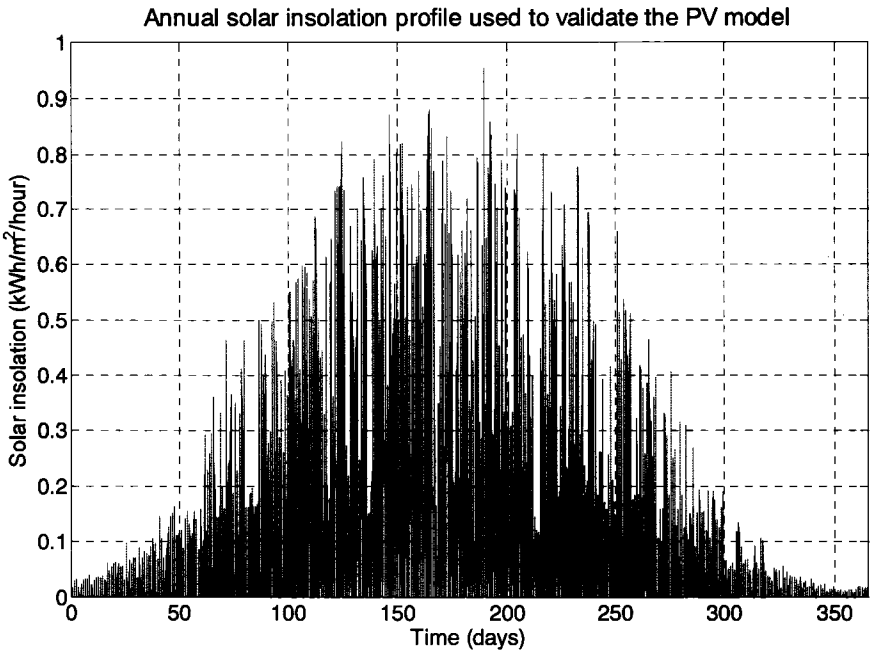

Fig. 4-15. Annual solar insolation profile used to validate the PV model.

Fig. 4-16 shows the Simulink® model for validating the PV model block. The rating of the PV array was selected as 30 kW with a panel efficiency of 17%. The total electrical energy produced for the given solar insolation profile using the Simulink® model was 29,288 kWh over the one year period.

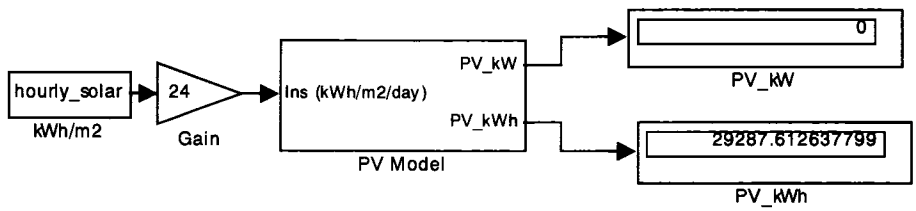

Fig. 4-16. Simulink® model for validating the PV model block.

Fig. 4-17 shows the HOMER model developed for validating the PV model block.

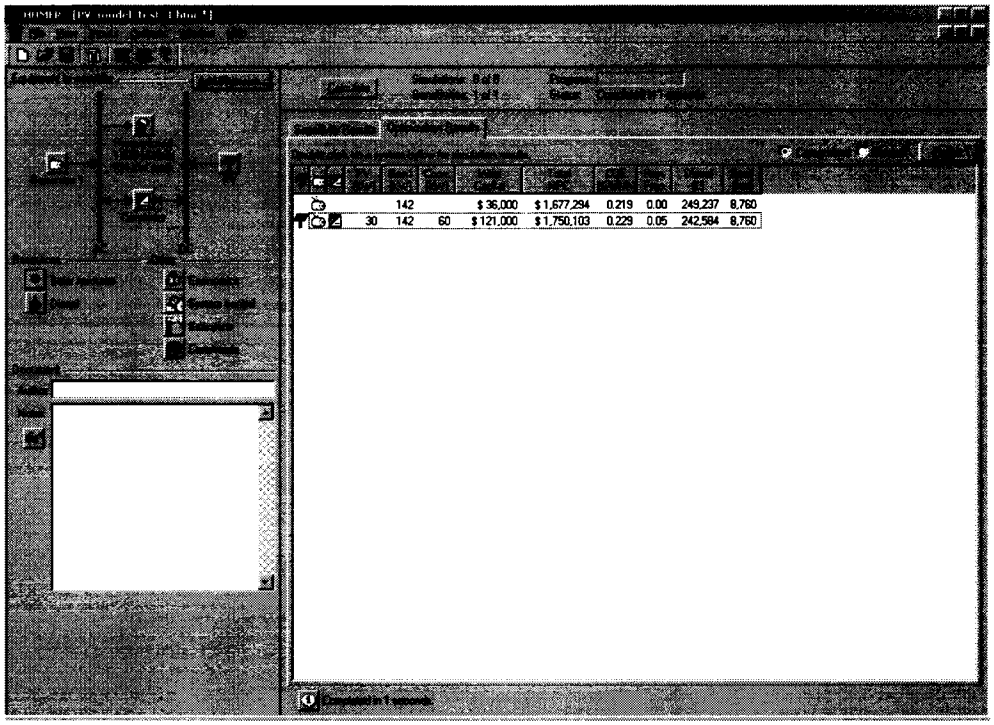

Fig. 4-17. Screenshot of the HOMER model to validate the PV model.

HOMER does not calculate the power available from the PV array unless the electrical load is connected. Therefore, to validate the PV model block, a hybrid power system model consisting of a PV array, a power converter, a DEG, and an electric load is used in HOMER. The total PV power obtained using HARPSim was then compared with the total PV power obtained using HOMER, for the same solar insolation values.

The total electrical energy produced for the given solar insolation profile using the HOMER model was 30,951 kWh. It was observed that the total electrical energy produced for the annual solar insolation profile using the HOMER model was about 5.4% more than that obtained from the Simulink® model. In the HOMER model the total electrical energy produced is calculated as follows:

$$P_{PV} = f_{PV} * Y_{PV} * \frac{I_T}{I_s} \quad (4\text{-}5)$$

where P_{PV} is the power obtained from the PV array, f_{PV} is the PV derating factor, Y_{PV} is the PV array capacity, I_T is the solar radiation incident on the PV array, and I_s is the standard amount of radiation used to rate the capacity of PV modules which is 1 kW/m^2.

The power obtained from the PV array in the Simulink® model is partly based on the efficiency of the solar panels. Increasing the efficiency of the PV array will result in an increase in power obtained from the PV array.

In this chapter the various components of the HARPSim model were validated. The results obtained for the DEG model developed in HARPSim were in close agreement with those predicted by HOMER and the experimental values obtained from the Nexus RTU. The power obtained from the wind model block and the PV model block developed in HARPSim were in close agreement with the power obtained from the wind model block and the PV model block developed using the HOMER software, respectively.

While this chapter validated the various components of the HARPSim model, Chapter 5 will describe the use of the HARPSim model to study the performance of the wind-diesel-battery hybrid power system installed at Wales Village, Alaska, the PV-diesel-battery hybrid power system installed at Lime Village, Alaska, and the design of a PV-wind-diesel-battery system for Kongiganak Village, Alaska.

5 Results and Discussions

In Chapter 4, various components of the HARPSim model were validated. The validation process of the DEG model involved the comparison of results for the UAF Energy Center DEG system from HARPSim with the experimental data and the HOMER model. The validation process for the WTG and the PV model involved the comparison of the power obtained from the WTG and the PV array with those predicted by the HOMER software for the same wind speed and solar insolation.

In this chapter, the validated model components are used to study the performance of three different hybrid power systems:

1) The wind-diesel-battery hybrid power system for Wales Village, Alaska.
2) The PV-diesel-battery hybrid power system for Lime Village, Alaska.
3) The design of a PV-wind-diesel-battery system for Kongiganak Village, Alaska.

5.1 Wales Village Analysis

Wales Village is located at the tip of Seward Peninsula, about 111 miles northwest of Nome, Alaska, at a northern latitude of 65.60917° and western longitude of 168.0875° as shown in Fig. 5-1.

As per the US 2000 census, the area of Wales Village is about 2.8 square miles, with approximately 152 people, 50 households, and 28 residing families. There is one school attended by 49 students, and one local hospital – Wales Health Clinic [57]. The occupations of Wales Village residents include hunting, fishing, whale trapping, native arts and crafts, and mining [58]. The average summer temperature of Wales Village is about 40 °F to 50 °F and the average winter

temperature is about -10 °F to 6 °F, with an average annual precipitation of about 10 inches and annual snowfall of about 35 inches. Due to its coastal location, there is frequent fog and blizzards in Wales Village [58].

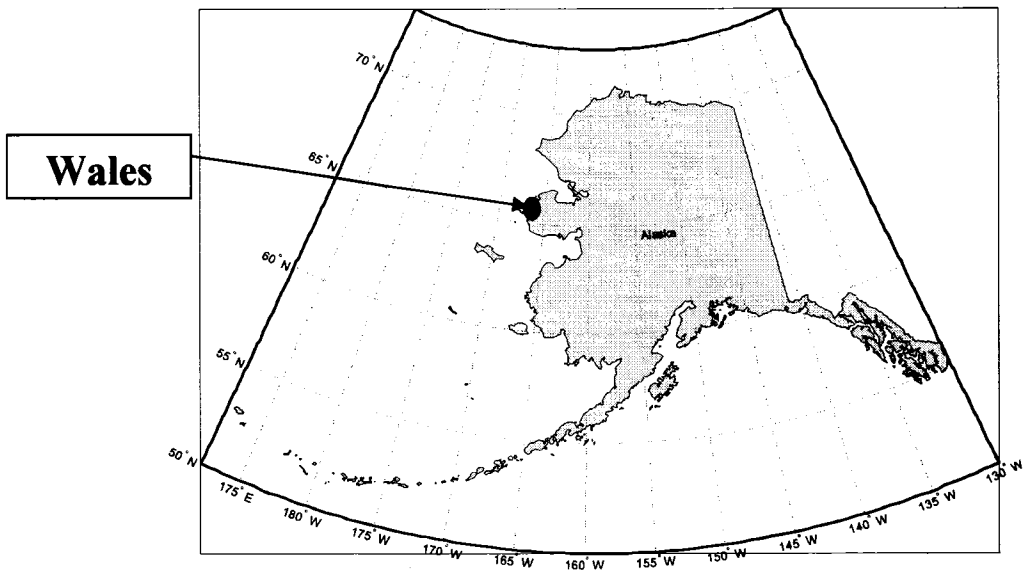

Fig. 5-1. Location of Wales Village, Alaska.

The electricity in Wales Village is provided by the Alaska Village Electric Cooperative (AVEC) using a hybrid wind-diesel-battery system. The hybrid system was installed in the summer of 2000 [8]. Before 2000, DEGs were the only source of electricity with a back-up battery bank.

In order to analyze the performance of the hybrid power system in Wales Village, simulations were performed using HARPSim's wind-diesel-battery hybrid power system model. The simulation results were compared with those predicted by the HOMER software.

5.1.1 Wales Village Hybrid Power System

The details of the Wales Village hybrid power system components are available in Appendix 6. The Wales Village hybrid power system consists of 3 DEGs as follows:

- Diesel #1: 168 kW, 1200 RPM Cummins LTA10.
- Diesel #2: 75 kW, 1800 RPM Allis-Chalmers 3500.
- Diesel #3: 168 kW, 1800 RPM Cummins LTA10.

The details of the Wales Village hybrid power system are shown in Fig. 5-2 [59].

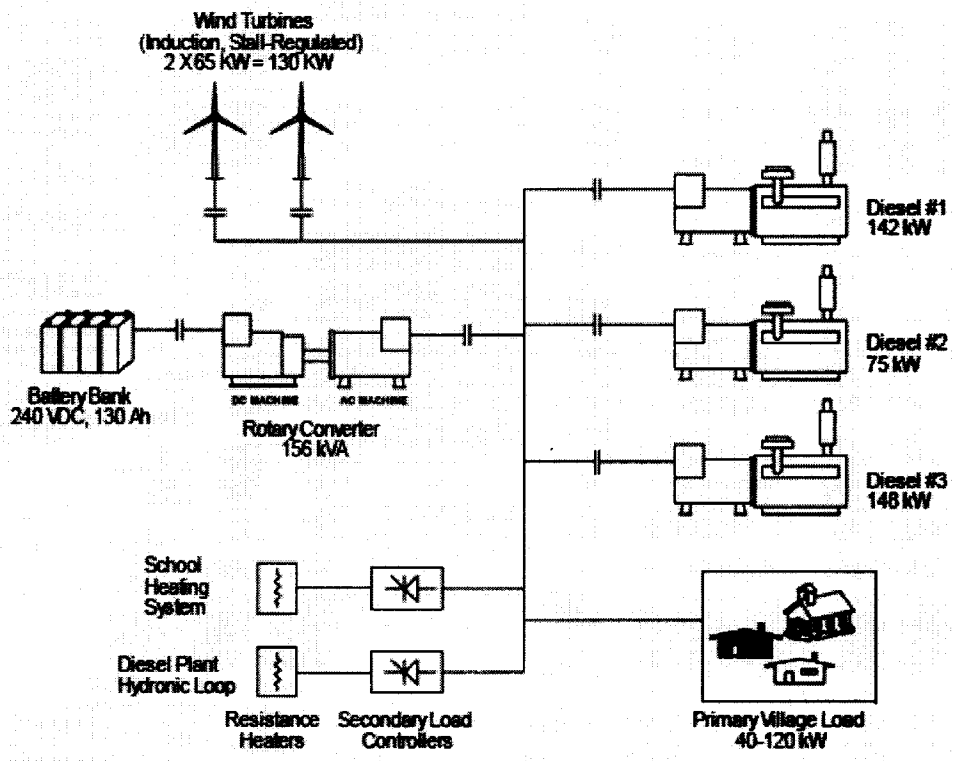

Fig. 5-2. Wales Village hybrid power system [59].

The Wales Village hybrid power system is operated as a single generator plant. DEG # 1 and DEG # 3 are cycled to supply the village load in conjunction with the WTGs. DEG#2, a less efficient generator, is brought online in case of scheduled maintenance or failures of either DEG#1 or DEG#3. The Wales Village hybrid power system also includes two WTGs with the total rated capacity of 130 kW, spaced 500 ft apart. These WTGs are manufactured by Atlantic Orient Corporation (AOC), currently known as Entegrity Wind Systems, Inc. The performance power curve for this 15/50 WTG is shown in Fig. 2-14.

Besides DEGs and WTGs, the hybrid power system of Wales Village also includes 200-1.2 volt each SAFT SPH130 Ni-Cad battery cells (sintered/plastic bonded electrode nickel cadmium batteries) with a total DC voltage rating of 240 VDC. The system also has a 156 kVA, 100 kW, rotary power converter with a roundtrip efficiency of 92% to supply power to and from the battery bank.

5.1.2 Development of Wales Village Model Using HOMER

The Wales Village hybrid power system model was implemented using the HOMER software. Fig. 5-3 shows the front-end for the hybrid power system of Wales Village as developed using the HOMER software. The system consists of two DEGs, two 15/50 AOC WTGs, a battery bank, a converter, and a primary AC load. The details of various components in HOMER are available in Appendix 7.

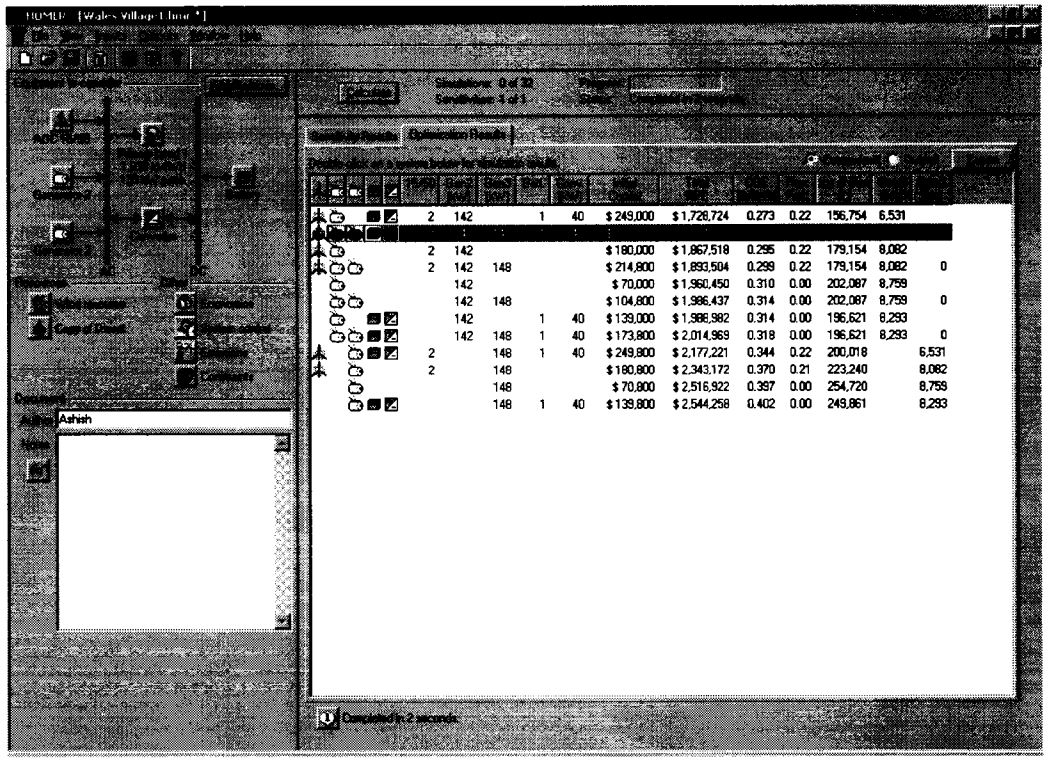

Fig. 5-3. Front-end of HOMER model for the Wales Village hybrid power system.

5.1.3 Wales Village Simulation

Simulations for the Wales Village hybrid wind-diesel-battery power system were performed for the annual load profile. The following assumptions are made for the simulations:

(i) Interest rate i = 7%.

(ii) Life cycle period for WTG (n) = 20 years.

(iii) Life cycle period for diesel-battery system = 5 years.

(iv) Life cycle period for diesel-battery system when operating in conjunction with WTG = 5.5 years.

The plots for the annual load profile and the annual temperature profile are shown in Fig. 5-4(a) and Fig. 5-4(b), respectively.

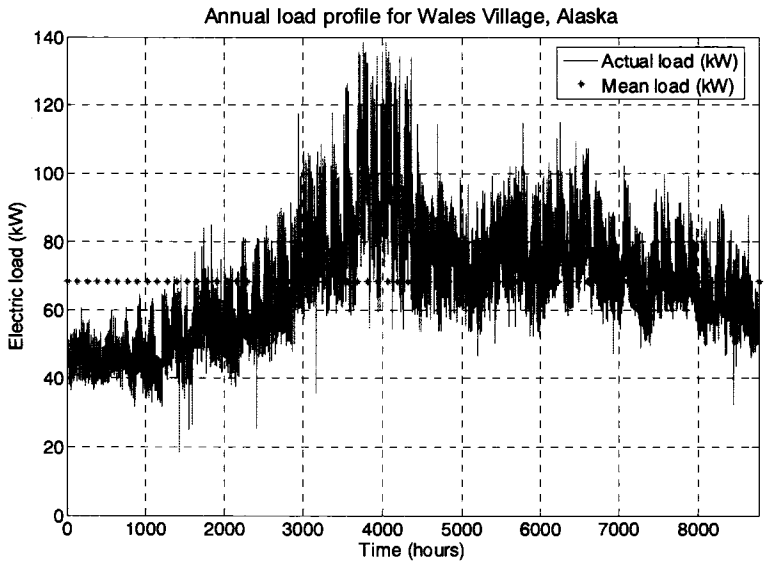

(a)

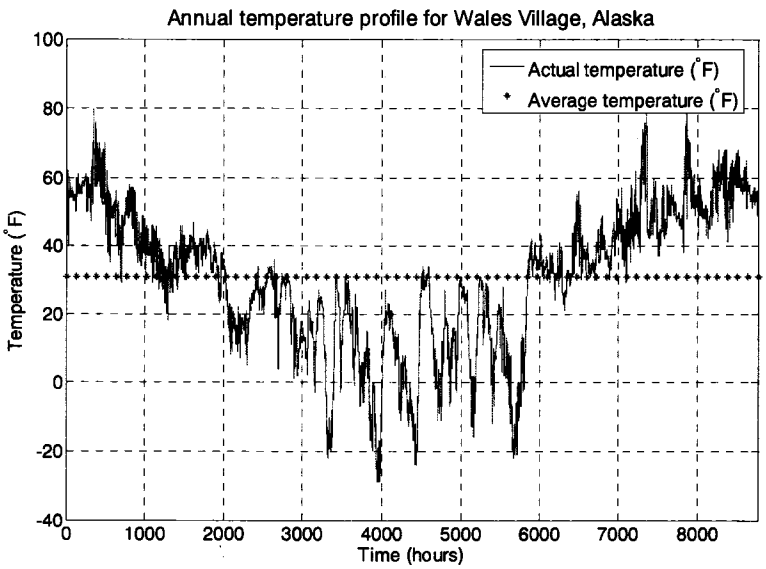

(b)

Fig. 5-4. Annual (a) load profile and (b) temperature profile for Wales Village.

The annual load data were recorded at Wales Village from August 1st, 1993 to July 31st, 1994 with the sampling period of 15 minutes. The annual temperature data could not be obtained for Wales Village. However, for analyses purposes, annual temperature data for Nome Village, which is located 90 miles southeast of Wales Village, were used. The temperature data for Nome Village with a one hour sampling period were obtained from the Alaska Climate Research Center located at the University of Alaska Fairbanks. It can be observed from Fig. 5-4(a) that the average annual load for Wales Village is about 68 kW and from Fig. 5-4(b) that the annual average temperature is about -0.55 °C (31 °F).

Fig. 5-5 shows the plot for the annual wind speed (m/s) for Wales Village. It can be observed that the average wind speed is about 8.4 m/s.

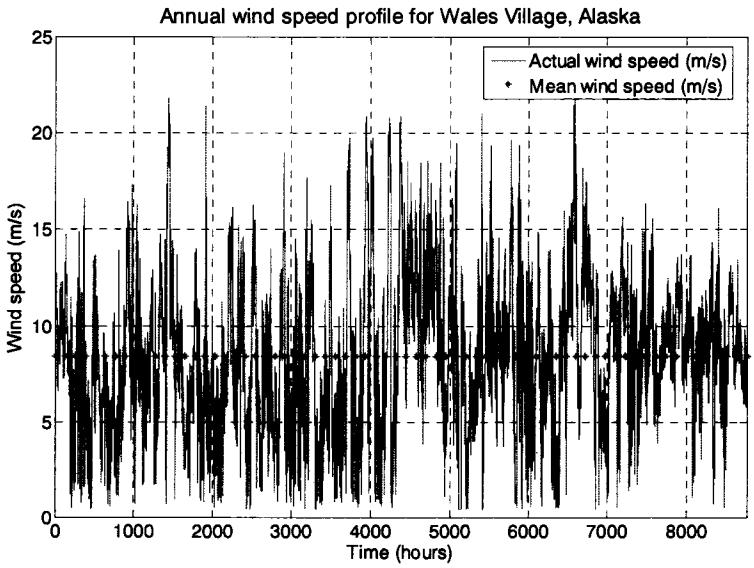

Fig. 5-5. Annual wind speed profile for Wales Village.

The second law efficiency of the WTGs is calculated using Eq. (2-13) and is shown in Fig. 5-6. It was observed that the average second law efficiency for the 15/50 AOC WTG installed at Wales Village is about 36%.

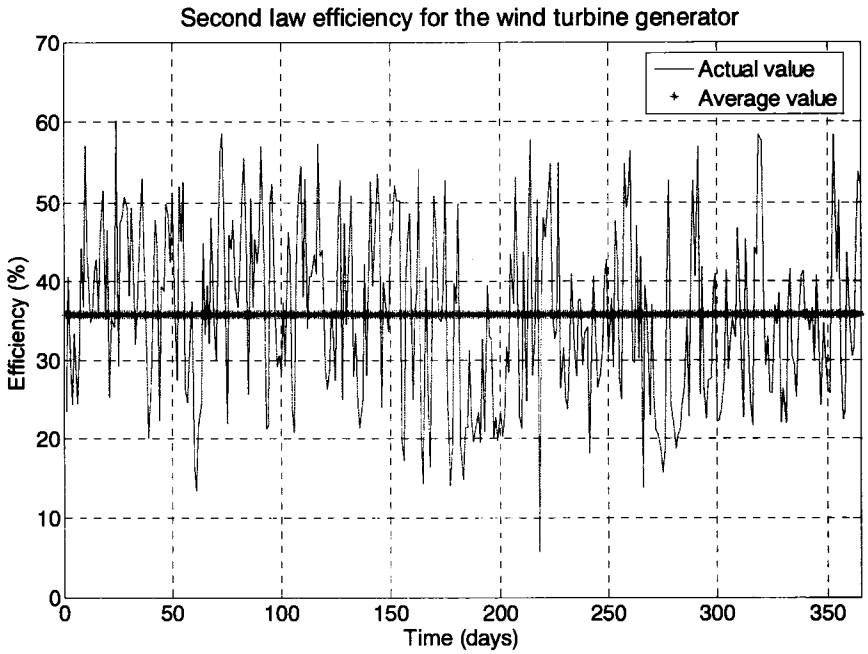

Fig. 5-6. Second law efficiency for the WTG.

5.1.4 Comparison of Wales Village Results from HARPSim and HOMER

The results from the HARPSim model were compared with those predicted by the HOMER software. TABLE 5-1 shows the overall comparison chart for the two models. It should be noted that the LCC analysis for 20 years with an investment rate of 7% is performed with the battery bank indoors. This is because in HOMER the battery bank is assumed to be kept at an optimal temperature. The results obtained with the battery bank kept outdoors are also presented in TABLE 5-1.

TABLE 5-1. Comparison of results for Wales Village with HOMER

Parameter	Simulink® Model			HOMER	
	Diesel-battery system	Wind-diesel-battery system		Diesel-battery system	Wind-diesel-battery system
	Battery Indoors (@ 20 °C)	Battery Indoors (@ 20 °C)	Battery Outdoors (Avg: -0.5 °C)	Battery Indoors (@ 20 °C)	Battery Indoors (@ 20 °C)
System cost (USD)	167,800	283,800	-	167,800	283,800
Engine efficiency (%)	29.55	29.55	29.55	29.4	29.55
kWh/liter (kWh/gallon) for the engine	3.13 (11.85)	3.13 (11.85)	3.13 (11.85)	3.09 (11.7)	3.13 (11.85)
Fuel consumed in liter (gallons)	199,890 (52,881)	155,762 (41,207)	185,020 (48,947)	196,621 (50,016)	156,653 (41,443)
Total cost of fuel (USD)	158,643	123,621	146,841	156,039	124,320
Energy generated					
(a) Diesel engine (kWh)	626,876	488,484	580,239	606,501	490,507
(b) WTG (kWh)	0	137,266	137,266	0	139,830
(c) Excess energy (kWh)	28,939	0	119,568	92.8	11,988
Energy supplied to load (kWh)	597,937	597,937	597,937	597,871	597,871
Operational life					
(a) Generator (years)	5.5	5.5	5.5	3.62	4.6
(b) Battery bank (years)	5.0	5.5	3.0	12	12
Net present value (USD) with i = 7% and n = 20 years	-	1,652,820	1,923,997	2,008,969	1,754,711
Cost of Electricity (USD/kWh)	0.32	0.28	0.32	0.32	0.28
Payback period for WTGs (years)	-	4.867	Never	-	-
Emissions					
(a) CO_2 in metric tons (US tons)	498.65 (549.67)	388.57 (428.33)	461.55 (508.77)	497.10 (547.96)	*402.41 (443.58)
(b) NOx in kg (Pounds)	5516.45 (12161.69)	4298.62 (9476.83)	5106.048 (11256.91)	-	-
(c) PM in kg (Pounds)	231.94 (511.34)	180.74 (398.49)	214.69 (473.3)	-	-

*Based on 88% carbon content in the diesel fuel

From HARPSim and HOMER, it can be observed that the wind-diesel-battery system is the most cost effective system with the least COE and NPV. In

HARPSim the battery bank charges and discharges while supplying the load. Therefore, the DEGs operate more efficiently resulting in fuel savings. This saving in the fuel is achieved at the expense of the battery life. In HOMER, the battery bank is used as a back-up source of power. Therefore, the life of the battery bank is much higher (12 years) as compared to the life of the battery bank in HARPSim (5.5 years). Overall, the NPV of the system using HARPSim is less than that using the HOMER software and the payback period of the WTG using HARPSim is less than 5 years.

5.1.4.1 Comparison of LCC and NPV of Wales Village from HARPSim and HOMER

Fig. 5-7 and Fig. 5-8 show the cost involved for various hybrid power system components throughout the 20-year life cycle of the project, therefore, the life cycle cost analysis of the hybrid power system using the Simulink® model and the HOMER software, respectively. It can be observed that the cost of the battery bank in HARPSim is greater than the cost predicted by HOMER. This is because in the HARPSim model, the battery bank acts as a source of power, rather than backup batteries. Therefore, the life of the battery bank in HARPSim is reduced due to the increase in charge-discharge cycles. Overall, the NPV of the system is less in the HARPSim model, mainly due to the savings in the fuel consumed by the DEGs.

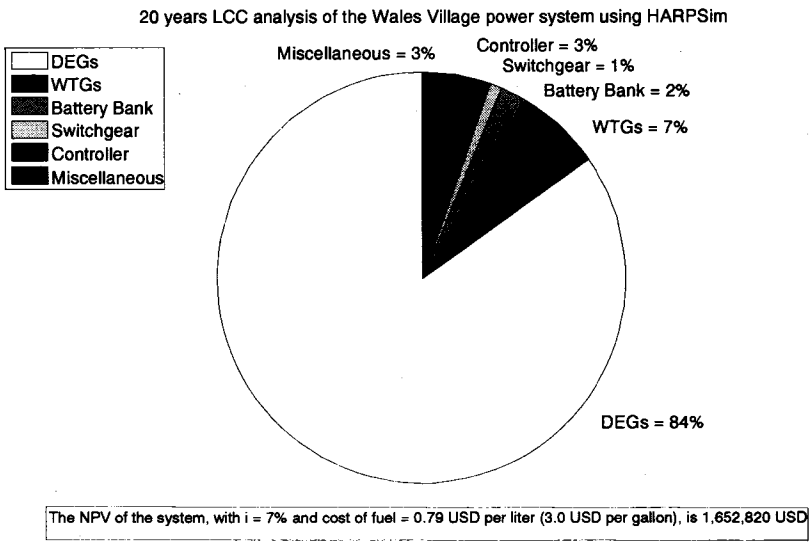

Fig. 5-7. LCC analysis of the hybrid power system of Wales Village, Alaska using HARPSim.

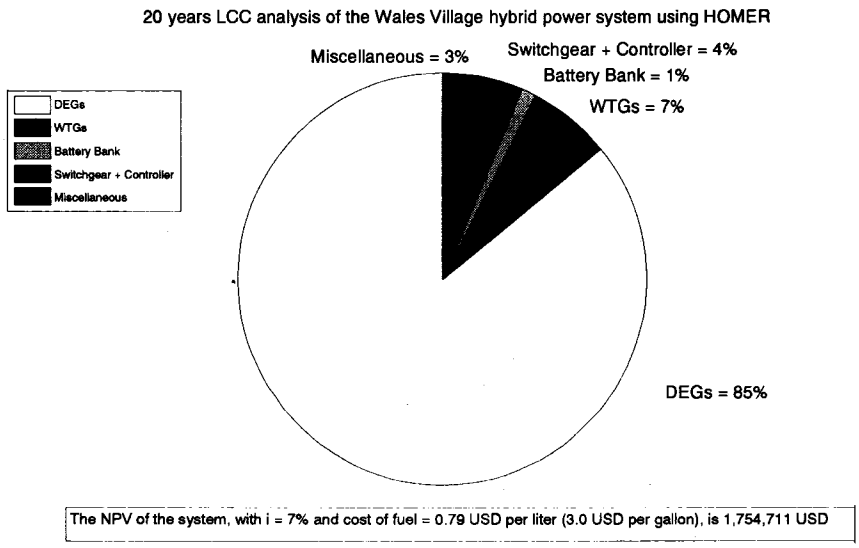

Fig. 5-8. LCC analysis of the hybrid power system of Wales Village, Alaska using HOMER.

Fig. 5-9 shows the sensitivity analysis of fuel cost and investment rate on the net present value (NPV) of the system of Wales Village. It can be observed that as the fuel cost increases and the investment rate decreases, the NPV of the system increases linearly.

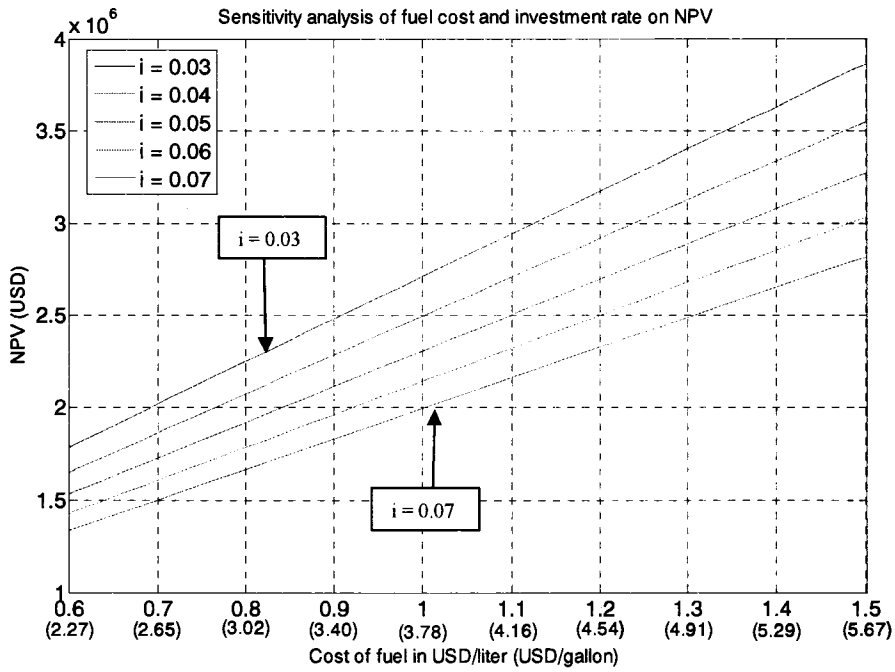

Fig. 5-9. Sensitivity analysis of fuel cost and investment rate on NPV for wind-diesel-battery system.

5.1.4.2 Comparison of COE of Wales Village from HARPSim and HOMER

TABLE 5-2 shows the annualized operating and maintenance cost for the hybrid power system of Wales Village. The data in the table is obtained from the actual system installed at Wales Village [8]. In order to calculate the COE for the system, data from TABLE 5-1 and TABLE 5-2 are used.

TABLE 5-2. Annualized cost for the hybrid system of Wales Village

Sr. No.	Item	Diesel- battery system	Wind-diesel-battery system
1	Annual inspection of WTGs	0 USD	500 USD
2	Generator oil change*	2,500 USD	2,500 USD
3	Generator valve adjustment**	625 USD	625 USD
4	Battery bank watering	200 USD	200 USD
5	Switchgear inspection & fuses	100 USD	100 USD
6	Inverter inspection & fuses	100 USD	100 USD
7	Freight, travel & misc.	1,000 USD	1,000 USD
8	Energy & fuel	158,643 USD	122,975 USD
	Total annual spending	**192,685 USD**	**168,852 USD**

*Assuming generator operating for 5000 hours in a year requiring oil change after every 250 hours @ $125 per oil change.
**Assuming generator requiring valve adjustment every 2000 hours @ $250.

The COE using data from TABLE 5-1 and TABLE 5-2 for the Simulink® model is calculated as follows:

$$\text{COE} = \frac{\text{Total annual spending (USD)}}{\text{Energy to the load (kWh)}} \tag{5-1}$$

$$\therefore \text{COE for wind\_diesel\_battery system} = \frac{168{,}852\,\text{USD}}{597{,}937\,\text{kWh}} = 28.24\,\text{US cents/kWh}$$

$$\therefore \text{COE for diesel\_battery system} = \frac{192{,}685\,\text{USD}}{597{,}937\,\text{kWh}} = 32.22\,\text{US cents/kWh}.$$

The COE obtained from the HOMER software for the wind-diesel-battery system and the diesel-battery system are 27.7 US cents/kWh and 31.8 US cents/kWh, respectively. The COE in the Simulink® model is higher compared to

the HOMER model because the main objective of the Simulink® model is to reduce the fuel consumption by the DEGs. In order to achieve this objective, the battery bank acts as a source of power and undergoes a large number of deep discharge cycles. This reduces the life of the battery bank. Therefore, the total spending in the Simulink® model is higher, increasing the COE of the system, as compared with the HOMER software.

Fig. 5-10 shows the effect of varying fuel price and the investment rate on the COE for the diesel-battery system and the wind-diesel-battery system. It is observed that as the fuel price increases and the investment rate decreases, the COE increases linearly. The linear increase in the COE with the increasing fuel prices was expected because the fuel consumption curve of the engine is a linear function of the load on the system. It can also be seen that the COE is higher for the diesel-battery system as compared to the wind-diesel-battery system.

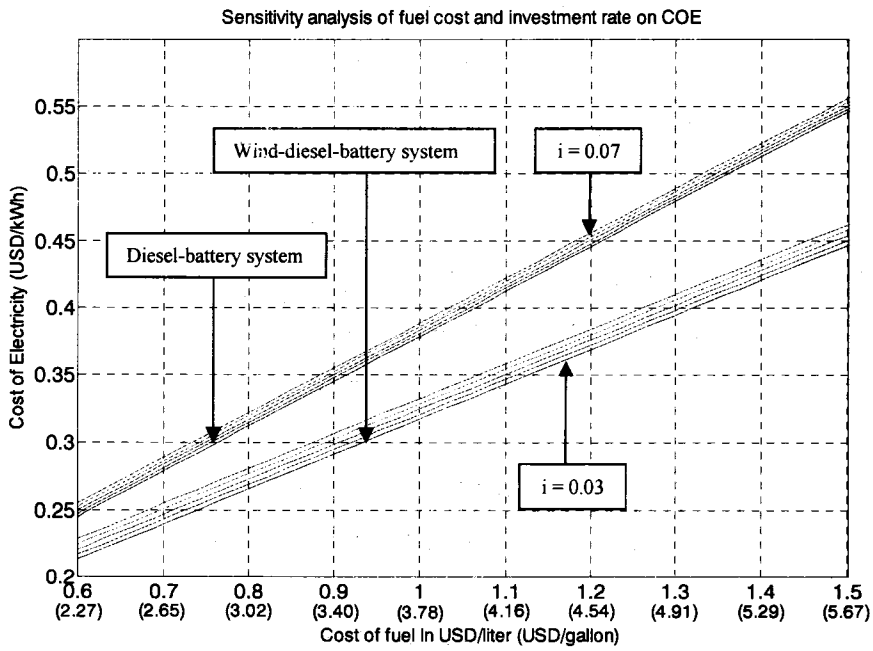

Fig. 5-10. Sensitivity analysis of fuel cost and investment rate on the COE.

5.1.4.3 Calculation of Payback Period for the WTGs

The simple payback period of the WTGs is calculated as described in Section 2.7.5 as follows:

$$\therefore \text{SPBT} = \frac{\text{Extra cost of PV system}}{\text{rate of saving per year}}$$

$$= \frac{(283{,}800 - 167{,}800)\ \text{USD}}{(192{,}685.1 - 168{,}852.07)\ \text{USD/year}} = 4.867\ \text{years}.$$

The term in the numerator is excess cost of the wind system obtained from the difference in the cost of the wind-diesel-battery system and the diesel-battery system as given in TABLE 5-1 and the term in the denominator is the rate of savings obtained from the difference in the annual spending of the two systems as given in TABLE 5-2.

Fig. 5-11 shows the sensitivity analysis of fuel cost and investment rate on the payback period of the WTGs. It is observed that as the cost of fuel increases and the investment rate decreases, the payback period of the WTGs decreases as a function of a fifth order polynomial. The decrease in the payback period with the increase in the cost of fuel was expected because the use of WTGs reduces the fuel consumed by the DEGs. The electrical efficiency versus the load curve used to model the DEG is a fifth order polynomial as described in Section 2.1. Therefore, the payback period for the WTGs is obtained as a function of a fifth order polynomial because the rate of fuel consumed by the DEG is a linear function of the load on the system.

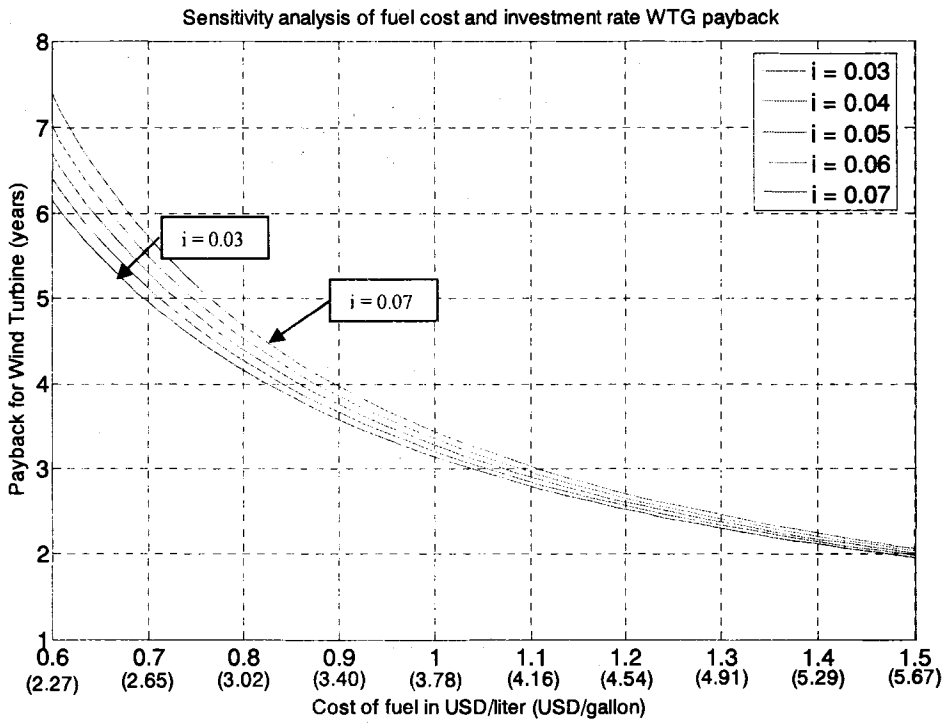

Fig. 5-11. Sensitivity analysis of fuel cost and investment rate on the payback period of WTGs.

5.1.4.4 Calculation of Avoided Cost of Pollutants for Wales Village

The use of a WTG with DEGs in Wales Village results in decreased emissions. The cost associated with the difference in the amount of emitted pollutants in called the avoided cost of emissions. The avoided cost of different pollutants: carbon dioxide (CO_2), nitrogen oxide (NOx), and particulate matter (PM_{10}) for the Wales Village hybrid power system are calculated as described in Section 2.8.4 as follows:

$$AC_{CO_2} = \frac{(168{,}206 - 192{,}685)\ \text{USD}}{(498.65 - 372.68)\ \text{tons}} = -194\ \text{USD/ton}.$$

Similarly, the avoided cost for NOx and PM_{10} are calculated. The avoided costs for various pollutants are tabulated in TABLE 5-3. The avoided costs of the pollutants are negative because the annual spending in the wind-diesel-battery system (low emissions plant) is less than the annual spending in the diesel-battery system (high emissions plant). The negative avoided cost shows that the wind-diesel-battery system is more economical and at the same time emitting less pollutants.

TABLE 5-3. Avoided cost for different pollutants

Emission	Avoided costs
CO_2	-194 USD/metric ton (176 USD/US ton)
PM_{10}	-478 USD/kg (-217 USD/lb)
NOx	-20 USD/kg (-9 USD/lb)

5.2 Lime Village Analysis

Lime Village is located on the south bank of the Stony River, about 111 air miles southeast of McGrath and 185 miles west of Anchorage [60]. The village is located at a northern latitude of 61°20'29" and a western longitude of 155°29'27" as shown in Fig. 5-12. According to the United States Census Bureau, Lime Village has a total area of 213.6 km² (82.5 mi²). According to the 2000 US Census the village has 25 housing units with 6 vacant [61]. The village has one K-12 school attended by 10 students [62]. Lime Village has a continental climate with temperatures ranging from -47°F to 82°F, an average annual precipitation of 22 inches, and an annual average snowfall of 85 inches. The main occupation of

people in the village is hunting, berry picking, fire fighting, and trapping. The mode of transportation in and out of the village is small airplanes and riverboats [61], [62].

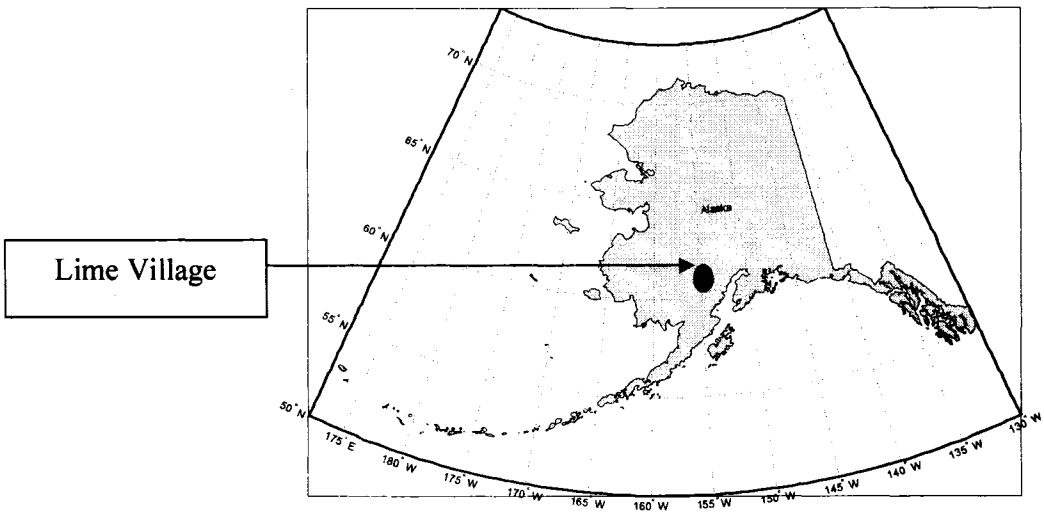

Fig. 5-12. Location of Lime Village, Alaska.

The electricity in Lime Village is provided by Lime Village Power Systems, operated and maintained by McGrath Light and Power, with the use of a hybrid PV-diesel-battery system. The hybrid PV-diesel-battery system was installed in the summer of 2001 [11]. Before 2001, DEGs were the only source of electricity with a back-up battery bank.

In order to analyze the performance of the hybrid power system in Lime Village, simulations were performed using the HARPSim's PV-diesel-battery hybrid power system model. The simulation results were compared with those predicted by the HOMER software.

5.2.1 Lime Village Hybrid Power System

The details of the Lime Village Hybrid Power System are available in Appendix 8. The Lime Village hybrid power system consists of two DEGs rated at 35 kW and 21 kW. The system is operated as a single generator plant with the other generator as a back-up generator. Besides DEGs, the system consists of 4 kW of Siemens PV panels and 8 kW of BP PV panels with a total PV capacity of 12 kW.

Besides the DEGs and the PV panels, the hybrid power system of Lime Village includes 95-2 volt GNB Absolyte IIP battery cells with a total DC voltage rating of 190 VDC and the battery capacity of 100 kWh. The system also has a 30 kVA bi-directional power converter to supply power to and from the battery bank. A block diagram of the Lime Village hybrid power system is shown in Fig. 5-13.

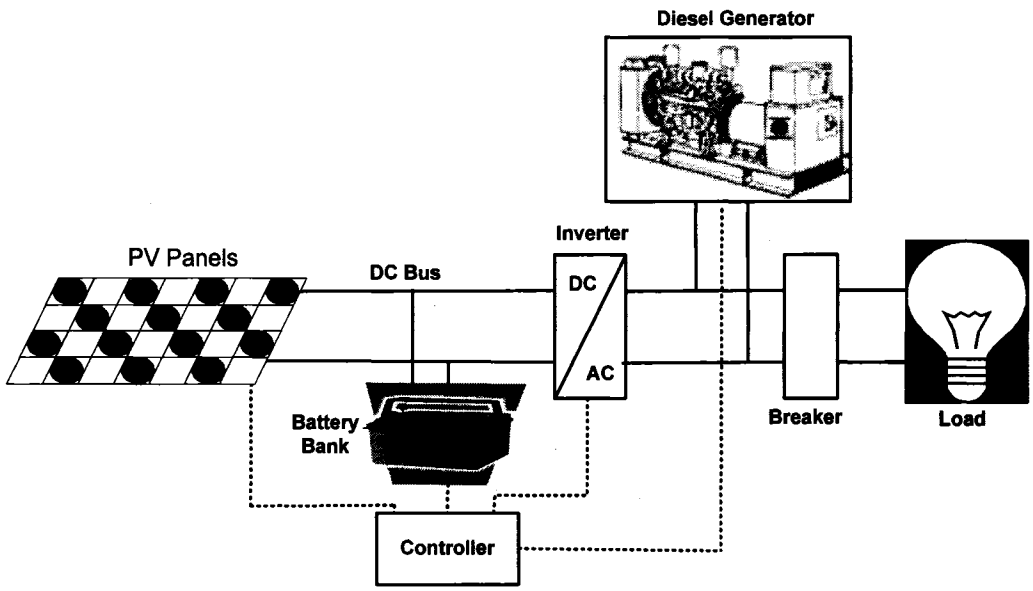

Fig. 5-13. Lime Village hybrid power system.

5.2.2 Development of Lime Village Model Using HOMER

The Lime Village hybrid power system model is implemented using the HOMER software. Fig. 5-14 shows the front-end for the hybrid power system of Lime Village, as developed using the HOMER software. The system consists of two DEGs, a 12 kW PV array, a battery bank, a converter, and a primary AC load. The details of the various components in HOMER are available in Appendix 9.

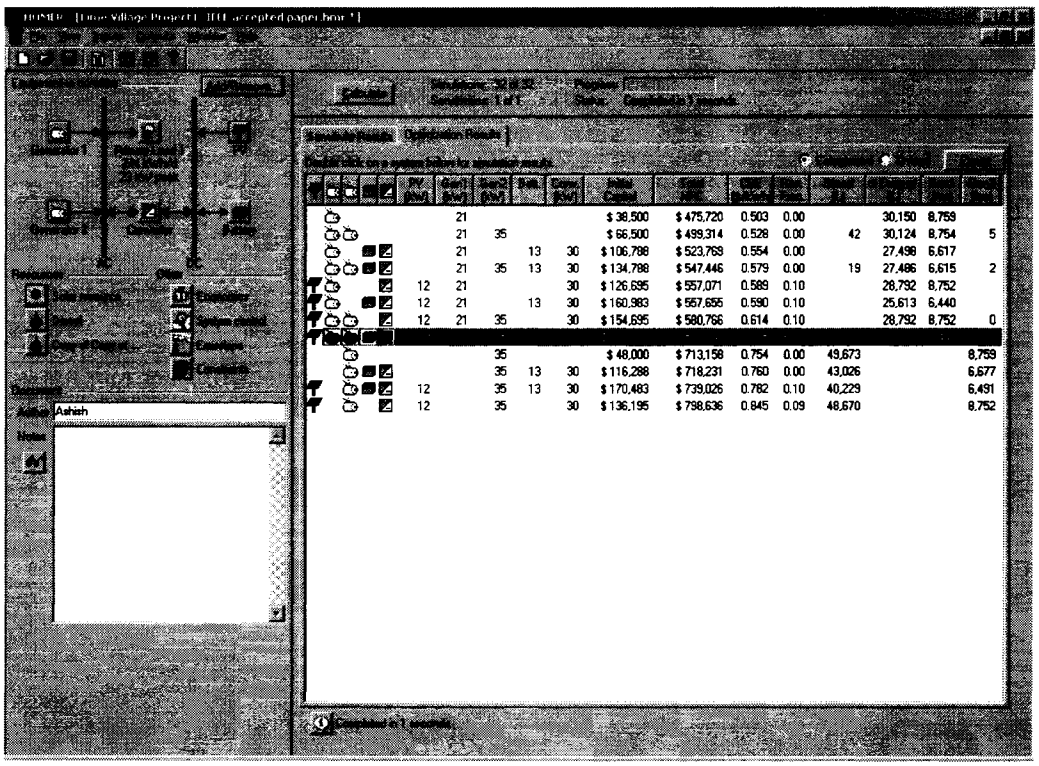

Fig. 5-14. Front-end of HOMER model for the Lime Village power system.

5.2.3 Lime Village Simulation

In Alaska, there is less sunlight available during winter months, therefore, very few PV-diesel-battery hybrid power systems are installed. As a result field data is not easily available for the PV-diesel-battery hybrid power system. In order

to study the performance of the PV-diesel-battery system installed at Lime Village, simulations were performed for the PV-diesel-battery system for the load profile shown in Fig. 5-15. This load profile was obtained by interpolating and averaging a 24-hour summer load profile with 10 minute samples and a 24-hour winter load profile with 15 minute samples obtained from Lime Village over a one year time period for the year 2000. Each data point represents a daily average. A second order polynomial fit to the data is used as shown in Fig. 5-15.

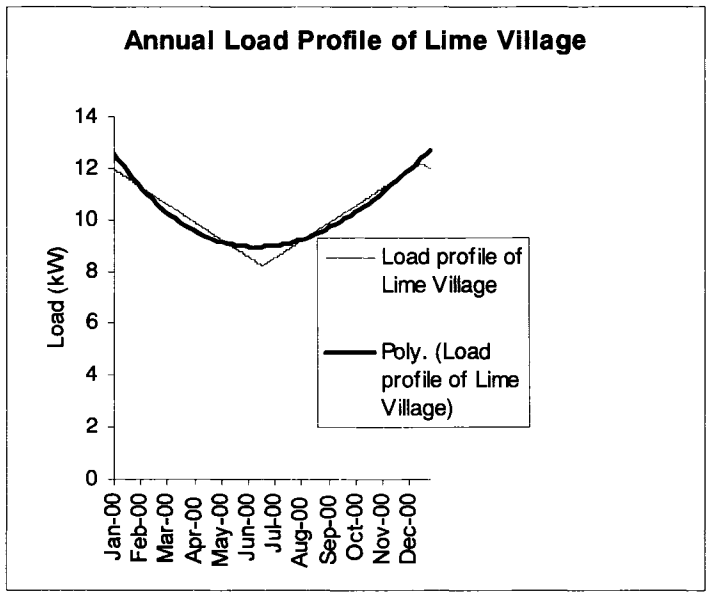

Fig. 5-15. Annual load profile for Lime Village, Alaska.

The solar insolation profile for Lime Village is shown in Fig. 5-16.

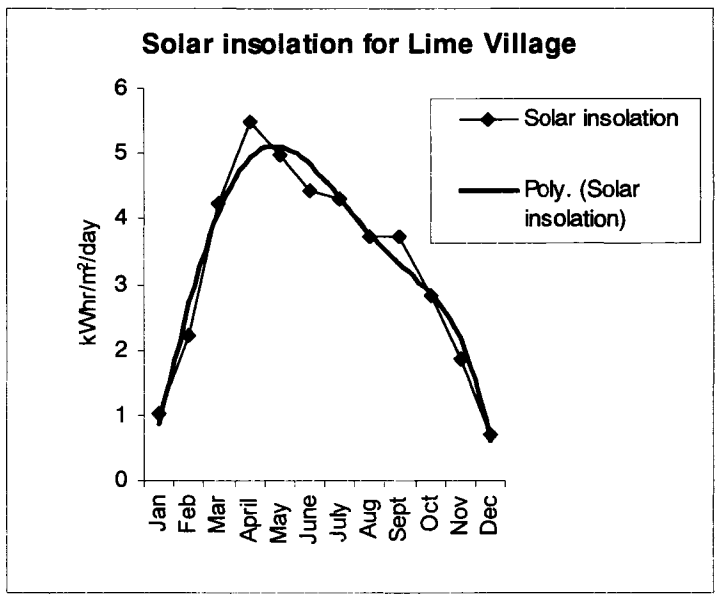

Fig. 5-16. Annual solar insolation profile for Lime Village, Alaska.

This solar insolation profile is obtained using the solar maps developed by the National Renewable Energy Laboratory (NREL) [63]. A third order polynomial fit to the data is used as shown in Fig. 5-16. It can be observed from this plot that during summer days there is abundant sunlight, hence the energy available from the sun is distributed throughout the day. If there is any extra power available from the PV array after supplying the load, it is utilized to charge the battery bank.

The following assumptions are made for the Lime Village simulations:

(i) Interest rate i = 7%.

(ii) Life cycle period for PV (n) = 20 years.

(iii) Life cycle period for diesel-battery system = 5 years.

(iv) Life cycle period for diesel-battery system when operating in conjunction with PV = 5.4 years.

The higher life cycle period for the diesel-battery system when operating in conjunction with the PV array is assumed because in the PV-diesel-battery system about 10% of the load is supplied by the PV array. So the life of the diesel-battery system will increase when operating in conjunction with the PV array.

5.2.4 Comparison of Lime Village Results from HARPSim and HOMER

Simulations were performed for the Lime Village hybrid power system using the annual load profile for three systems: (i) Diesel-only system, (ii) Diesel-battery system, and (iii) PV-diesel-battery system. The post simulation results obtained from the HARPSim model were compared with those obtained from the HOMER software.

TABLE 5-4 shows the costs of the different components installed at Lime Village. The costs of the different components were obtained from the various manufacturers. The engineering cost, commissioning, installation, freight and other miscellaneous costs were obtained from a report prepared by the Alaska Energy Authority (AEA) [11]. Due to the remoteness of the site, the cost for transporting and installing the various components is relatively high.

TABLE 5-5 shows the results obtained from the HARPSim model. In this model the roundtrip efficiency of the rectifier/inverter and the internal loss in the battery bank per cycle was considered as 90%. The collector efficiency for the PV array is assumed as 12%. As mentioned in HOMER, the heating value of fuel is assumed to be 48.5 MJ/kg (20,852 BTU/lb) and the density of fuel is assumed to be 840 kg/m^3 (52.44 lb/ft^3). The post-simulation analysis includes an economic and environmental component illustrating the simple payback and avoided cost of emissions using the PV array.

TABLE 5-4. Component and installation costs for Lime Village

Item	Cost per unit (USD)	No of units	Diesel-only system (USD)	Diesel-battery system (USD)	PV-diesel-battery system (USD)
35 kW diesel generator	28,000	1	28,000	28,000	28,000
21 kW diesel generator	18,500	1	18,500	18,500	18,500
Switch gear to automate control of both diesels	16,000	1	16,000	16,000	16,000
Rectification/Inversion	18,000	1	0	18,000	18,000
New Absolyte IIP 6-90A13 battery bank	2,143	16	0	34,288	34,288
BP275 Solar	329	105	0	0	34,545
Siemens M55 Solar	262	75	0	0	19,650
Engineering		1	3,000	3,500	4,000
Commissioning, Installation, freight, travel, miscellaneous		1	13,000	14,000	16,000
		TOTAL	**78,500**	**132,288**	**188,983**

TABLE 5-5. Simulation results of Lime Village using HARPSim

Parameter	Diesel-only system	Diesel-battery system	PV-diesel-battery system
System cost (USD)	78,500	132,288	188,983
System efficiency (%)*	26.22%	29.94%	29.96%
kWh/liter (kWh/gallon)	2.81 (10.61)	3.20 (12.1)	3.20 (12.1)
Fuel consumed in liters (gallons)	31,789.80 (8410)	27,847.26 (7367)	24,883.74 (6583)
Total cost of fuel (USD)**	33,640	29,470	26,340
CO_2 emitted in metric tons (US tons)	81.05 (89.34)	70.93 (78.19)	63.64 (70.15)
PM_{10} emitted in kg (lbs)	33.01 (72.77)	32.84 (72.4)	27.18 (59.92)
NOx emitted in kg (lbs)	785.17 (1731)	784.71 (1730)	646.37 (1425)
System load (kWh)	89220	89220	89220
Energy supplied			
(a) DEG (kWh)	101900	100100	89500
(b) PV (kWh)	0	0	9445
Electrical efficiency of DEG (%)	87.56	89.13	90.17

*In this project System efficiency is the ratio of the total electrical energy supplied by the diesel generator to the total energy available from the fuel.
**Based on a diesel fuel price of 1.057 USD per liter (4.00 USD per gallon) for Lime Village, Alaska.

The results obtained from HARPSim for the three systems shows that the addition of the battery bank and the PV array with the DEGs improves the system efficiency and reliability and decreases the fuel consumption and the environmental pollutants. TABLE 5-6 shows the comparison of results from HARPSim with HOMER for the Lime Village hybrid power system.

TABLE 5-6. Comparison of results for Lime Village with HOMER

Parameter	**HOMER**	**HARPSim**
System cost (USD)	188,983	188,983
System efficiency (%)	29.9	29.96
kWh/liter (kWh/gallon)	3.13 (11.84)	3.20 (12.1)
Fuel consumed in liters (gallons)	25,768.26 (6,817)	24,883.74 (6,583)
Total cost of fuel (USD)	27,058	26,340
Energy generated		
(a) Diesel engine (kWh)	87,064	82,497
(b) PV (kWh)	9,444	9,445
Energy supplied to load (kWh)	89,224	89,220
Operational life		
(a) Generator (years)	4.62	5.4
(b) Battery bank(years)	6.07	5.4
Net present value (NPV) (USD)	581,350	557,154
Emissions		
(a) CO_2 in metric tons (US tons)	*68.58 (75.60)	63.64 (70.15)
(b) NOx in kg (lbs)	-	646.37 (1425)
(c) PM_{10} in kg (lbs)	-	27.18 (59.92)

*Based on 88% carbon content in the diesel fuel.

From TABLE 5-6, it can be observed that the NPV of the system using HARPSim is less than that using the HOMER software. This is because in HARPSim the battery bank charges and discharges while supplying the load. Therefore, the DEGs operate more efficiently resulting in the fuel savings while emitting less pollutant. This saving in the fuel is achieved at the expense of the battery life.

5.2.4.1 Comparison of LCC and NPV of Lime Village from HARPSim and HOMER

Fig. 5-17 and Fig. 5-18 show the LCC analysis of the PV-diesel-battery hybrid power system for Lime Village using the HARPSim model and the HOMER software, respectively. The 20 year life cycle costs for each component in the system using HARPSim are in close agreement with HOMER.

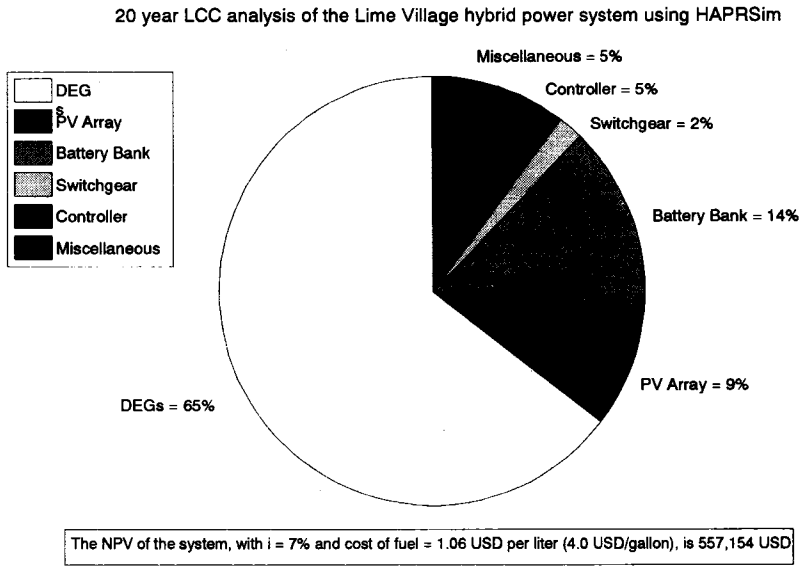

Fig. 5-17. 20 year LCC analysis of the Lime Village hybrid power system using the Simulink® model.

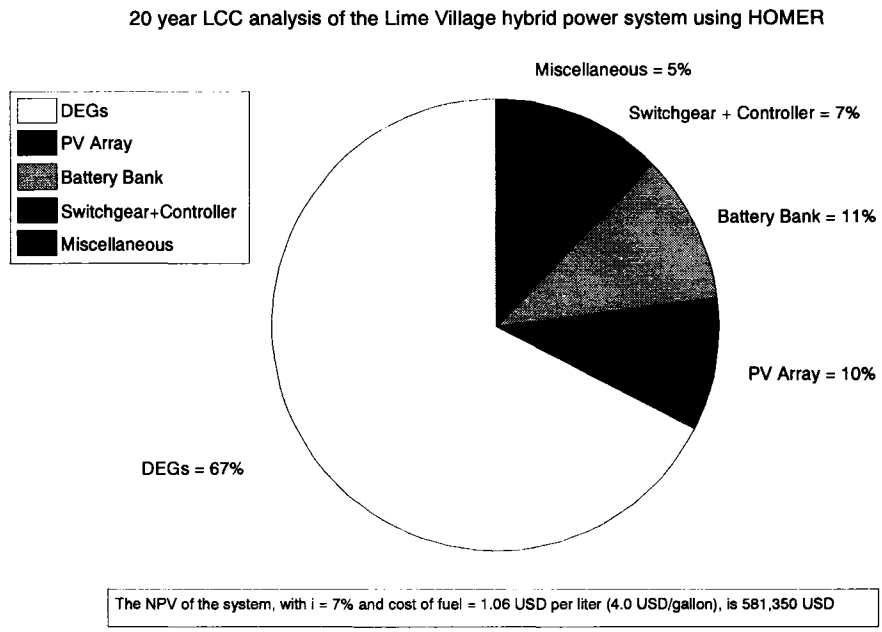

Fig. 5-18. 20 year LCC analysis of the Lime Village hybrid power system using the HOMER software.

It can be seen that in the HARPSim model, the cost of the battery bank is 3% more while the cost of the DEGs is 2 % less than in the HOMER model. This is because in the HARPSim model, the battery bank acts as a source of power rather than as the backup power source used in the HOMER software. Therefore, the life of the battery bank is less in the HARPSim model due to the annual increase in charge/discharge cycles. This is achieved with the reduction in the fuel consumed by the DEGs. Overall, the LCC analysis shows a reduced NPV in the HARPSim model, compared to the HOMER software.

Fig. 5-19 shows the sensitivity analysis of the fuel cost and the investment rate on the NPV. It can be seen that as the cost of fuel increases and the investment rate decreases, the NPV of the system increases linearly. The NPV plays an important role in deciding on the type of the system to be installed. The NPV of a system includes the total spending on the installation, maintenance, replacement,

and fuel cost for the type of system over the life-cycle of the project. Knowing the NPV for different system configurations, the user can install a system with minimum NPV.

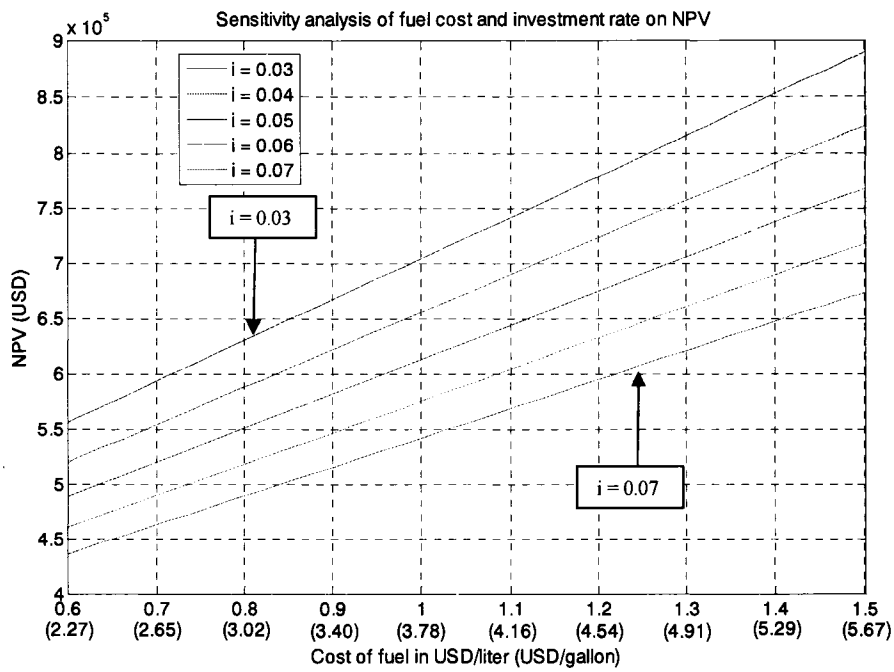

Fig. 5-19. Sensitivity analysis of fuel cost and investment rate on the NPV for PV-diesel-battery system.

5.2.4.2 Calculation of COE for Lime Village

In order to calculate the COE for the diesel-battery (high emissions plant) system and the PV-diesel-battery (low emissions plant) system, it is necessary to know the A/P ratio for the system, where 'A' is the annual payment on a loan whose principal is 'P' at an interest rate *'i'* for a given period of 'n' years [44].

The ratio A/P is given as follows:

$$\frac{A}{P} = \frac{i(1+i)^n}{(1+i)^n - 1} \tag{5-2}$$

$$\therefore \frac{A}{P}(\text{for PV array}) = \frac{0.07(1+0.07)^{20}}{(1+0.07)^{20} - 1} = 0.09439.$$

Similarly, A/P for other cases is calculated and tabulated in TABLE 5-7.

TABLE 5-7. A/P and COE for various cases

Parameter	Diesel-battery system	PV-diesel-battery system
A/P for PV array	-	0.09439
A/P for Diesel-battery system	0.2439	0.2287
Annual cost of electricity (USD)	61,735	61,946

The annual COE for different systems with a fuel price of 1.057 USD per liter (4.00 USD per gallon) and an investment rate of 7% is calculated as follows:

$$COE_L = 0.09439\,(C_{PV} - C_{DB}) + 0.2341\,(C_{DB}) + C_F \quad \text{and} \tag{5-3}$$

$$COE_H = 0.2439\,(C_{DB}) + C_F \tag{5-4}$$

where C_{PV} is the cost of the PV-diesel-battery system, C_{DB} is the cost of the diesel-battery system and C_F is the annual cost of fuel.

Substituting the values from TABLE 5-4, TABLE 5-5, and TABLE 5-7, the COE of the low emissions plant is calculated as follows:

$$COE_L = 0.09439\,(56{,}695) + 0.2287\,(132{,}288) + 26{,}340 = \$61{,}946.$$

Similarly, COE_H with a fuel cost of 1.057 USD per liter (4.00 USD per gallon) and an investment rate of 7% is calculated as 61,735 USD.

Fig. 5-20 shows the plot for the sensitivity analysis of fuel cost and investment rate on the COE. It can be observed that as the cost of fuel increases and the investment rate increases, the COE increases linearly as described in Section 5.1.4.2.

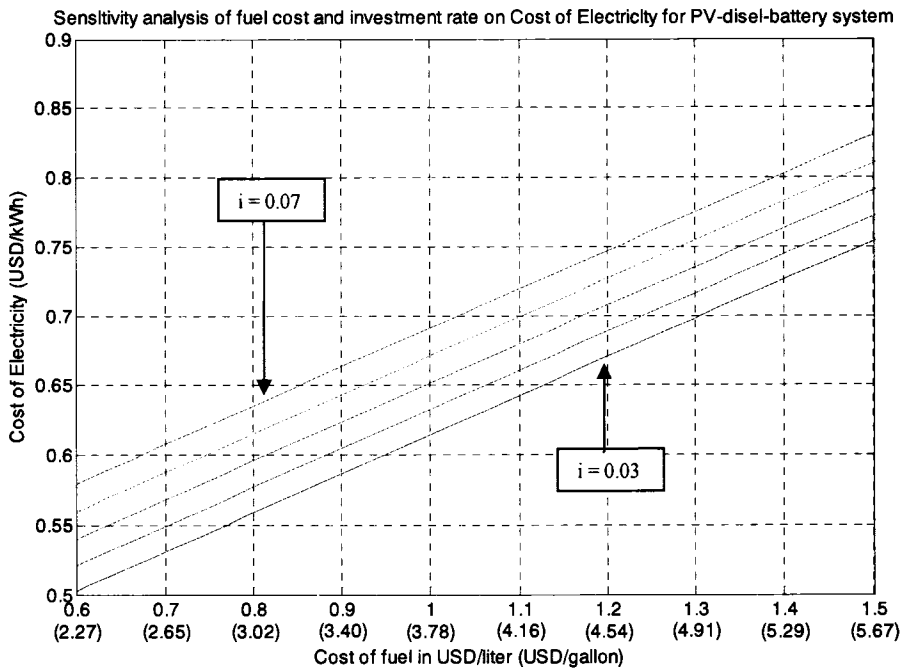

Fig. 5-20. Sensitivity analysis of fuel cost and investment rate on COE for the PV-diesel-battery hybrid power system.

Fig. 5-21 shows the plot for the sensitivity analysis of fuel cost and investment rate on the COE for the diesel-battery system of Lime Village. It can be observed that as the cost of the fuel and the investment rate increases, the COE increases linearly.

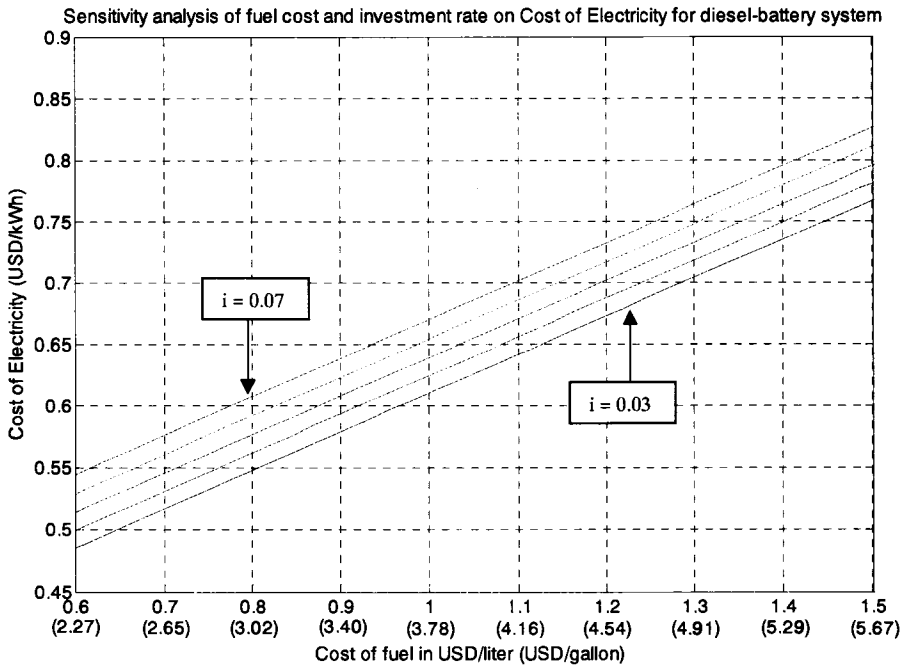

Fig. 5-21. Sensitivity analysis of fuel cost and investment rate on COE for the diesel-battery hybrid power system.

5.2.4.3 Calculation of Payback Period for the PV Array

The simple payback period for the PV array is calculated using data from TABLE 5-4 and TABLE 5-5 as described in Section 2.7.5 as follows:

$$\text{SPBT} = \frac{\text{Extra cost of PV system}}{\text{rate of saving per year}}$$

$$= \frac{188{,}983\ \text{USD} - 132{,}288\ \text{USD}}{(29{,}470 - 26{,}340)\ \text{USD/year}} = 18.11\ \text{years}\ .$$

The extra cost of the PV system is obtained as the difference between the system cost of the PV-diesel-battery system and the diesel-battery system from TABLE

5-4 and the rate of savings per year is obtained from the savings in the cost of fuel per year as given in TABLE 5-5.

Fig. 5-22 shows the sensitivity analysis of fuel cost on the payback period of the PV array.

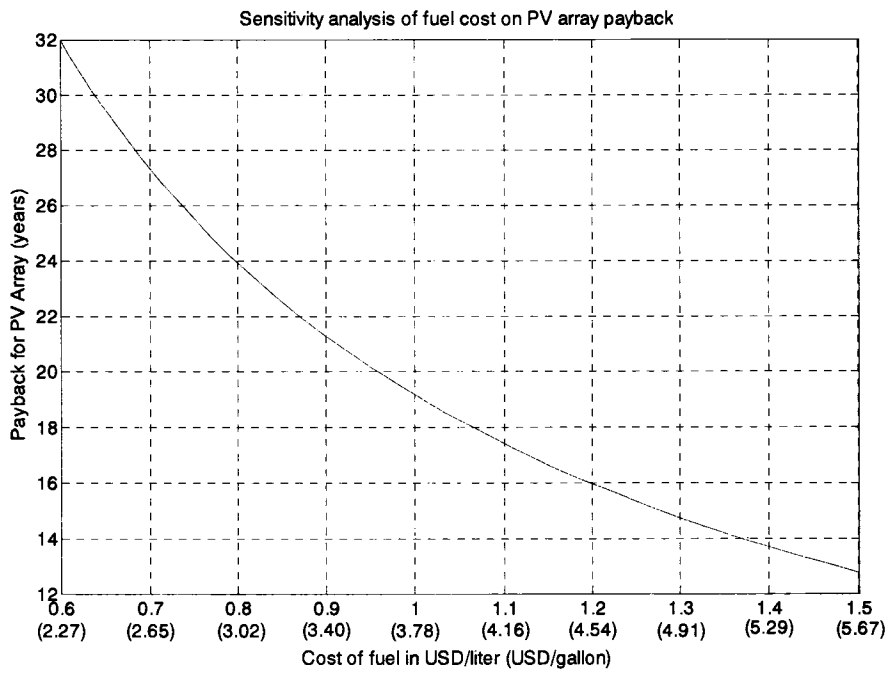

Fig. 5-22. Sensitivity analysis of fuel cost on PV array payback.

It can be seen that the payback period of the PV array decreases as a function of a fifth order polynomial with the increase in the cost of fuel. The payback period for the PV array follows a trend similar to the one described in Section 5.1.4.3 for the WTGs.

A large amount of energy is required in the construction of the PV array. In order to calculate the energy payback time (EPBT) for the PV array it is essential to know the energy required in the construction of the PV array, also called the embodied energy. In [64], Knapp and Jester describe a method to calculate the

embodied energy of a PV array. In this method, the total energy required is the sum of energies required for raw materials and the energy required in the various processes involved to convert the raw materials into the PV array. The embodied energy of a PV system is given as follows:

$$kWh_e = 5{,}600 * kW_p \text{ and} \tag{5-5}$$

$$EPBT = \frac{kWh_e}{\dot{E}} \tag{5-6}$$

where kWh_e is the embodied energy, the number 5,600 is the amount of energy (kWh) required in the production of a 1 kW PV array [64], kW_p is the rated power (kW) of the PV array, and $\dot{E}$ (kWh/year) is the energy generation rate of the PV array.

For Lime Village the PV array is rated to produce 12 kW and from TABLE 5-5 the value for $\dot{E}$ is 9445 kWh/yr.

$$\therefore kWh_e = 5{,}600 * 12 = 67{,}200\,kWh \text{ and}$$

$$EPBT = \frac{67{,}200\,kWh}{9445\,kWh/year} = 7.11\,years.$$

It can be observed that in HOMER the energy generated by the diesel engine is higher because the battery bank is designed to cycle between 40% and 82% of its kWh rating rather than between 20% and 95% in the HARPSim model. The inverter and rectifier are operating with much less efficiency in HOMER as compared to the Simulink® model (about 20% difference). In HOMER the DEG is loaded anywhere between 6.3 kW to 21 kW with the average load of 13.4 kW and

hence operates with a lower electrical efficiency than in the HARPSim model. In the HARPSim model the battery bank acts as a source of power. So whenever the DEG is 'on', it operates at 95% of its rated power, therefore with a higher electrical efficiency. If the load on the DEG is less than 95% of its rated power, the excess power is utilized to charge the battery bank. It can also be observed that the efficiencies for the diesel-battery and PV-diesel-battery models calculated in HARPSim are the same as those predicted by the HOMER software.

5.2.4.4 Calculation of Avoided Cost of Pollutants for Lime Village

The use of a PV array with DEGs in Lime Village results in decreased emissions. The cost associated with the difference in the amount of emitted pollutants is called the avoided cost of emissions. The avoided cost of different pollutants: carbon dioxide (CO_2), nitrogen oxide (NOx), and particulate matter (PM_{10}), for the Lime Village hybrid power system are calculated as described in Section 2.8.4 as follows:

$$AC = \frac{COE_L - COE_H}{E_H - E_L} = \frac{(61{,}946 - 61{,}735)\ \text{USD}}{(70.93 - 63.64)\ \text{tons}} = 28.94\ \text{USD/ton}$$

where 'AC' is the avoided cost in USD/metric ton (USD/US ton), 'COE_L' is the annual COE from the low emissions plant, 'COE_H' is the annual COE from the high emissions plant, 'E_H' is the amount of emissions from the high emissions plant in metric ton (US ton), and 'E_L' is the amount of emissions from the low emissions plant in metric ton (US ton).

Using Eq. (5-9) and the data from Section 5.2.4.2 the avoided costs for various pollutants for the fuel price of 1.057 USD per liter (4.00 USD per gallon) and an investment rate of 7% are calculated and are listed in TABLE 5-8.

TABLE 5-8. Avoided cost of emissions

Emission	Avoided costs
CO_2	28.94 USD/metric ton (26.31 USD/US ton)
PM_{10}	37.28 USD/kg (16.91 USD/pound)
NOx	1.52 USD/kg (0.69 USD/pound)

The avoided cost of CO_2 is in the range of estimates provided by the Intergovernmental Panel on Climate Change (IPCC) [65] which has estimated the cost for CO_2 capture at power stations to be in the range of 30 USD – 50 USD per metric ton (US tons) of avoided CO_2. The California Air Resources Board (CARB) [66] estimated a cost of about 25 USD per pound of PM_{10} avoided by retrofitting buses with diesel particle filters (DPF). CARB [67] also reported 23 USD and 13 USD per pound for PM_{10} and NOx, respectively, as averages paid for emissions offsets transactions in 35 California districts.

5.3 Kongiganak Village

Kongiganak Village is located on the west shore of Kuskokwim bay, about 451 miles west of Anchorage. The village is located at a northern latitude of 59.96° and a western longitude of 162.89° as shown in Fig. 5-23. According to the United States 2000 Census Bureau, Kongiganak Village has 90 housing units with 11 vacant. The village has one school attended by 116 students. Kongiganak Village has a marine climate with temperatures ranging from 6°F to 57°F, an average annual precipitation of 22 inches, and an average annual snowfall of 43 inches [68].

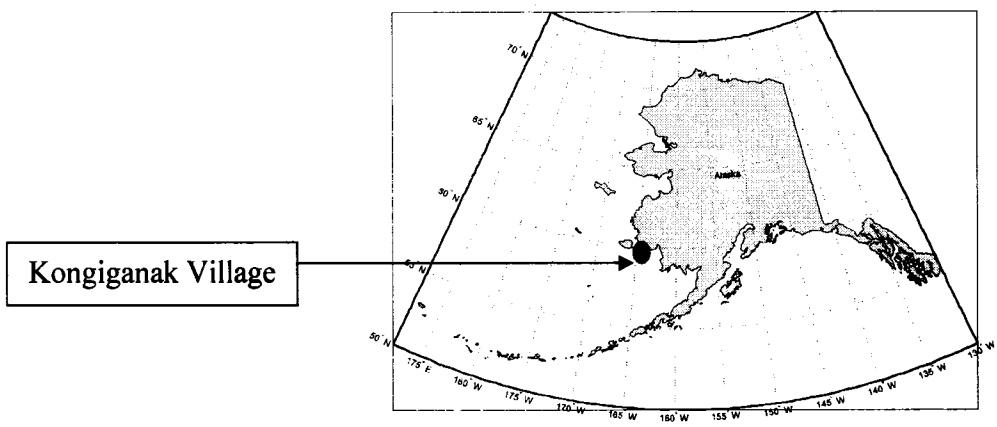

Fig. 5-23. Location of Kongiganak Village, Alaska.

The electricity in Kongiganak Village is provided by Puvurnaq Power Company with the help of 4 DEGs. In order to analyze the performance of the DEG system in the presence of a PV array and a WTG, simulations were performed using HARPSim for a PV-diesel-battery system, a wind-diesel-battery system, and a PV-wind-diesel-battery system. The simulation results were compared with those predicted by the HOMER software.

5.3.1 Kongiganak Village Hybrid Power System

The Kongiganak Village power system consists of four DEGs rated at 235 kW, 190 kW, 190 kW and 140 kW. One DEG is sufficient to supply the village load. Currently, a PV array and a WTG are not installed in the system.

The system performance is analyzed by incorporating a 100 kWh absolyte IIP battery bank (similar to the one installed at Lime Village), a 12 kW PV array (similar to the one installed at Lime Village, a 65 kW 15/50 AOC WTG (similar to the one installed at Wales Village), and a 100 kVA bi-directional power converter. The hybrid power system of Konginganak Village is as shown in Fig. 5-24.

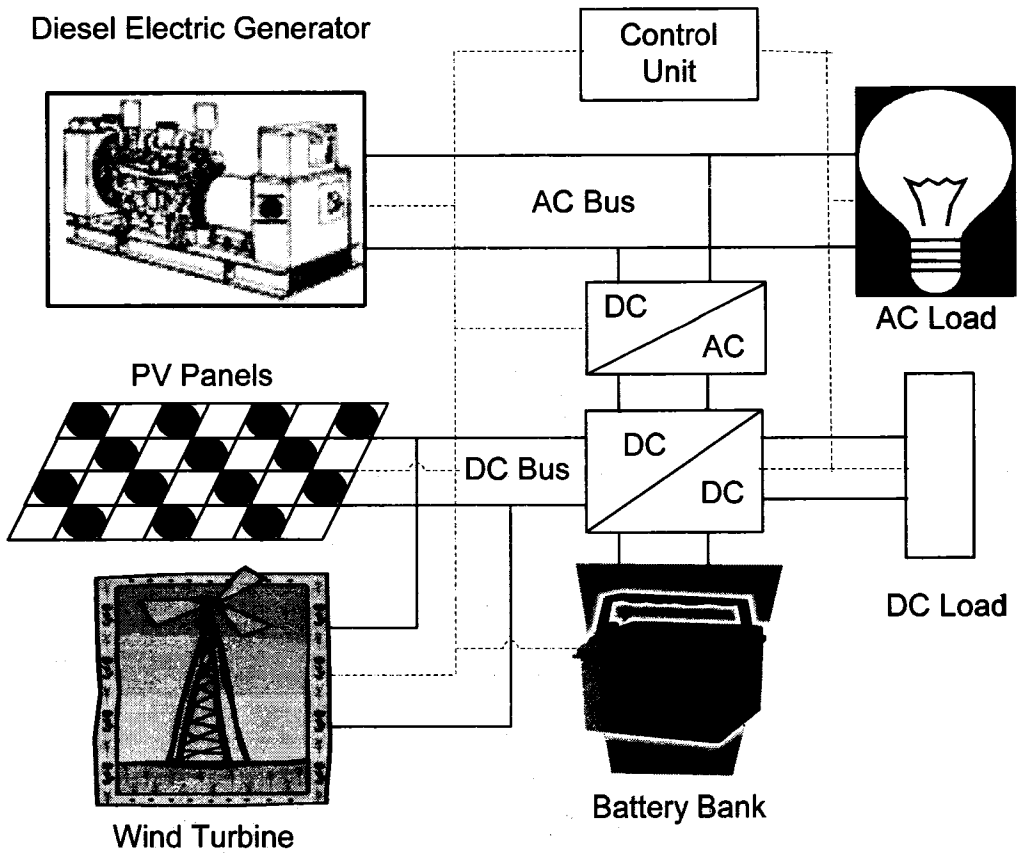

Fig. 5-24. Kongiganak Village hybrid power system.

5.3.2 Development of Kongiganak Village Model Using HOMER

The Kongiganak Village hybrid power system model is implemented using the HOMER software. Fig. 5-25 shows the front-end for the hybrid power system of Kongiganak Village as developed using the HOMER software. The system consists of two DEGs, a 12 kW PV array, a 100 kWh battery bank, a 100 kVA converter, a 65 kW 15/50 AOC WTG, and a primary AC load.

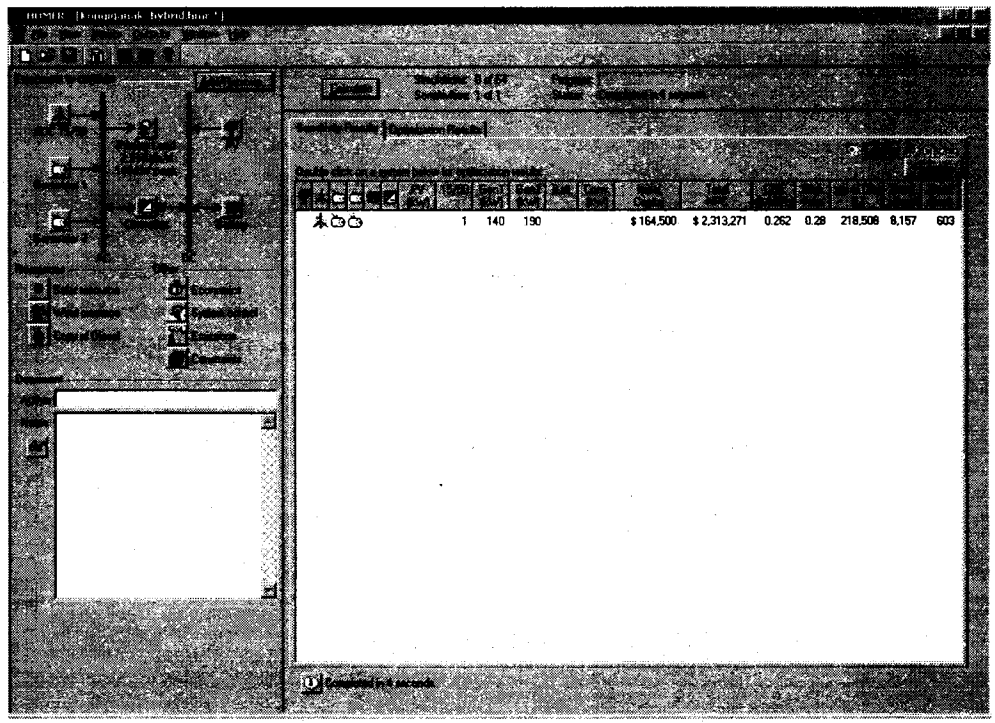

Fig. 5-25. Front-end of HOMER model for the Kongiganak Village power system.

5.3.3 Kongiganak Village Simulation

The annual synthetic load profile from January 1st, 2003 to December 31st, 2003 with one hour samples, the annual synthetic wind speed profile, and the annual solar flux profile used for analyzing the performance of the Kongiganak Village are shown in Fig. 5-26, Fig. 5-27, and Fig. 5-28, respectively. The clearness index data for the solar insolation profile is obtained using the solar maps developed by the National Renewable Energy Laboratory (NREL) [63]. It can be observed from Fig. 5-26 that the maximum load of the system is about 150 kW, the minimum load is about 45 kW and the average load is about 95 kW. From Fig. 5-27 it can be observed that the annual average wind speed is about 7 m/s (15.66 miles/hr). From Fig. 5-28 it can be observed that the village has low solar flux during winter months and high solar flux during summer months.

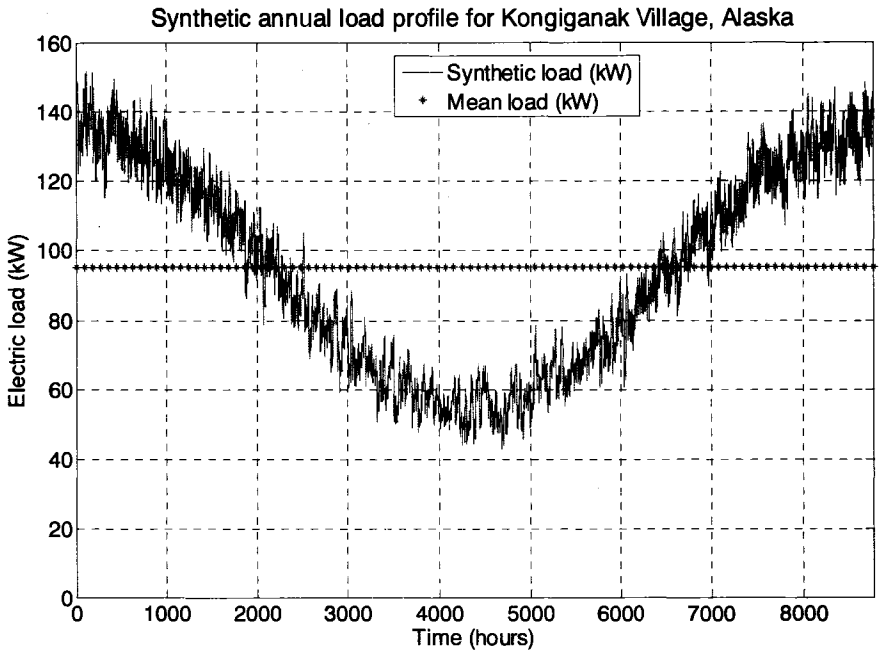

Fig. 5-26. Synthetic annual load profile for Kongiganak Village, Alaska.

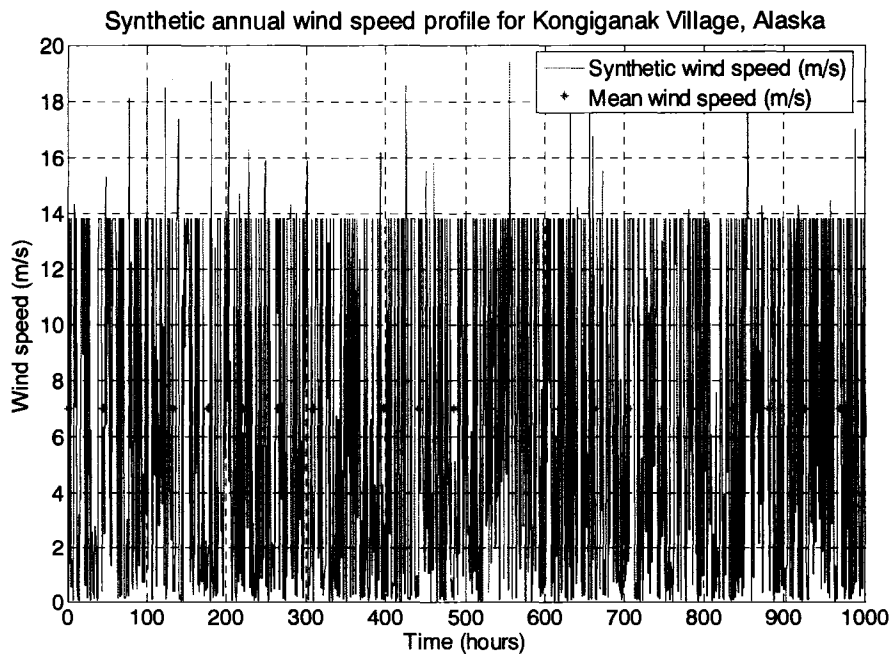

Fig. 5-27. Synthetic annual wind speed profile for Kongiganak Village, Alaska.

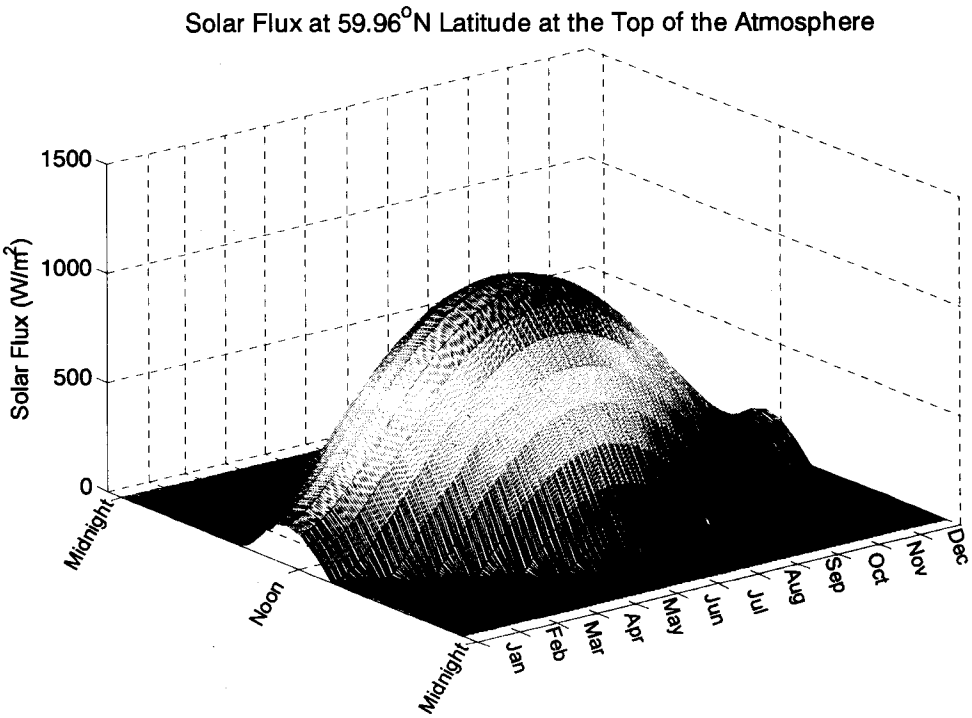

Fig. 5-28. Annual solar flux for Kongiganak Village, Alaska.

The following assumptions are made for the Kongiganak Village simulations:

(i) Interest rate $i = 7\%$.

(ii) Life cycle period for PV (n) = 20 years.

(iii) Life cycle period for diesel-battery system = 5 years.

(iv) Life cycle period for diesel-battery system when operating in conjunction with PV or WTG or both = 5.5 years.

5.3.4 Comparison of Kongiganak Village Results from HARPSim and HOMER

Simulations were performed for the Kongiganak Village hybrid power system using the annual load profile for four systems: (i) diesel-battery system, (ii) PV-diesel-battery system, (iii) wind-diesel-battery system, and (iv) PV-wind-diesel-battery system. TABLE 5-9 shows the installation cost (USD) for different components for the Kongiganak Village hybrid power system.

The post simulation results obtained from the HARPSim model were compared with those obtained from the HOMER software. TABLE 5-10 shows the comparison of results from the HARPSim model with HOMER for the Kongiganak Village hybrid power system. It can be observed from the table that the wind-diesel-battery system is the most cost effective system with the lowest NPV, COE, and payback period. This is because of the high energy available from the WTG. The WTG penetration level is observed as 28%. Due to its location, the solar flux available in this region is low resulting in low energy penetration from the PV array. The payback period of the WTG is obtained a little over a year and the payback period for the PV array and the WTG for the PV-wind-diesel-battery system is obtained as a little over two years. It can also be observed that the NPV of the wind-diesel-battery system using HARPSim is less than HOMER. This is because in HARPSim the battery bank charges and discharges while supplying the load. Therefore, the DEGs operate more efficiently resulting in the fuel savings while emitting less pollutant. This saving in the fuel is achieved at the expense of the battery life.

TABLE 5-9. Installation cost for different components for Kongiganak Village

Item	Cost per unit (USD)	No of units	Diesel-only system (USD)	Diesel-battery system (USD)	PV-diesel-battery system (USD)	Wind-diesel-battery system (USD)	PV-wind-diesel-battery system (USD)	2 wind-diesel-battery system (USD)
140 kW diesel generator	40,000	1	40,000	40,000	40,000	40,000	40,000	40,000
190 kW diesel generator	45,000	1	45,000	45,000	45,000	45,000	45,000	45,000
Switch gear to automate control of the system	16,000	1	16,000	18,000	20,000	20,000	22,000	30,000
Rectification/Inversion	18,000	1	0	18,000	18,000	18,000	18,000	28,000
New Absolyte IIP 6-90A13 battery bank	2,143	16	0	34,288	34,288	34,288	34,288	68,576
AOC 15/50 wind turbine generator	55,000	1	0	0	0	55,000	55,000	110,000
Siemens M55 solar panels	262	180	0	0	47,160	0	47,160	0
Engineering		1	3,000	3,500	4,000	4,000	4,500	6,000
Commissioning, Installation, freight, travel, miscellaneous		1	13,000	14,000	16,000	18,000	20,000	30,000
		TOTAL	**117,000**	**172,788**	**224,448**	**234,288**	**285,948**	**357,576**

TABLE 5-10. Comparison of results for Kongiganak Village with HOMER

Item	Diesel-battery system		PV-diesel-battery system		Wind-diesel-battery system		PV-wind-diesel-battery system	
	HARPSim	HOMER	HARPSim	HOMER	HARPSim	HOMER	HARPSim	HOMER
System cost (USD)	172,788	172,788	224,448	224,450	234,288	234,288	285,948	285,950
Engine efficiency (%)	29.3	28.63	29.3	28.51	29.3	27.03	29.3	26.88
kWh/liter (kWh/gallon) for the engine	3.11 (11.75)	3.04 (11.48)	3.11 (11.75)	3.02 (11.43)	3.11 (11.75)	2.87 (10.84)	3.11 (11.75)	2.85 (10.78)
Fuel consumed in liters (gallons)	267,662 (70,810)	273,910 (72,463)	264,834 (70,062)	272,568 (72,108)	193,249 (51,124)	216,027 (57,150)	190,837 (50,486)	214,776 (56,819)
Total cost of fuel (USD)	212,429	217,390	210,185	216,325	153,373	171,451	151,458	170,456
Energy supplied								
(a) Diesel engine (kWh)	832,152	832,205	823,368	823,422	597145	619,504	588,362	612,287
(b) WTG (kWh)	-	-	-	-	235,007	238,000	235,007	238,000
(c) PV array (kWh)	-	-	8,784	8,783	-	-	8,784	8,783
Energy supplied to load (kWh)	832,152	832,205	832,152	832,205	832,152	832,205	832,152	832,205
Operational life								
(a) Generator (years)	5	1.87	5	1.87	5	1.8	5	1.8
(b) Battery bank (years)	5	12	5.5	12	5.5	12	6	12
Net present value (USD) with i = 7% and n = 20 years	-	1,992,488	2,545,084	2,945,502	1,954,127	2,383,766	1,974,389	2,421,502
Cost of Electricity (USD/kWh)	0.301	22.6	0.304	0.334	0.237	0.27	0.24	0.275
Payback period for renewable (years)	-	-	Never	-	1.07	-	2.12	-
Emissions								
(a) CO_2 in metric tons (US tons)	660 (728)	703 (775)	653 (720)	700 (772)	477 (526)	555 (612)	471 (519)	552 (608)
(b) NOx in kg (lbs)	7,322 (16,143)	-	7,245 (15,972)	-	5,288 (11,657)	-	5,222 (11,512)	-
(c) PM_{10} in kg (lbs)	308 (679)	-	305 (672)	-	222 (490)	-	220 (484)	-

Since the wind-diesel-battery system was observed to be the most cost effective system, further work was carried out to study the effect of installing another WTG into the wind-diesel-battery system. The addition of a second WTG required an increase in the capacity of the battery bank to accommodate more energy storage. Therefore, the battery bank capacity and the inverter rating were increased from 100 kW and 100 kVA to 200 kW and 200 kVA, respectively.

TABLE 5-11 shows the comparison of results from the HARPSim model with HOMER for the two wind-diesel-battery hybrid power system for Kongiganak Village.

TABLE 5-11. Comparison of results for two wind-diesel-battery hybrid power system

Item	Two wind-diesel-battery system	
	HARPSim	HOMER
System cost (USD)	357,576	357,576
Engine efficiency (%)	29.3	26.6
kWh/liter (kWh/gallon) for the engine	3.11 (11.75)	2.78 (10.53)
Fuel consumed in liters (gallons)	151,252 (39,961)	201,444 (53,222)
Total cost of fuel (USD)	119,883	159,876
Energy supplied		
(a) Diesel engine (kWh)	469,542	561,741
(b) WTG (kWh)	470,015	475,999
Energy supplied to load (kWh)	832,152	832,205
Operational life		
(a) Generator (years)	5	1.8
(b) Battery bank (years)	5.5	12
Net present value (USD) with i = 7% and n = 20 years	1,748,988	2,407,895
Cost of Electricity (USD/kWh)	0.22	0.273
Payback period for WTG (years)	1.56	-
Emissions		
(a) CO_2 in metric tons (US ton)	367 (405)	517 (570)
(b) NOx in kg (lbs)	4,068 (9,112)	-
(c) PM_{10} in kg (lbs)	171 (383)	-

It can be observed that the addition of the second WTG into the wind-diesel-battery hybrid power system resulted in the further reduction in the NPV and the COE, while the payback period with the two WTGs increased slightly. The WTG penetration level increases to 50% for this case. The payback period of the WTGs has increased to 1.56 years due to the extra cost involved in the addition of the second WTG.

5.3.4.1 Comparison of LCC and NPV of Lime Village from HARPSim and HOMER

Fig. 5-29 and Fig. 5-30 show the LCC analysis of the PV-wind-diesel-battery hybrid power system for Kongiganak Village using HARPSim and HOMER, respectively. It can be seen that in HARPSim, the cost of DEGs in 4% less while the cost of battery bank is 2% more than in HOMER. This is because in HARPSim, the battery bank acts as a source of power rather than as the backup power source used in HOMER. Therefore, the life of the battery bank in less in HARPSim due to the annual increase in charge/discharge cycles. This results in more efficient operation of the DEGs while reducing the fuel consumption and saving in the cost of the DEGs. Overall, the LCC analysis shows a lower NPV in HARPSim than in HOMER.

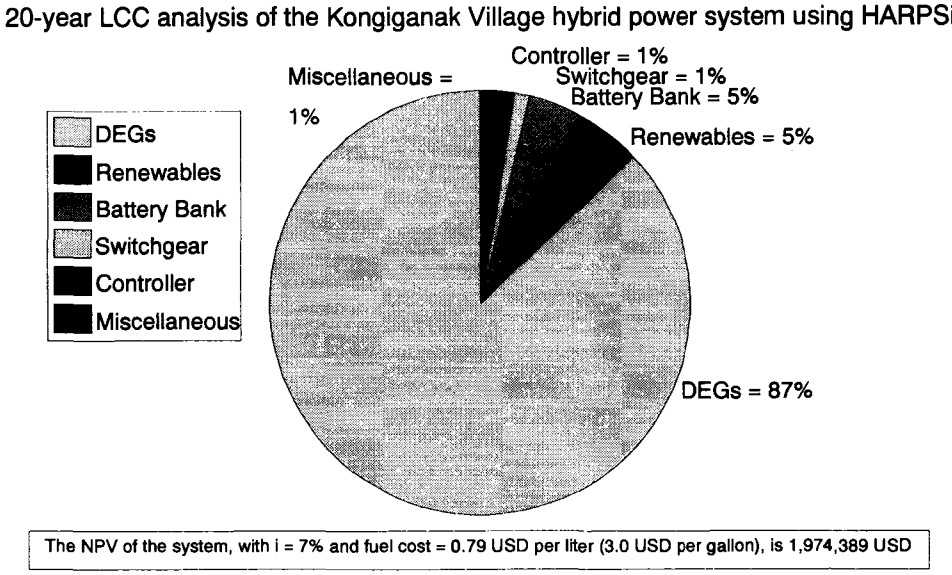

Fig. 5-29. 20-year LCC analysis of the Kongiganak Village hybrid power system using the Simulink® model.

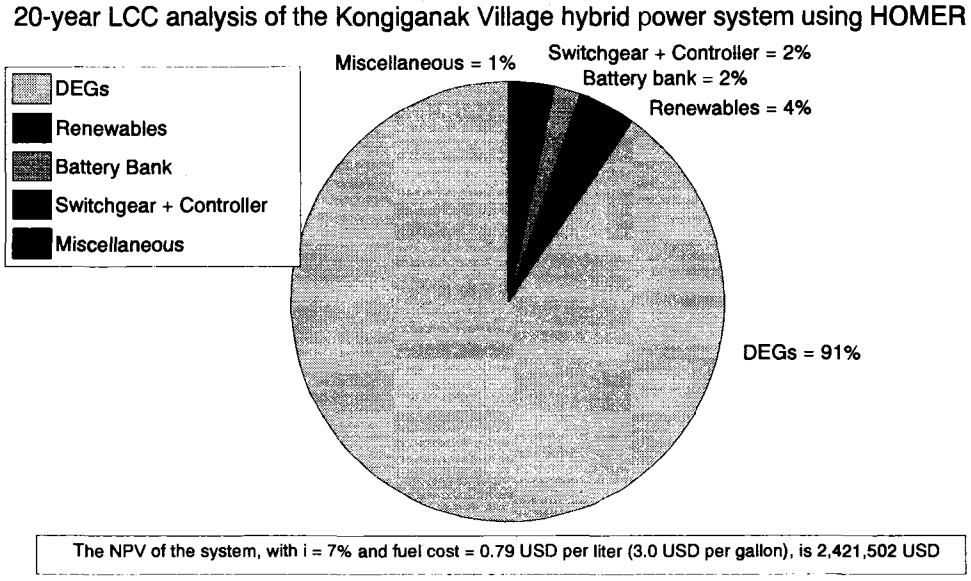

Fig. 5-30. 20-year LCC analysis of the Kongiganak Village hybrid power system using the HOMER software.

5.3.4.2 Sensitivity Analysis Results for Kongiganak Village

The sensitivity analysis plots for the Kongiganak Village hybrid power system are similar to the sensitivity analysis plots for the Wales Village hybrid power system and the Lime Village hybrid power system as explain in Section 5.1.4 and Section 5.2.4. The plots of sensitivity analysis of fuel costs and investment rate on the NPV, the COE, and the payback period for the PV-wind-diesel-battery system are shown in Fig. 5-31, Fig. 5-32 and Fig. 5-33, respectively.

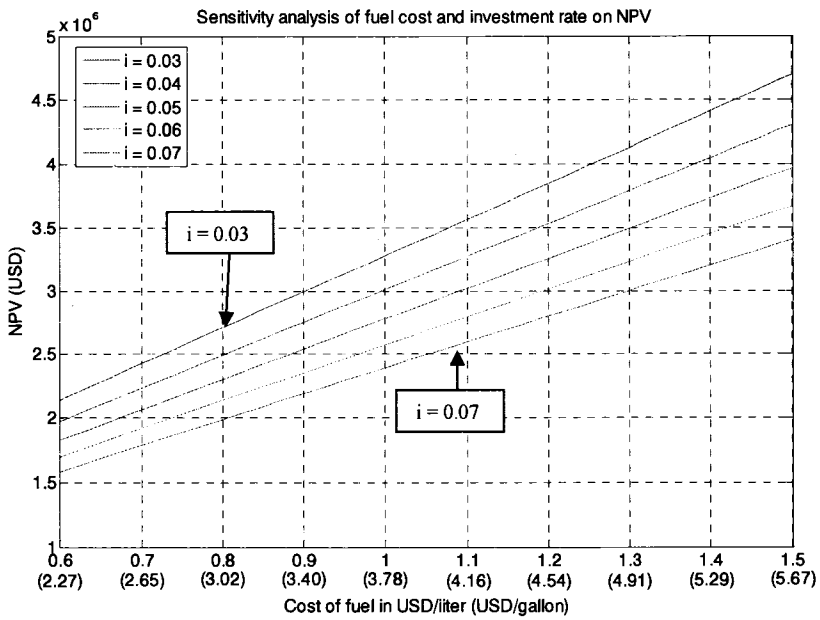

Fig. 5-31. Sensitivity analysis of fuel cost and investment rate on the NPV.

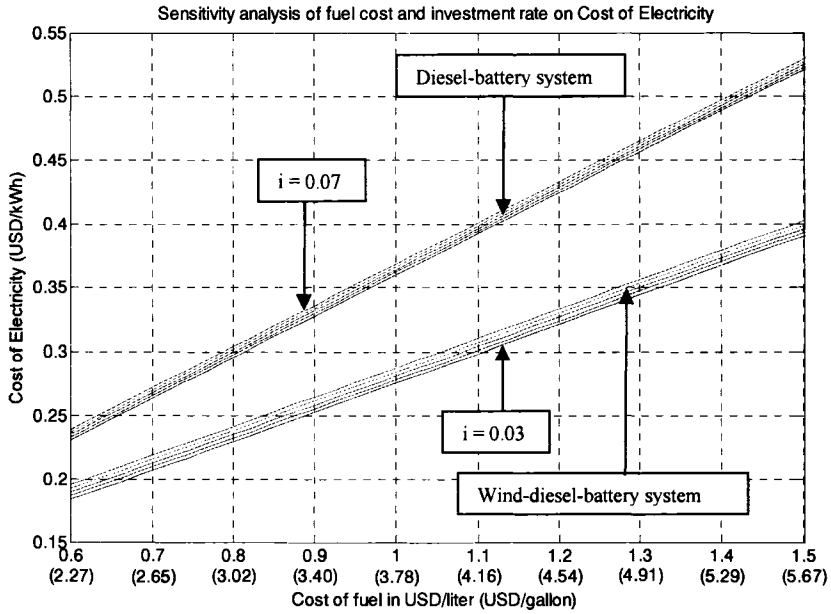

Fig. 5-32. Sensitivity analysis of fuel cost and investment rate on the COE.

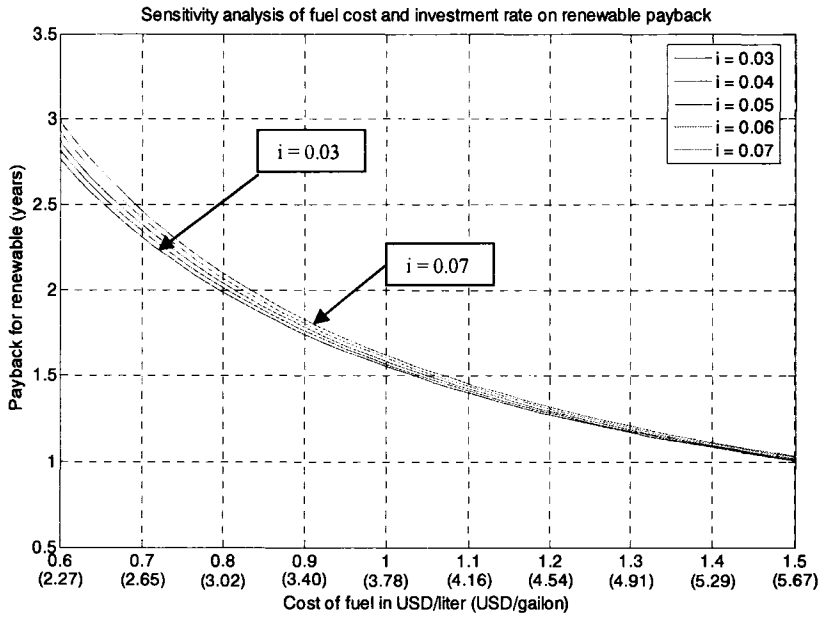

Fig. 5-33. Sensitivity analysis of fuel cost and investment rate on the payback period.

This chapter described the use of the HARPSim model for analyzing the long-term performance of three systems:

1) The wind-diesel-battery hybrid power system of Wales Village, Alaska.
2) The PV-diesel-battery hybrid power system of Lime Village, Alaska.
3) The design of a PV-wind-diesel-battery hybrid power system for Kongiganak Village, Alaska.

The sensitivity analysis of fuel cost and investment rate on the NPV, the COE, and the payback period were studied for the three villages. The environmental analysis involved the avoided cost calculations for different pollutants. The results obtained from the HARPSim model were in close agreement with those predicted by the HOMER software.

Chapter 6 will summarize this dissertation and present conclusions based on for the various hybrid power system models. The latter part of Chapter 6 will describe the scope for future work in the development of the HARPSim model.

6 Summary, Conclusions, and Scope for Future Work

6.1 Summary

This dissertation focused on the need for developing more efficient hybrid power systems for remote arctic villages. Various technical challenges for studying the performance of hybrid power systems for arctic villages include the lack of data and poor power quality data, lack of DEG optimization techniques, remoteness of the site, harsh environmental conditions, high fuel costs, and new environmental standards. In order to study the performance of hybrid power systems in remote arctic villages, the development of a software analysis tool was necessary.

This dissertation presents the development of simulation software called HARPSim to study the performance of hybrid power systems for remote arctic villages. HARPSim can produce synthetic system data, optimize multiple DEGs, model the system performance in arctic climates, and compute the economic and environmental parameters of the system. The various economic parameters involved in the study included the LCC analysis of the system, the payback period calculation, and the COE calculation. The environmental analysis part included the avoided cost calculation for various pollutants including CO_2, NOx, and PM_{10}.

Various system components modeled in HARPSim include a DEG model, a heat exchanger model, a boiler model, a WTG model, a PV array model, and a battery bank model. These component models were developed using MATLAB® Simulink®. The component models were validated and integrated to form different hybrid power systems. The validation process for the DEG model involved the comparison of results obtained from HARPSim for the UAF Energy Center DEG system with those obtained from the Nexus RTU and the HOMER software. The validation process for the PV array and the WTG involved the comparison of results obtained from the HARPSim model with those obtained from the HOMER

software. The results obtained from the Nexus RTU and the HOMER software for the DEG system and the HOMER software for the PV array and the WTG were in close agreement with those obtained from the HARPSim model.

The different hybrid power system models developed in HARPSim are: the diesel-battery model, the wind-diesel-battery model, the PV-diesel-battery model, and the PV-wind-diesel-battery model. HARPSim was used to study the performance of the following systems:

1) A wind-diesel-battery system installed at Wales Village, Alaska.
2) A PV-diesel-battery system installed at Lime Village, Alaska.
3) A PV-wind-diesel-battery system design for Kongiganak Village, Alaska.

The results obtained for the wind-diesel-battery system of Wales Village, the PV-diesel-battery system of Lime Village, and the PV-wind-diesel battery system designed for Kongiganak Village were is close agreement with those predicted by the HOMER software.

6.2 Conclusions

The preliminary results reported here demonstrate that the integration of a WTG and a PV array into a diesel-battery stand-alone hybrid power system reduces the operating costs, the greenhouse gases, and particulate matter emitted to the atmosphere. The sensitivity analysis of fuel cost and investment rate showed that as the price of fuel rises at the global level, the payback period of the WTG and the PV array decreases. The COE and the NPV increases linearly with the increase in the fuel price.

The wind-diesel-battery hybrid power system of Wales Village has been in reliable operation since the summer of 2000. A Simulink® model for the hybrid

power system was developed. The model was validated by comparing the results obtained from the Simulink® model, for supplying an annual load profile, with those obtained from the HOMER software. The LCC and air emissions results of the Simulink® model were comparable with those obtained from the HOMER software. It was observed that the COE for the wind-diesel-battery hybrid power system is less than the COE for the diesel-battery system, thus making the wind-diesel-battery system more economical while emitting less pollution. The payback period of the WTG with a fuel cost of 0.793 USD per liter (3.00 USD per gallon) was less than 5 years and it decreases with the increase in the cost of fuel.

The PV-diesel-battery hybrid power system of Lime Village has been in reliable operation since July 2001. A Simulink® model for the hybrid power system was developed. The model was validated by comparing the results obtained from the Simulink® model, for supplying an annual load profile, with those obtained from the HOMER software. The LCC and air emissions results of the Simulink® model were comparable to those obtained from the HOMER software. Although there is a significant capital investment to purchase a PV system for this application, the PV system may have acceptable 20-year life cycle costs for many remote locations. Furthermore, over its life cycle the PV-diesel-battery hybrid power system will consume less fuel and emit less CO_2, NOx, and PM_{10} than the diesel-battery system. If the external costs associated with these emissions are taken into account, the PV system payback period will decrease further, thus making these systems more viable and affordable. A simple payback period for the PV array of Lime Village with a fuel cost of 1.057 USD per liter (4.00 USD per gallon) was about 18 years and it decreases with the increase in the cost of fuel.

Currently, DEGs are the only source of power for the load demand of the Kongiganak Village, Alaska. HARPSim was used to study the feasibility of integrating a PV array, a WTG, and a battery bank with the existing DEGs to meet the village load demand. Various hybrid power systems studied in this analysis

include the diesel-battery system, the PV-diesel-battery system, the wind-diesel-battery system, and the PV-wind-diesel-battery system. The hybrid power system models were validated by comparing the results obtained from HARPSim, for supplying an annual load profile, with those obtained from the HOMER software. A payback period for the PV array and the WTG for the PV-wind-diesel-battery system, with a fuel cost of 0.79 USD per liter (3.00 USD per gallon), was about 2.1 years and it decreases with the increase in the cost of fuel. The payback period for the WTG for the wind-diesel-battery system, with a fuel cost of 0.79 USD per liter (3.00 USD per gallon), was about one year and decreases with the increase in the cost of fuel. The addition of second WTG in the wind-diesel-battery system increased the payback period of the WTGs, but improved the system economics. Overall, the two wind-diesel-battery system was the most cost effective system with lowest NPV and COE.

The rising price of crude oil, the depleting oil resources, the developments in the energy storage technologies, reduced installation costs of WTGs, increasing efficiency of photovoltaic cells, growing pollutant taxes in some parts of the world, and newly emerging renewable energy technologies are encouraging the use of hybrid power systems. These hybrid power systems combine renewable energy sources with other fossil fuel based energy sources like oil and gas while optimizing the system economics. Hybrid energy systems which result in more economical and efficient generation of electrical energy would not only enhance the capability of automated and precision generation systems, but would also help to extend the life of non-renewable energy sources.

6.3 Scope for Future Work

In this project, the hybrid power system analysis tool developed is used to study the long term performance of the system by performing LCC analysis, COE analysis, payback analysis, and the avoided cost of pollutant analysis. Further work

needs to be carried out to study the dynamic effects of load fluctuations, wind speed and direction fluctuations, and solar flux variations on the system. Thus, dynamic analysis components need to be incorporated into the Simulink® model for more thorough analysis.

Currently, HARPSim can model a maximum of two DEGs. In the future, multiple DEGs can be integrated and an optimizing technique can be developed to supply the load at the maximum possible efficiency. Various other energy sources including biomass, hydro-electric power, geothermal, nuclear, flywheels, flow batteries, and various energy converting devices including transformers, fuel cells, DC-DC converters, and DC-AC converters can be modeled and integrated into HARPSim to study the performance of the hybrid power system.

A controller can be programmed using Simulink® and can be integrated with HARPSim via the Hardware in the Loop (HIL) feature of Simulink® to control real time operations of the hybrid power systems in remote locations through the secure networks. Furthermore, work needs to be carried out to develop and maintain a secure network so that users can download and use HARPSim.

Also, studies need to be carried out by incorporating a Maximum Power Point Tracker (MPPT) with the PV array and the WTG. The use of a MPPT would increase the power obtained from the PV array and the WTG, but at the same time the system will be more complex to control. The benefit to cost ratio will play an important role in the decision process of installing a MPPT with the system.

With the rising oil prices and depleting oil resources, hybrid energy systems containing wind, PV, and other renewable energy sources are promising future energy technologies for remote arctic communities.

7 References

1. Agrawal, A. N., "Modeling and Optimization of Hybrid Electric Power Systems for Remote Locations in Extreme Northern Climates", Master's Thesis, *University of Alaska Fairbanks*, Fairbanks, AK, Aug 2003.
2. Wies, R. W., Johnson, R. A., Agrawal, A. N., and Chubb, T. J., "Using HOMER and Simulink® for Long-Term Performance Analysis of a Hybrid Electric Power System in a Remote Alaskan Village", *Proceedings of the 2004 NREL World Renewable Energy Congress VIII*, Denver, CO, 2004.
3. Wies, R. W., Johnson, R. A., and Agrawal, A. N., "Integration of Wind-Turbine Generators (WTGs) into Hybrid Distributed Generation Systems in Extreme Northern Climates", poster presentation at the *Rural Energy Conference*, Valdez, AK, 2005.
4. Provol, S and Coleman, M., "Renewable Energy and Fuels: In the Mainstream", *Power Engineering Magazine*, p. 6, Mar 2006.
5. Alaska Energy Policy Task Force, "Statewide Energy Issues – An Overview", a *report prepared by AIDEA and AEA*, Anchorage, Alaska, Sep 2003.
6. Gutierrez-Vera, J., "Options for Rural Electrification in Mexico", *IEEE Transactions on Energy Conversion*, Vol. 7, No. 3, pp. 426-433, 1992.
7. Kruangpradit, P. and Tayati, W., "Hybrid Renewable Energy System Development in Thailand", *Proceedings of the 1996 World Renewable Energy Congress of Renewable Energy*, pp. 514-517, 1996.
8. Drouilhet, S. and Shirazi, M., "Wales, Alaska High-Penetration Wind-Diesel Hybrid Power System, Theory of Operation", *National Renewable Energy Laboratory*, Golden, Colorado, NREL/TP-500-31755, May 2002.
9. Reeve, B., "Kotzebue Wind Farm Operational Experience", *Wind Diesel Workshop 2004*, Anchorage, AK, 2004.

10. TDX Power, "St. Paul, Alaska Operational Experience", *Wind Diesel Workshop 2004*, Anchorage, AK, 2004.
11. Meiners, D. "Lime Village Power System Alternatives", *Alaska Energy Authority*, 2001.
12. Official Webpage for the Department of Energy, "Geothermal Technologies Program: Alaska", Available at: http://www.eere.energy.gov/geothermal/pdfs/36548.pdf, accessed Oct 8th, 2005.
13. Conner, A. M. and Francfort, J. E., "US Hydropower Resource Assessment for Alaska", *U.S. Department of Energy*, Contract DE-AC07-94ID13223, Nov 1997.
14. Mark A. Foster and Associates, "Rural Alaska Energy Plan: Initiatives Aimed at Improving Rural Energy Efficiency and Reliability, Draft Diesel Efficiency Chapter", *a report prepared for Alaska Energy Authority*, Anchorage, Alaska, Dec 2002.
15. Official Webpage for the US Department of Energy, available at http://www.eia.doe.gov/emeu/international/energyconsumption.html, accessed Dec 12th, 2005.
16. US Department of Energy Website, available at http://www.energy.gov/news/1919.htm, accessed Mar 22nd, 2006.
17. Energy Information Administration, "International Energy Outlook 2005", *a report prepared by Department of Energy, Energy Information Administration*, report # DOE/EIA – 0484 (2005), Jul 2005.
18. Fariley, P., "Steady as She Blows", *IEEE Spectrum*, pp. 35-39, Aug 2003.
19. Australia Wind Energy Association. "A Progress Report on Australian Wind Energy Industry", available online at http://www.auswea.com.au/auswea/downloads/Tradewinds_report.pdf, accessed Apr 2006.

20. Somers, D. M., "The S827 and the S828 Airfoils Period of Performance: 1994-1995", *a report prepared by Airfoils, Inc., National Renewable Energy Laboratory*, report # NREL/SR – 500 – 36343, Jan 2005.
21. Tangler, J. M. and Somers, D. M., "Airfoils for Wind Turbines", *US Patent # 5,562,420*, Oct 1996.
22. Olsen, T., Lang, E., Hansen, A. C., Cheney, M. C., Quandit, G., Vandenbosche, J., and Meyer, T., "Low Wind Speed Turbine Project Conceptual Design Study: Advanced Independent Pitch Control", *a report prepared by Advanced Energy System, Inc. et al, National Renewable Energy Laboratory*, report # NREL/SR – 500 – 36755, Dec 2004.
23. Erdman, W. and Behnke, M., "Low Wind Speed Turbine Project Phase II: The Application of Medium – Voltage Electrical Apparatus to the Class of Variable Speed Multi – Megawatt Low Wind Speed Turbines", *a report prepared by Behnke, Erdman & Whitaker Engineering, National Renewable Energy Laboratory*, report # NREL/SR – 500 – 38686, Nov 2005.
24. Bir, G. and Migliore, P., "Preliminary Structure Design of Composite Blades for Two and Three-Blade Rotors", *a report prepared by Midwest Research Institute, National Renewable Energy Laboratory*, report # NREL/TP – 500 – 31486, Sep 2004.
25. Official Webpage for the United States Department of Energy, available at http://www.eere.energy.gov/RE/solar_photovoltaics.html, accessed Feb 7th, 2006.
26. Official Webpage for the United States Department of Energy, available at http://www.eia.doe.gov/kids/energyfacts/sources/renewable/geothermal.html, accessed Jul 8th, 2006.
27. Official Webpage for the University of Alaska, available at http://www.uaf.edu/energyin/webpage/pages/renewable_energy_tech/geothermal.htm, accessed Jul 8th, 2006.

28. Official Webpage for the Chena Hot Springs Resort, available at http://www.yourownpower.com/, accessed Jul 2006.
29. Sale, M. J., Cada, G. F., Carlson, T. J., Dauble, D. D., Hunt, R. T., and Sommers, G. L., "DOE Hydropower Program Annual Report for FY 2002", *a report prepared by Oak Ridge National Lab et al , United States Department of Energy*, report # DOE/ID-11107, Jul 2003.
30. National Renewable Energy Laboratory, "Biofuel for Sustainable Transportations", *a report prepared by National Renewable Energy Laboratory, United States Department of Energy*, report # DOE/GO-102000-0812, Jun 2000.
31. Official Webpage for the National Renewable Energy, available at http://www.nrel.gov/otec/, accessed Mar 22nd, 2006.
32. Farret, F and Simoes, M. G., "Integration of Alternative Sources of Energy", *John Wiley and Sons, Inc.*, Chapter 15, pp. 379-418, 2006.
33. Official Webpage of Maui Solar Energy Software Corporation, available at http://www.mauisolarsoftware.com/, accessed May 2006.
34. Valentin Energie Software, "User Manual for PV*SOL® Version 2.4", Available online at http://www.valentin.de/downloads/docu/pvsolshortmanual.pdf, accessed May 2006.
35. Official Webpage for RETScreen®, Available at http://www.retscreen.net/, accessed May 2006.
36. Manwell, J. F., McGowan, J. G., and Abdulwahid, U., "Simplified Performance Model for Hybrid Wind Diesel Systems", available online at http://www.ceere.org/rerl/projects/software/WindScreenPaper.pdf, accessed May 2006.
37. Official Webpage for Mistaya Engineering Inc., available at http://www.mistaya.ca/products/windographer.htm, accessed Jul 8th, 2006.

38. Malosh, J. A. and Johnson, R. A., "Part-Load Economy of Diesel-Electric Generators", *a report prepared for Department of Transportation and Public Facilities*, report # AK-RD-86-01, Jun 1985.

39. Sonntag, R. E., Borgnakke, C., and Wylen, G. J. V., "Fundamentals of Thermodynamics", *John Wiley & Sons, Inc.*, Fifth Edition, 1998.

40. Official Webpage for the Atlantic Orient Corporation, available online at http://www.aocwind.net/1550brochure.pdf, accessed Nov 2002.

41. Patel, M., "Wind and Solar Power Systems", *Florida: CRC Press LLC*, 1St Edition, 1999.

42. Official Webpage of the National Renewable Energy, available at http://www.nrel.gov/gis/solar.html, accessed Mar 22nd, 2006.

43. Winsor, W. D. and Butt, K. A., "Selection of Battery Power Supplies for Cold Temperature Application", *Technical report, C-CORE Publication* No. 78-13, Sep 1978.

44. Sandia National Laboratories, "Stand-Alone Photovoltaic Systems - A Handbook of Recommended Design Practices", *a report prepared by Sandia National Laboratories*, report # SAND87-7023, Mar 1995.

45. Official Webpage of the United States Environmental Pollution Agencies, available at http://yosemite.epa.gov/OAR/globalwarming.nsf/content/Emissions.html, accessed Mar 28th, 2006.

46. Robinson, A. B., Baliunas, S. L., Soon, W., and Robinson, Z. W., "Environmental Effects of Increased Atmospheric Carbon Dioxide", *Oregon Institute of Science and Medicine*, available at http://www.oism.org/pproject/s33p36.htm, accessed Mar 28th, 2006.

47. Cengel, Y. A. and Boles, M. A., "Engineering Thermodynamics", *McGraw Hill Publications*, 4th ed., 2002.

48. United States Environmental Protection Agencies (USEPA), "Evaluating Ozone Control Programs in the Eastern United States: Focus on the NOx

trading budget Program, 2004", *a report prepared by USEPA*, report # EPA 454-K-05-001, Aug 2005.

49. Official Webpage for the United States Environmental Pollution Agencies, available at http://www.epa.gov/oar/particlepollution/health.html, accessed Mar 28th, 2006.
50. Narula, R. G., Wen, H., Himes, K., and Power, B., "Incremental Cost of CO_2 Reduction in Power Plants", *ASME Turbo Expo*, 2002.
51. Devine, M and Baring-Gould, E. I., "Alaska Village Electric Load Calculator", *a report prepared by the National Renewable Energy Laboratory*, report # NREL/TP-500-36824, Oct 2004.
52. Hartmann, D. L., "Global Physical Climatology", *Academic Press*, 1994.
53. Chubb, T., "Performance Analysis for Remote Power Systems in Rural Alaska", Master's thesis, *University of Alaska Fairbanks*, Fairbanks, AK, Dec 2004.
54. Johnson, R. A. "Cogeneration and Diesel Electric Power Production", *University of Alaska Fairbanks*, Fairbanks, AK, Sep 1989.
55. Official Webpage of House needs, available at http://www.houseneeds.com/shop/HeatingProducts/HydronicHeating/heatexchangers/shellandtube/shellandtubebuypage.asp, accessed Apr 2006.
56. Official Website of NASA, available at http://eosweb.larc.nasa.gov/cgi-bin/sse/sse.cgi?na#s03, accessed Apr 2006.
57. Wikipedia Official Webpage, http://en.wikipedia.org/wiki/Wales,Alaska #Demographics, accessed Apr 2006.
58. Official Webpage for the Department of Commerce, available at http://www.commerce.state.ak.us/dca/commdb/CF_BLOCK.cfm, accessed Apr 2006.
59. Drouilhet, S., "Overview of the High Penetration Wind-Diesel System in Wales, Alaska", *Wind Diesel Workshop 2004,* Anchorage, AK, 2004.

60. Official Webpage for the Alaska Wilderness Recreation and Tourist Association, available at http://www.awrta.org/comminfo/communities.cfm?city=Lime % 20Village, accessed May 2006.
61. Official Webpage for the Department of Commerce, available at http://www.commerce.state.ak.us/dca/commdb/CIS.cfm?Comm_Boro_name=Lime%20Village, accessed May 2006.
62. Official Webpage of School at Lime Village, available at http://lvd.schoolaccess.net/, accessed, May 2006.
63. Official Webpage of National Renewable Energy Laboratory, available at http://rredc.nrel.gov/solar, accessed Oct 2003.
64. Knapp, K. E. and Jester, T. L., "PV Payback", *Home Power # 80*, Dec 2000.
65. Official webpage of Intergovernmental Panel on Climate Change, available at http://www.grida.no/climate/ipcc, "Climate Change 2001: Working Group III: Mitigation: 3.8.4.4 Technical CO_2 Removal and Sequestration", accessed Nov 2003.
66. Official Webpage of California Resources Board, available at http://www.arb.ca.gov/regact/bus02/appf.pdf, "Staff Analysis of PM Emission Reductions and Cost-Effectiveness, Appendix F", accessed Nov 2003.
67. Kats, G., "The Costs and Financial Benefits of Green Buildings", *a report prepared for California's Sustainable Building Task Force*, 2003.
68. Official Webpage of Communities and Fisheries, available at http://www.beringsea.com/communities/index.php?community=198, accessed Jul 2006.
69. Wies, R. W., Johnson R. A., and Agrawal, A. N., "Life Cycle Cost Analysis and Environmental Impacts of Integrating Wind-Turbine Generators (WTGs) into Standalone Hybrid Power Systems", *WSEAS Transactions on Systems*, Issue 9, Vol. 4, 1383-1393, Aug 2005.

70. Wies, R. W., Johnson, R. A., Agrawal, A. N., and Chubb, T. J., "Simulink® Model for Economic Analysis and Environmental Impacts of a PV with Diesel-Battery System for Remote Villages", *IEEE Transactions on Power Systems*, Vol. 20, No. 2, 692-700, May 2005.

71. Wies, R. W., Agrawal, A. N., and Chubb, T. J., "Optimization of a PV with Diesel-Battery System for Remote Villages", *International Energy Journal*, Vol. 6, No.1, part 3, 107-118, May 2005.

8 Appendices

Appendix 1: Data-Sheet for Marathon Electric Generator

MARATHON ELECTRIC GENERATORS

TYPICAL SUBMITTAL DATA

Section 3600

Page 25

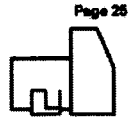

10/31/2001

MODEL : 283PSL1506

BASE MODEL: 283PSL1506 Winding WC- 1506

Submittal Data: 480 Volts*, 25 kW, 31.25 kVA, 0.8 P.F., 1800 RPM, 60 Hz, 3 Phase

Kilowatt ratings at	1800 RPM	60 Hertz	12 LEADS	Standard 3 phase					
kW (kVA)	3 Phase	0.8 Power Factor					Dripproof or Open Enclosure		
	Class B	Class F					Class H		
Voltage*	80° C ① Continuous	90° C ① Lloyds	95° C ① ABS	105° C British Standard	105° C Continuous	130° C ① Standby	125° C British Standard	125° C Continuous	150° C ① Standby
480/240	20 (25)	21 (26.3)	22 (27.5)	23 (28.8)	23 (28.8)	25 (31.3)	24 (30)	25 (31.3)	27 (33.8)
460/230	20 (25)	21 (26.3)	22 (27.5)	23 (28.8)	23 (28.8)	25 (31.3)	24 (30)	25 (31.3)	27 (33.8)
440/220	20 (25)	21 (26.3)	22 (27.5)	23 (28.8)	23 (28.8)	25 (31.3)	24 (30)	25 (31.3)	27 (33.8)
416/208	20 (25)	21 (26.3)	22 (27.5)	23 (28.8)	23 (28.8)	25 (31.3)	24 (30)	25 (31.3)	26 (32.5)
380/190	18 (22.5)	19 (23.8)	20 (25)	20 (25)	21 (26.3)	22 (27.5)	21 (26.3)	22 (27.5)	23 (28.8)

①Rise by resistance method, Mil-Std-705, Method 650.1b. British Standard Rating per BS 5000

Submittal Data: 480 Volts*, 25 kw, 31.25 kVA, 0.8 P.F., 1900 RPM, 60 Hz, 3 Phase STD. CONNECTION

Mil-Std-706B Method	Description	Value
301.1b	Insulation Resistance	>1.5 Meg
302.1a	High Potential Test	
	Main Stator	2000 Volts
	Main Rotor	1500 Volts
	Exciter Stator	1500 Volts
	Exciter Rotor	1500 Volts
	PMG Stator	NS**
401.1a	Stator Resistance, Line to Line	
	High Wye Connection	0.681 Ohms
	Rotor Resistance	0.654 Ohms
	Exciter Stator	23 Ohms
	Exciter Rotor	0.12 Ohms
	PMG Stator	NS**
410.1a	No Load Exciter Field Amps at 240/480 Volts Line to Line	0.48 A DC
420.1a	Short Circuit Ratio	0.571
421.1a	Xd Synchronous Reactance	2.05 p.u.
		14.951 ohms
422.1a	X2 Negative Sequence React.	0.182 pu
		1.327 ohms
423.1a	X0 Zero Sequence Reactance	0.052 pu
		0.379 ohms
425.1a	X'd Transient Reactance	0.139 pu
		1.014 ohms
426.1a	X"d Subtransient Reactance	0.118 pu
		0.861 ohms
--	Xq Quadrature Synch. React.	Not Available
427.1a	T'd Transient Short Circuit Time Constant	0.03 sec.
428.1a	T"d Subtransient Short Circuit Time Constant	0.009 sec.
430.1a	T'do Transient Open Circuit Time Constant	0.45 sec
432.1a	Ta Short Circuit Time Constant of Armature Winding	0.007 sec.

Mil-Std-705B Method	Description	Value
505.3b	Overspeed	2250 RPM
507.1c	Phase Sequence CCW-ODE	ABC
508.1c	Voltage Balance, L-L or L-N	0.20%
601.4a	L-L Harmonic Maximum - Total (Distortion Factor)	3.0%
601.4a	L-L Harmonic Maximum - Single	2.5%
601.1c	Deviation Factor	6.0%
---	TIF (1960 Weightings)	< 50
---	THF (IEC, BS & NEMA Weightings)	< 2 %
652.1a	Shaft Current	< 0.1 ma
---	Main Stator Capacitance to ground	@NA mfd
	Additional Prototype Mil-Std Methods are Available on Request.	
--	Generator Frame	283
--	Type	MAGNAPLUS
--	Insulation	Class H
--	Coupling - Single Bearing	Flexible
--	Amortisseur Windings	Full
--	Excitation	Ext. Voltage Regulated, Brushless
--	Voltage Regulator	SE350
--	Voltage Regulation	1.00%
--	Cooling Air Volume	250 CFM
--	Heat rejection rate	257 Btu's/min
--	Full load current	38 amps
--	Minimum input hp required	39.6
	Efficiency at rated load :	84.7%
--	Full load torque	116 Lb-ft

(3) Excitation support system or PMG required to sustain short circuit currents.

* Voltages refer to wye (star) connection, unless otherwise specified.

** Not supplied as standard equipment.

Date rev. : 09/01/98

Version : 2001.2

Section 3600
Page 26

MARATHON ELECTRIC
GENERATORS

TYPICAL DYNAMIC CHARACTERISTICS

MODEL : 283PSL1506
BASE MODEL: 283PSL1506 Winding WC- 1506
Submittal Data: 480 Volts*, 25 kW, 31.25 kVA, 0.8 P.F., 1800 RPM, 60 Hz, 3 Phase

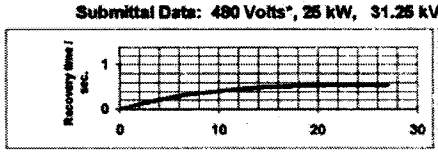

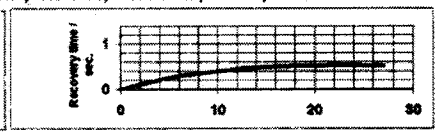

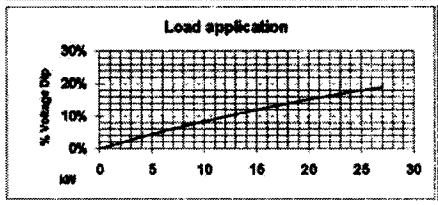

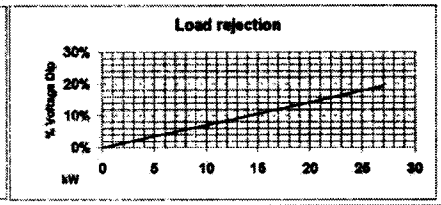

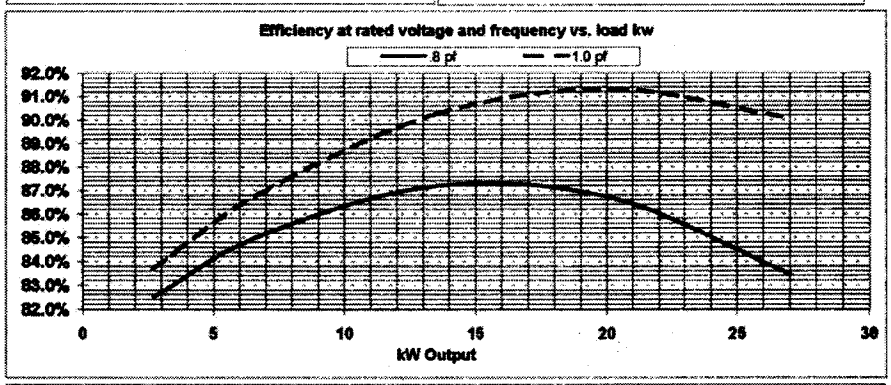

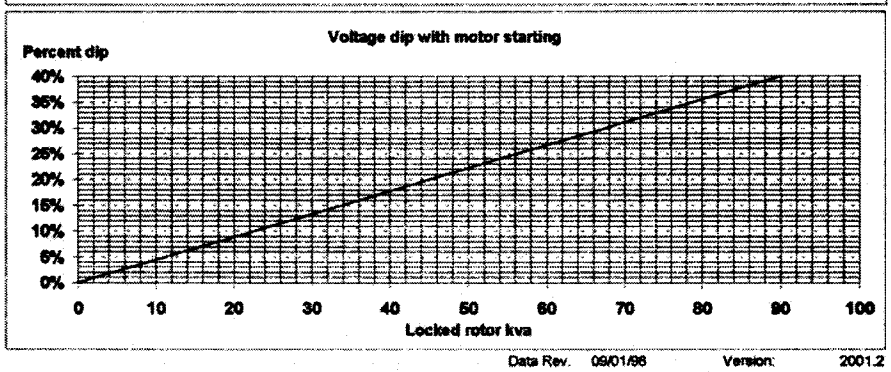

Data Rev. 09/01/98 Version: 2001.2

Appendix 2: Data-Sheet for John Deere Engine

ENGINE PERFORMANCE CURVE

POWERTECH 2.0 L Engine*
Model: **4020TF***

Rating: Net Power
Application: Generator, *Prime* ..... 32.6 hp (24.3 kW)* @ 1800 rpm
Generator, *Standby* ..... 36.1 hp (26.9 kW)* @ 1800 rpm
Recommended Gen-Set Ratings:
Prime 21* kW @ 1800 rpm (Based on 87%* Generator Efficiency
Standby 22* kW @ 1800 rpm (Based on 86%* Generator Efficiency

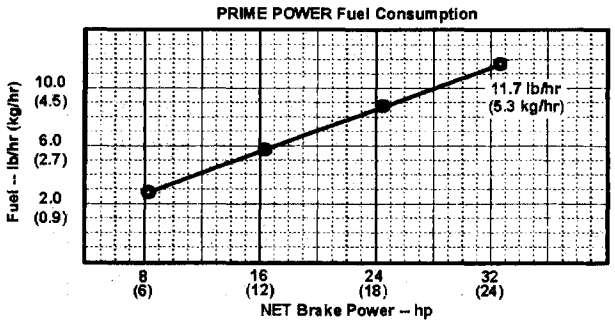

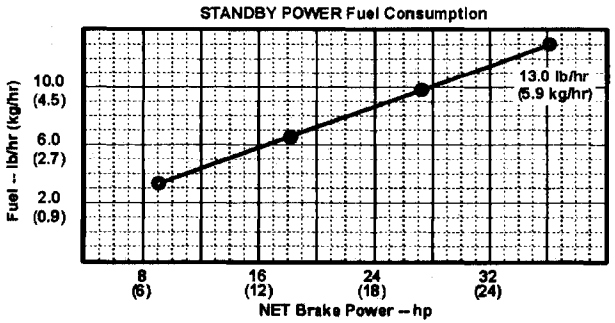

Air Intake Restriction ..... 12 in.H_2O (3 kPa)
Exhaust Back Pressure ..... 30 in.H_2O (7.5 kPa)

NET power guaranteed within + or - 5% at SAE J1995 and ISO 3046 conditions:
77 °F (25 °C) air inlet temperature
29.31 in.Hg (99 kPa) barometer
104 °F (40 °C) fuel inlet temperature
0.853 fuel specific gravity @ 60 °F (15.5 °C)
Conversion factors:
Power: kW = hp x 0.746
Fuel: 1 gal = 7.1 lb, 1 L = 0.85 kg
Torque: N•m = lb-ft x 1.356

All values are from currently available data and are subject to change without notice.

Notes:

Emission Certifications	Certified by:
CARB; EEC; EPA	R. J. Schuh
Ref: Engine Emission Label	1 DEC 95

* Revised Data
Curve 4020TFGS ..... Sheet 1 of 2
December 1995

Engine Specification Data

General Data

Model	4020TF*
Number of Cylinders	4
Bore and Stroke--in. (mm)	3.31 x 3.54 (84 x 90)*
Displacement--in.^{3} (L)	121.7 (1.994)*
Compression Ratio	18:1*
Valves per Cylinder--Intake/Exhaust	1/1
Firing Order	1-3-4-2
Combustion System	Direct Injection
Engine Type	In-Line, 4-Cycle
Aspiration	Turbocharged
Engine Crankcase Vent System	Open
Maximum Crankcase Pressure--in. H_2O (kPa)	2 (0.5)

Physical Data

Length--in. (mm)	32.2 (819)*
Width--in. (mm)	21.6 (548)*
Height--in. (mm)	34.2 (869)*
Weight, dry (power unit)--lb (kg) (includes flywheel & electrics)	506 (230)*
Center of Gravity Location	
From Rear Face of Block (X-axis)--in. (mm)	7.32 (186)
Right of Crankshaft (Y-axis)--in. (mm)	-0.18 (-4.6)*
Above Crankshaft (Z-axis)--in. (mm)	3.62 (92)
Max. Allow. Static Bending Moment at Rear Face of Flywhl Hsg w/5-G Load--lb-ft (N-m)	159 (218)
Thrust Brng. Cont. Load Limit (Forward)--lb (N)	639 (2842)

Electrical System

Recommended Battery Capacity (CCA)	
12 Volt System--amp	600
Maximum Allowable Starting Circuit Resistance	
12 Volt System--Ohm	0.0012
Starter Rolling Current--12 Volt System	
At 32°F (0 °C)--amp	350

Air System

Maximum Allowable Temp Rise--Ambient Air to Engine Inlet--°F (°C)	18 (10)
Maximum Air Intake Restriction	
Dirty Air Cleaner--in.H_2O (kPa)	25 (6.25)
Clean Air Cleaner--in.H_2O (kPa)	12 (3)
Engine Air Flow--ft^3/min (m^3/min)	
Prime	99 (2.8)*
Standby	109 (3.1)*
Recommended Intake Pipe Diameter--in. (mm)	1.97 (50)

Exhaust System

Exhaust Flow--ft^3/min (m^3/min)	
Prime	196 (5.6)*
Standby	226 (6.4)*
Exhaust Temperature--°F (°C)	
Prime	842 (450)*
Standby	896 (480)*
Max. Allow. Back Pressure--in. H_2O (kPa)	51.3* (12.3)
Rec'd. Exhaust Pipe Diameter--in. (mm)	2.36 (60)

Cooling System

Engine Heat Rejection--BTU/min (kW)	
Prime	910 (16.0)*
Standby	1008 (17.7)*
Coolant Flow--gal/min (L/min)	15.6 (60)*
Thermostat Start to Open--°F (°C)	160 (71)
Thermostat Fully Open--°F (°C)	185 (85)
Max. Water Pump Inlet Restriction--in. H_2O* (kPa)	40* (10)
Engine Coolant Capacity--qt (L)	5.4 (5.2)*
Recommended Pressure Cap--psi (kPa)	12.8 (88)
Maximum Top Tank Temp--°F (°C)	221 (105)*
Recommended Air to Boil--°F (°C)	117 (47)

Fuel System

Fuel Injection Pump	Yanmar
Governor Regulation	8% max
Governor Type	Mechanical
Fuel Consumption--lb/hr (kg/hr)	
Prime	11.7 (5.3)*
Standby	13.0 (5.9)*
Maximum Allowable Fuel Pump Suction	
Clean System-psi (kPa)	1.13* (7.8)
Fuel Filter Micron Size @ 98% Efficiency	10

Lubrication System

Oil Pressure at Rated Speed--psi (kPa)	49.7 (343)
Oil Pressure at Low Idle--psi (kPa)	39.9 (275)*
In Pan Oil Temperature--°F (°C)	240 (115)
Oil Pan Capacity, High--qt (L)	9.4 (9.0)
Oil Pan Capacity, Low--qt (L)	6.7 (6.4)*
Total Engine Oil Capacity with Filters--qt (L)	10 (9.8)*
Engine Angularity Limits (Continuous)	
Any Direction--degrees	25

Performance Data (NET)

Net Rated Power--hp (kW)	
Prime	32.6 (24.3)*
Standby	36.1 (26.9)*
Rated Speed--rpm	1800
Low Idle Speed--rpm	1200
BMEP--psi (kPa)	
Prime	116.1 (801)*
Standby	128.6 (887)*
Altitude Capability--ft (m)	4921 (1500)*
Ratio--Air : Fuel	22:1
Smoke @ Rated Speed--Bosch No. *	3*
Noise--dB(A) @ 1 m	88*

Fuel Consumption @ 1800 rpm--lb/hr (kg/h)

Percent Power	*Prime*	*Standby*
25%	2.9 (1.3)	3.3 (1.5)
50%	5.9 (2.7)	6.5 (3.0)
75%	8.8 (4.0)	9.8 (4.4)
100%	11.7 (5.3)	13.0 (5.9)

All values at rated speed and power with standard options unless otherwise noted.

* Revised Data

Curve 4020TFGS ... Sheet 2 of 2

December 1995

Appendix 3: Data-Sheet for 15/50 AOC Wind Turbine Generator

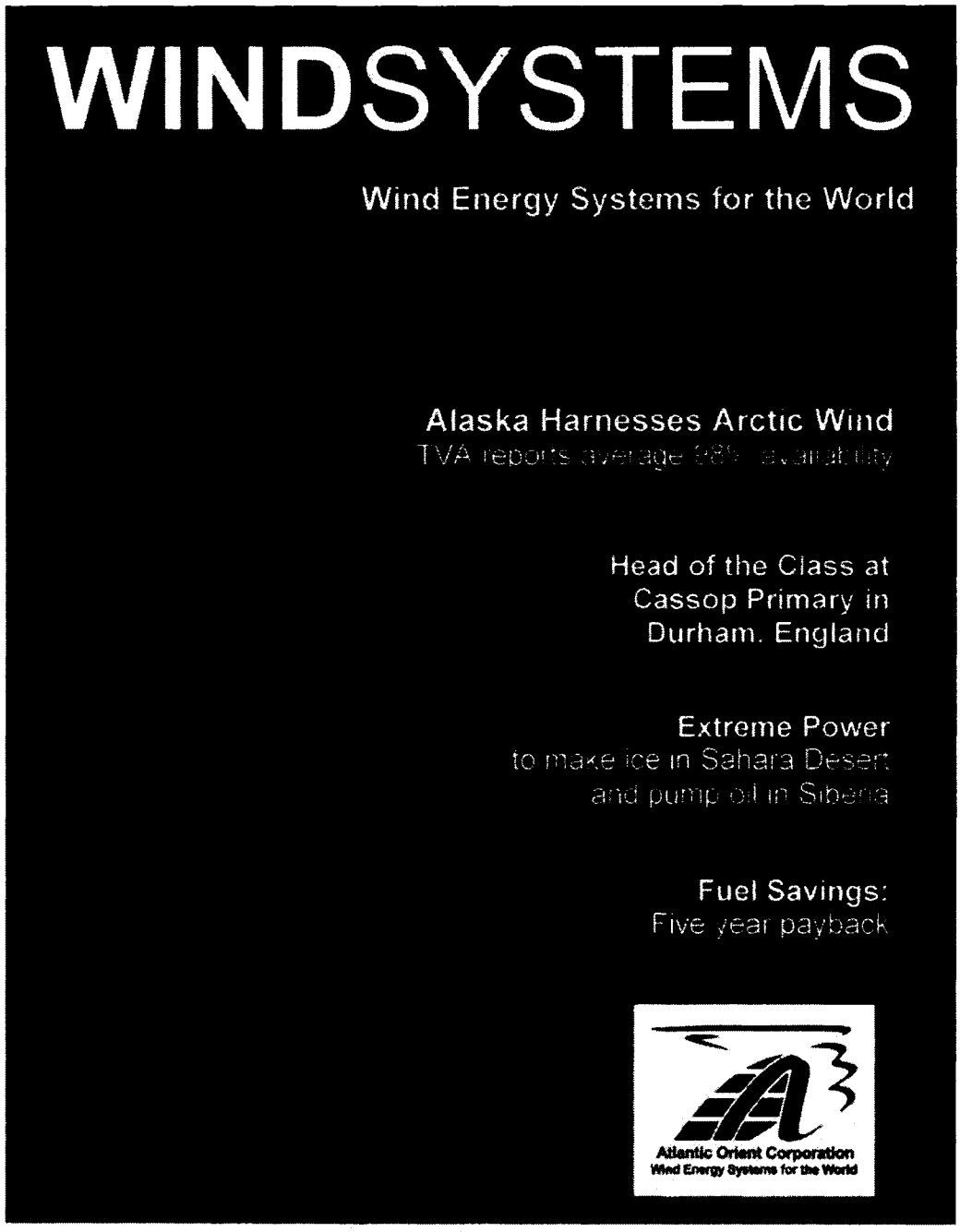

Atlantic Orient Corporation designs and builds state-of-the-art wind turbine generators. Our turbines are reliable, durable, cost-effective and environmentally friendly.

THE COMPANY
Atlantic Orient Corporation (AOC), headquartered in Norwich, Vermont, designs and manufactures a mid-sized advanced wind turbine system for integration with diesel generators and installation in rural and remote regions of the world. The specific purpose of the AOC wind turbine energy system is to dramatically reduce the amount of very expensive diesel fuel consumed in these remote areas and to offset the retail price of electricity. In many applications the fuel savings alone will provide a payback within five years.

PROVEN DESIGN
Since 1986, AOC has designed and built state-of-the-art wind turbine generators. Design innovations, exhaustive testing, and advanced technology have led to a wind turbine generator with high availability, even in extreme Arctic or desert conditions. Our turbine's performance consistently meets or exceeds design specifications and requires low maintenance throughout its expected operating life.

EXPERIENCE
Atlantic Orient Corporation has extensive utility systems experience to efficiently integrate wind energy into your system. Our engineering team is composed of individual talents yet one goal: to design the highest value wind turbine generators for your application. Our engineering capabilities are widely recognized and respected in the wind energy industry worldwide.

RELIABLE
Our goal is robust simplicity and failsafe reliability with minimal maintenance requirements over a thirty year design life in extreme environmental conditions. Our design process utilizes peer review, international standards, component qualification testing and field testing. Independent analysis and testing at the National Renewable Energy Laboratory (NREL), the Netherlands Energy Research Foundation ECN, RISO Laboratory in Denmark,

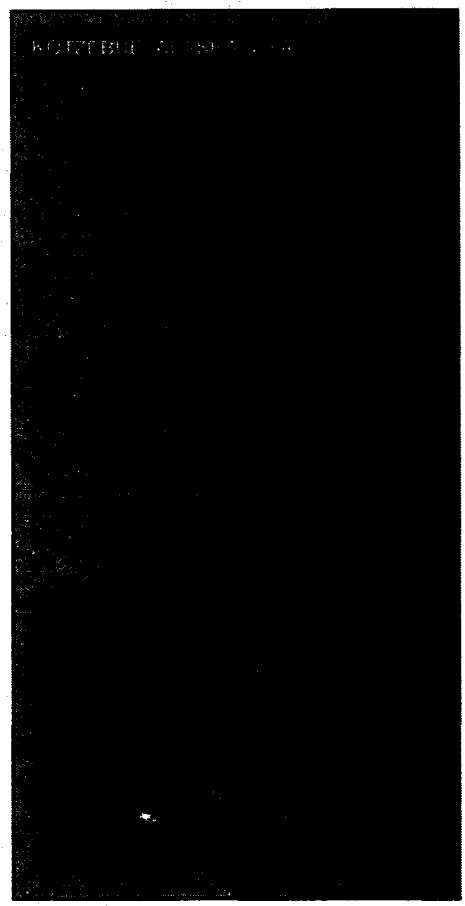

The AOC 15/50 Wind Turbine Generator

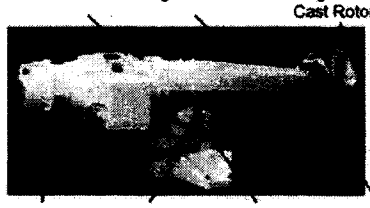

The AOC 15/50 wind turbine consists of a 15 meter rotor which produces 50 kW at an 11.3 m/s wind speed (60 Hz model). The turbine was developed in conjunction with the U.S. Department of Energy and the National Renewable Energy Laboratory (NREL) under their Advanced Wind Turbine (AWT) Program. The goal of this cost shared program was to produce economic wind generated electricity in a moderate average wind resource. This was achieved with simplicity in design, high availability and failsafe reliability.

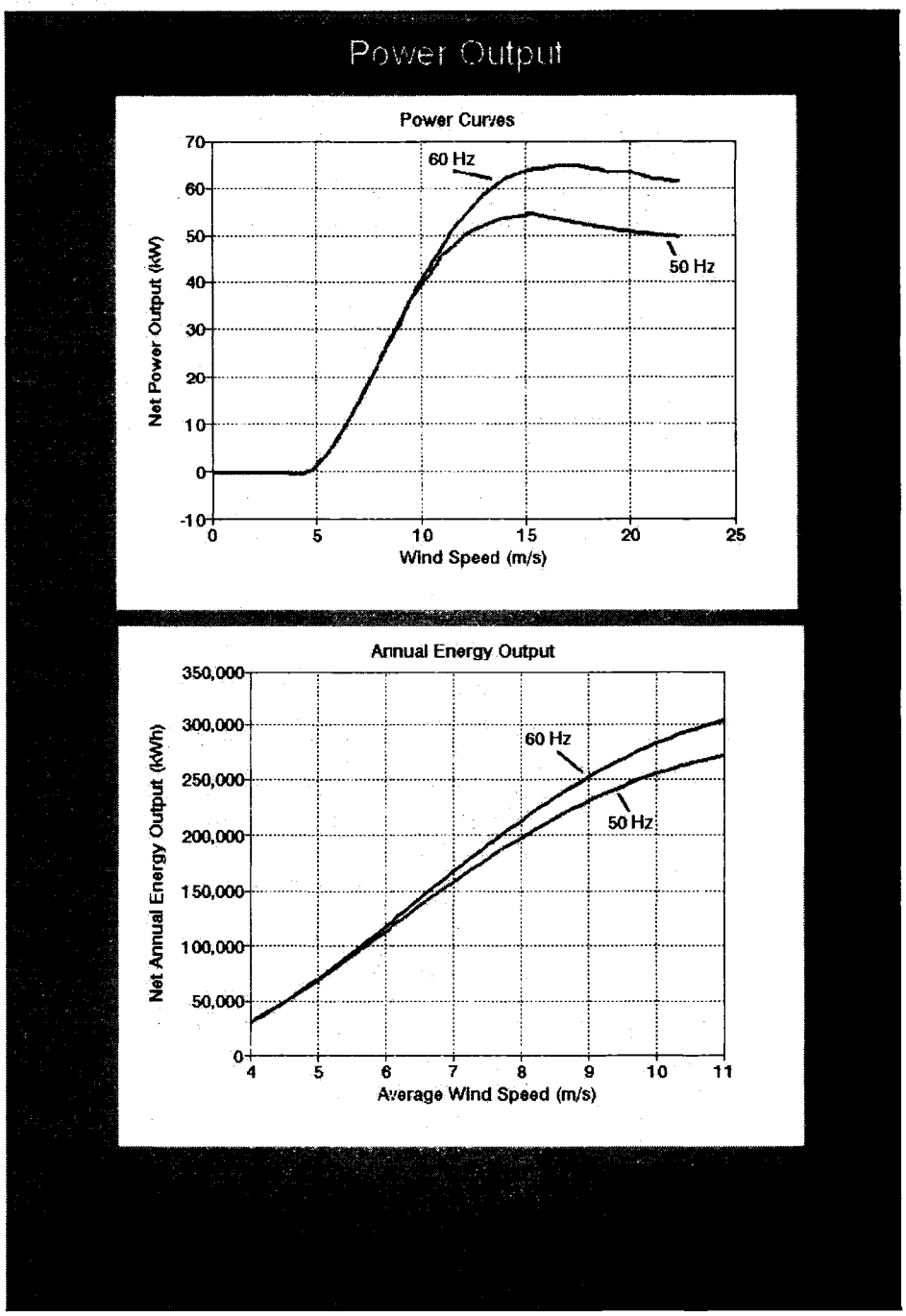

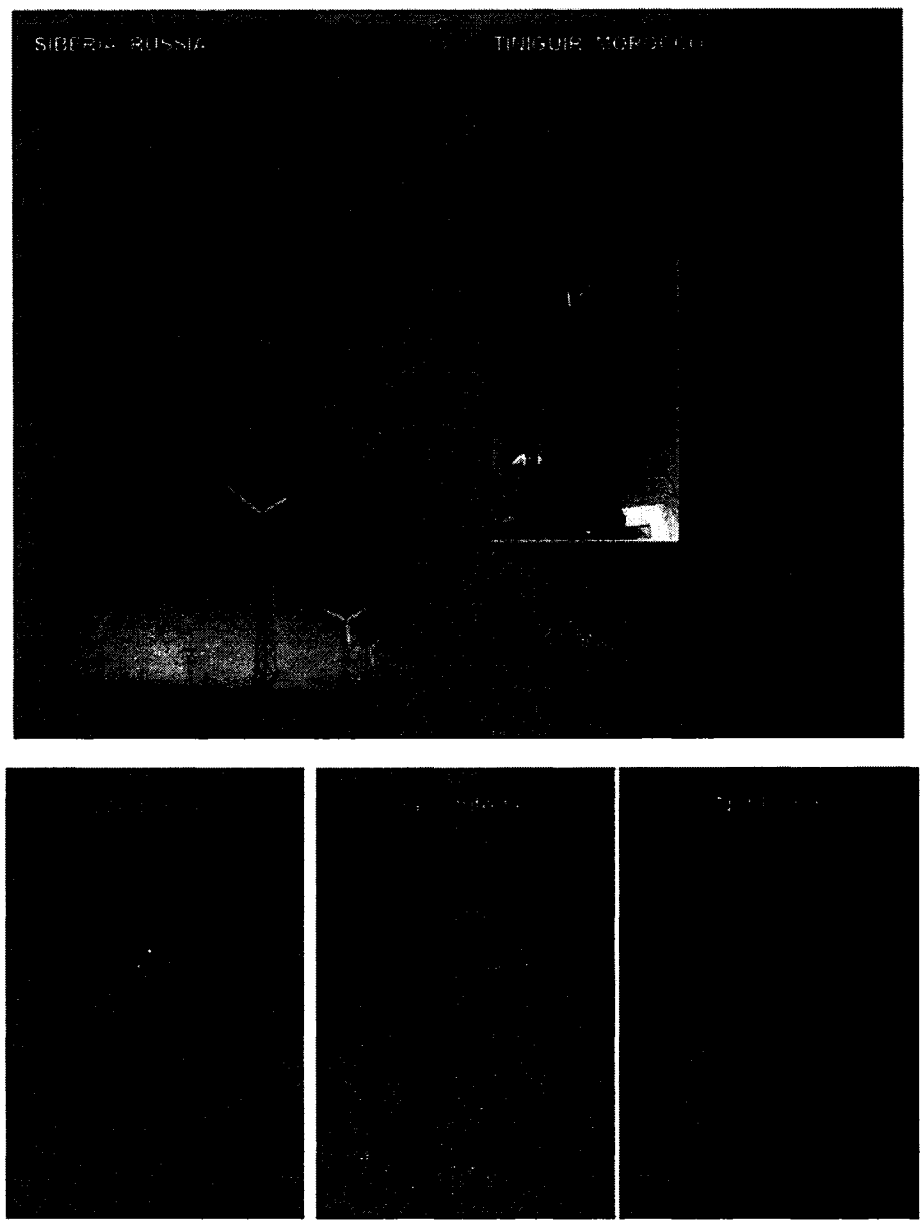

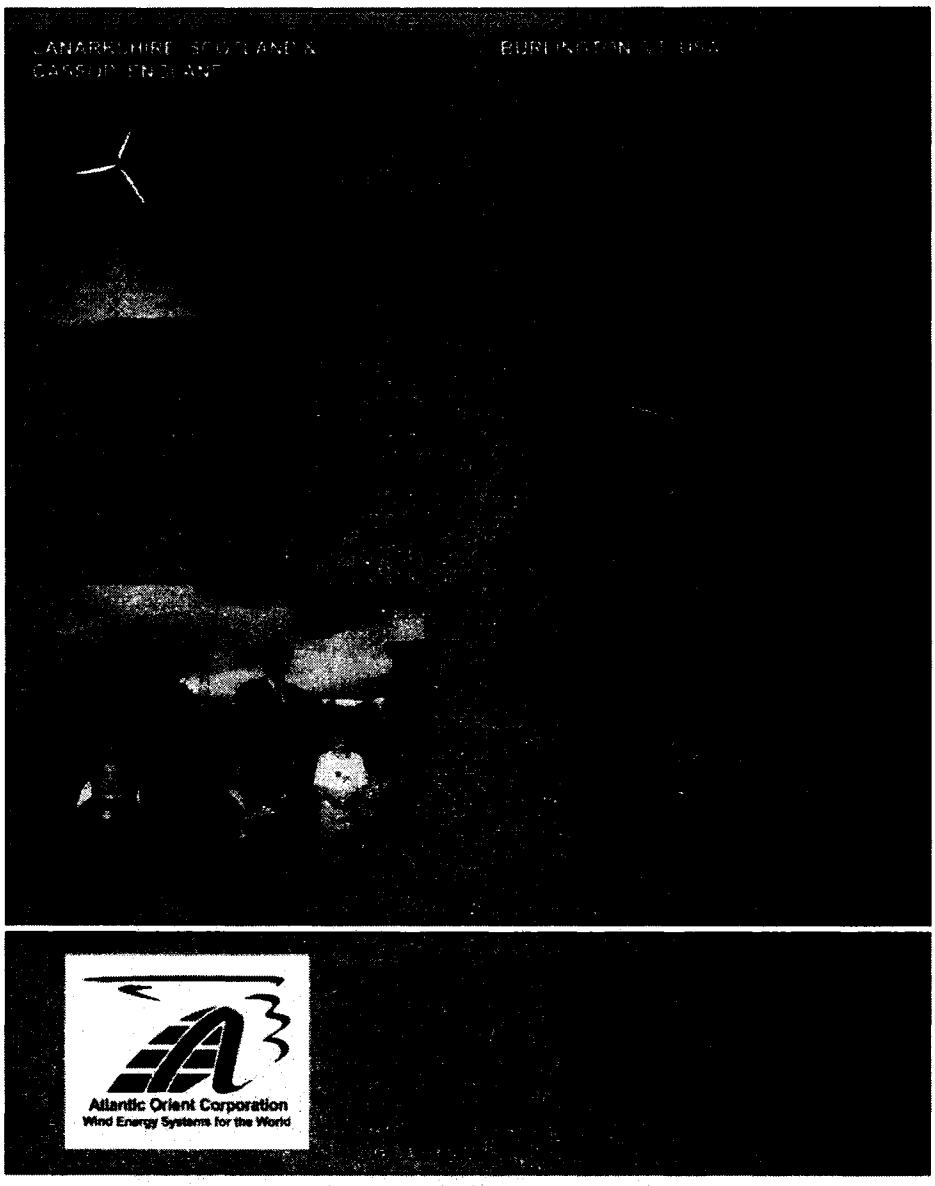

Appendix 4: Data-Sheet for Siemens PV Array

SIEMENS

Solar module SM55

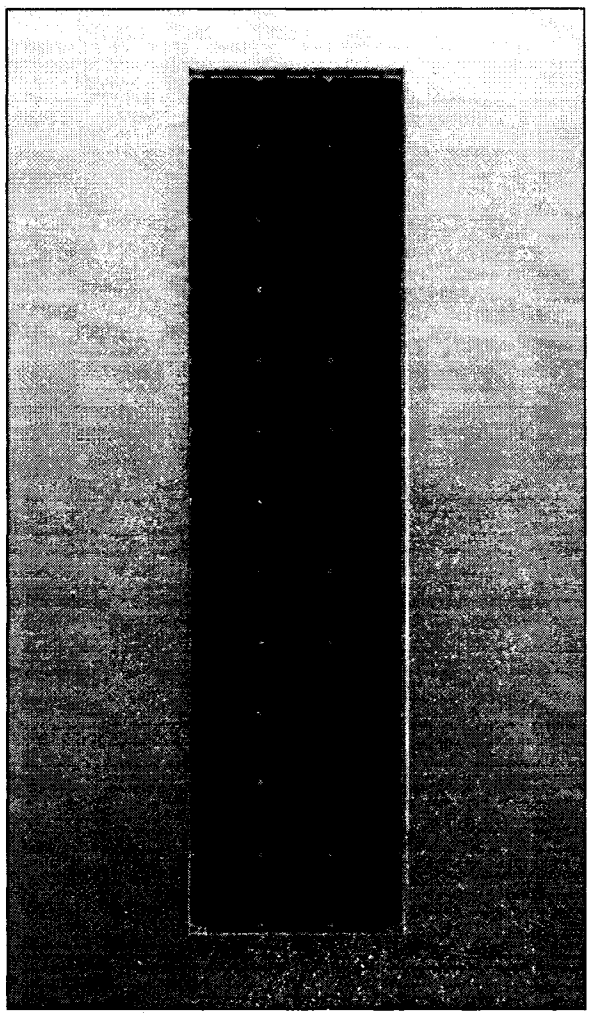

When it comes to reliable and environmentally-friendly generation of electricity from sunlight, solar modules from Siemens provide the perfect solution. Manufactured in compliance with the most stringent quality standards, Siemens Solar modules are designed to withstand the toughest environmental conditions and are characterized by their long service life. Siemens Solar modules are covered by a 25-year limited warranty on power output – your guarantee of trouble-free solar power generation.

PowerMax® technology
Siemens' proprietary PowerMax® technology optimizes the energy production of individual cells and solar modules for all types of environmental conditions. PowerMax® process optimization includes a special refining technique for ingots, a clean room semiconductor grade production process, and a multistage proprietary TOPS™ (Texture Optimized Pyramidal Surface) process. The TOPS process incorporates the formation of textured pyramids on the surface of the solar cell. These pyramids are then specially treated to passivate the surface which optimizes the cell's optical properties for maximum absorption of photons from the sun's light. TOPS also maximizes photon absorption from direct and diffused light (typical under cloudy conditions). This means that light absorption is especially high, even at low light levels. Siemens PowerMax® solar cells deliver maximum energy throughout the day.

Solar module
Model: SM55
Rated power: 55 Watts
Limited warranty: 25 Years

Certifications and Qualifications
- UL-Listing 1703
- TÜV safety class II
- JPL Specification No. 5101-161
- ESTI-IEC 1215/CECC803
- MIL Standard 810
- CE mark
- FM Certification (SM55-J)

Intelligent module design

- All cells are electrically matched to assure the greatest power output possible
- Ultra-clear tempered glass provides excellent light transmission and protects from wind, hail, and impact.
- Torsion and corrosion-resistant anodized aluminum module frame ensures dependable performance, even through harsh weather conditions and in marine environments.
- Built-in bypass diodes (12V configuration) help system performance during partial shading.

High quality

- Every module is subject to final factory review, inspection, and testing to assure compliance with electrical, mechanical, and visual criteria
- 36 PowerMax® single-crystalline solar cells deliver excellent performance even in reduced light or poor weather conditions
- Cell surfaces are treated with the Texture Optimised Pyramidal Surface (TOPS™) process to generate more energy from available light.
- Fault tolerant multi-redundant contacts on the front and back of each cell provide superior reliability.
- Solar cells are laminated between a multi-layered polymer backsheet and layers of ethylene vinyl acetate (EVA) for environmental protection, moisture resistance, and electrical isolation.
- Durable back sheet provides the module underside with protection from scratching, cuts, breakage, and most environmental conditions.
- Laboratory tested and certified for a wide range of operating conditions.
- Ground continuity of less than 1 ohm for all metallic surfaces.
- Manufactured in ISO 9001 certified facilities to exacting Siemens quality standards.

Easy installation

- Standard ProCharger™-S terminal enclosures are designed for trouble-free field wiring and environmental protection. (Modified versions also available, e.g. as SM55-J with the special ProCharger™-CR junction boxes.)
- Lightweight aluminum frame and pre-drilled mounting holes for easy installation.
- Modules may be wired together in series or parallel to attain required power levels.

Performance warranty

- 25 Year limited warranty on power output.

Further information on solar products, systems, principles, and applications is available in the Siemens Solar product catalog.

Siemens modules are recyclable.

Solar module SM55

Electrical parameters		
Maximum power rating P_{max}	$[W_p]$[1]	[illegible]
Rated current I_{MPP}	[A]	3.15
Rated voltage V_{MPP}	[V]	[illegible]
Short circuit current I_{SC}	[A]	3.45
Open circuit voltage V_{OC}	[V]	[illegible]
Thermal parameters		
NOCT[2]	[°C]	45±2
Temp. coefficient: short-circuit current		[illegible]
Temp. coefficient: open-circuit voltage		-.077 V / °C
Qualification test parameters[4]		
Temperature cycling range	[°C]	-40 to +85
Humidity freeze, Damp heat	[% RH]	[illegible]
Maximum permitted system voltage	[V]	600 (1000 V per ISPRA)
Wind Loading	PSF [N/m²]	[illegible]
Maximum distortion[3]	[°]	1.2
Hailstone impact	Inches [mm]	[illegible]
	MPH [m/s]	52 [v=23]
Weight	Pounds [kg]	[illegible]

[1] W_p (Watt peak) = Peak power (Minimum W_p = 50 Watts)

Air Mass	AM	= 1.5
Irradiance	E	= 1000 W/m²
Cell temperature	T_C	= 25 °C

[2] Normal Operating Cell Temperature at:

Irradiance	E	= 800 W/m²
Ambient temperature	T_U	= 20 °C
Wind speed	v_W	= 1 m/s

[3] Diagonal lifting of the module plane

[4] Per EIC 1215 test requirements

[5] 12 Volt configuration

Voltage-current characteristic[5]

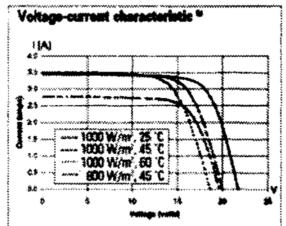

Module dimensions

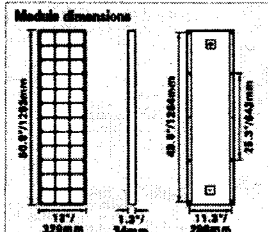

Hole diameter 0.26 inch (6.6 mm)
Mounting hole dimensions are center to center

ProCharger™-S Junction-box
Maximum cable diameter: 4 mm²
Type of protection: IP54

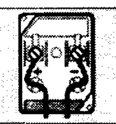

Your address for photovoltaics from Siemens Solar

Status 3/98 – Subject to modification

Siemens Solar GmbH
A joint venture of
Siemens AG and Bayernwerk AG
Postfach 46 07 05
D-80915 München
Germany

Siemens Solar Industries
P.O. Box 6032
Camarillo, CA 93011, U.S.A.
Tel. 805-482-6800
Fax: 805-388-6395
Web site: www.siemenssolar.com
E-mail: sunpower@solarpv.com

Siemens Showa Solar Pte. Ltd.
Blk. 164 Kallang Way
#05-14/15 Kolam Ayer Industrial Park
Singapore 349248
Tel: 65-842-3886
Fax: 65-842-3887

Printed in U.S.A.
Order No. 019895, Rev. 8

Appendix 5: Data-Sheet for Absolyte IIP Battery Bank

GNB

ABSOLYTE IIP

Section 26.12

I & O MANUALS

- 20 Year life expectancy
- 105 to 1140 AH
- Highest energy density
- Single cell module for ease of handling
- Recyclable to world standards
- UL recognized component

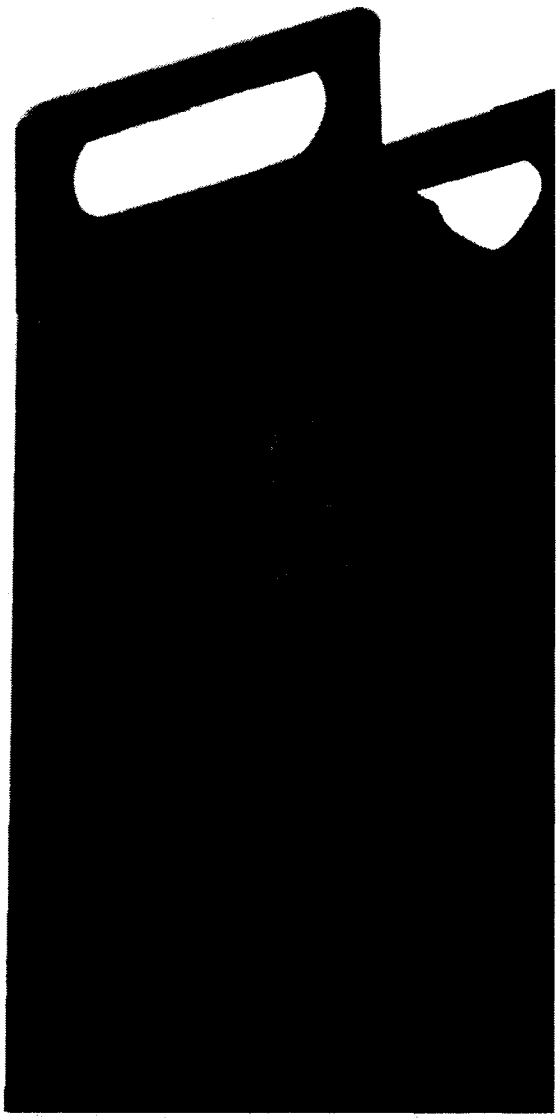

ABSOLYTE IIP

THE WORLD LEADER IN SEALED BATTERY POWER

Proven field experience since 1983. The Absolyte IIP represents the third generation of the Absolyte product line. Without an increase in size, it offers 15% more capacity than its predecessor, the Absolyte II.

Patented MFX positive grid alloy* provides long-life. This proprietary alloy gives Absolyte IIP superior cycling performance and excellent float characteristics: 1200 cycles to 80% D.O.D. and a twenty year life in float service @ 25°C (77°F). This alloy also has low gassing characteristics and is designed to allow for deep discharge recovery.

Absorbed glass mat separators for efficient operation. The positive and negative plates are separated by a highly porous fiberglass mat which functions as the electrolyte retainer and provides the highest oxygen recombination efficiency. In addition, the low resistance of the glass mat improves high rate discharge performance.

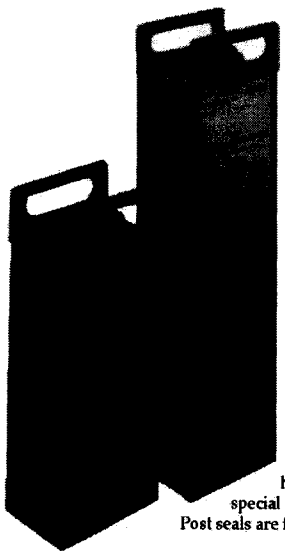

Reduced installation and maintenance time. The Absolyte IIP cells are housed in protective, individual steel trays with convenient lifting handles for easy transport to remote locations. The single cells may be operated in the horizontal (preferred) or vertical position. With the sealed design, maintenance is also kept to a minimum. No water additions or scheduled equalization charges are required. Periodic visual inspections, voltage readings and connection retorquing is all that is required.

Highest reliability is assured by GNB's quality program. Cell covers are hermetically sealed using a special GNB double-sealing process. Post seals are formed by fusing the lead bushing to the post with a robotic welder. Cells are checked by an automated, ultra-sensitive helium leak detection unit prior to the electrolyte "fill by weight" process. These steps virtually eliminate any potential for leaking cells. Finally, all cells are capacity tested prior to shipment to verify attainment of specified ratings.

APPLICATIONS

The Absolyte IIP Single Cell Modules are ideal for numerous applications including:

- Railroad Signal and Communications
- Photovoltaics
- Cellular Radio
- Alternative Energy Systems
- Telecommunications

ADDED FEATURES & BENEFITS

- Does not require separate battery room
- Can be integrated into other equipment enclosures
- Recombination efficiency greater than 99%
- Freezing tolerant
- Deep discharge recovery
- Accepts high rate charge

CELL SPECIFICATIONS

Container and Cover—Polypropylene is standard. Flame retardant, UL94 V-0/ 28% L.O.I. is optional.

Separators—Spun glass, microporous matrix.

Safety Vent—400mb (6 psi) nominal, self-resealing (patented).

Terminals—Integral solid copper core.

Positive Plate—Patented MFX grid alloy*.

Negative Plate—Lead calcium grid alloy.

Life—20 years float @25°C (77°F).

Self Discharge—0.5 to 1% per week maximum @25°C (77°F).

Float Voltage—2.23 to 2.27 VPC (2.25 recommended) @25°C (77°F).

*U.S. Patent 4,401,730

ABSOLYTE IIP

Absolyte IIP Single Cell Module Weights and Dimensions

CELL TYPE	NOM AH CAP (8 HR)	LENGTH		WIDTH		DEPTH OR HEIGHT		WEIGHT	
		IN	MM	IN	MM	IN	MM	LB	KG
50A									
50A05	105	3.80	97	6.49	165	16.00	406	32	15
50A07	160	3.80	97	6.49	165	16.00	406	39	18
50A09	210	3.80	97	6.49	165	16.00	406	43	20
50A11	265	4.55	116	6.49	165	16.00	406	50	23
50A13	320	5.30	134	6.49	165	16.00	406	58	26
50A15	370	6.05	154	6.55	166	16.00	406	66	30
50A17	425	6.80	173	6.67	169	16.00	406	82	37
50A19	475	7.67	195	6.67	169	16.00	406	91	41
50A21	530	8.40	214	6.67	169	16.00	406	99	45
50A23	580	9.17	233	6.67	169	16.00	406	107	49
50A25	635	9.92	252	6.67	169	16.00	406	116	52
50A27	685	10.67	271	6.67	169	16.00	406	124	56
90A									
90A05	175	3.80	97	6.49	165	23.31	592	80	23
90A07	265	3.80	97	6.49	165	23.31	592	61	28
90A09	350	3.80	97	6.49	165	23.31	592	67	30
90A11	440	4.55	116	6.49	165	23.31	592	79	36
90A13	530	5.30	135	6.49	165	23.31	592	92	42
90A15	615	6.05	154	6.55	166	23.31	592	104	47
90A17	700	6.80	173	6.67	169	23.31	592	128	58
90A19	790	7.67	195	6.67	169	23.31	592	141	64
90A21	880	8.40	213	6.67	169	23.31	592	155	70
90A23	965	9.17	233	6.67	169	23.31	592	168	76
90A25	1055	9.92	252	6.67	169	23.31	592	180	82
90A27	1140	10.67	271	6.67	169	23.31	592	193	88

Note: Design and / or specifications subject to change without notice. If questions arise, contact your local GNB sales representative for clarification.

• For additional performance data, refer to section 26.10.

Absolyte IIP Performance Specifications*
Amperes to 1.75 Final Volts PerCell @ 25°C (77°F)

CELL TYPE	HOURS													
	100	72	36	24	20	16	12	10	8	6	4	3	2	1
50A														
50A05	1.4	1.9	3.5	5.1	6.0	7.3	9.3	11	13	16	20	27	40	66
50A07	2.1	2.9	5.5	7.7	9.1	11	14	16	19	24	3	41	56	87
50A09	2.9	3.8	7.2	10	12	14	18	22	26	33	43	58	75	118
50A11	3.6	4.9	9.1	13	15	18	23	27	33	41	56	69	94	146
50A13	4.2	5.8	11	15	18	22	28	33	39	49	67	83	113	175
50A15	5.1	6.9	12	18	21	25	32	38	46	57	78	97	131	204
50A17	5.8	7.9	14	20	24	29	37	44	52	66	88	110	150	233
50A19	6.5	8.9	16	23	27	33	42	49	59	74	101	125	169	262
50A21	7.3	9.9	18	25	30	36	46	55	65	82	112	138	188	291
50A23	8.0	10	20	28	33	40	51	60	72	90	123	153	206	321
50A25	8.7	11	22	31	36	43	56	66	78	98	134	167	225	349
50A27	9.5	12	23	33	39	47	60	71	85	107	146	181	244	379
90A														
90A05	2.4	3.2	6.0	8.6	10	12	16	18	21	27	37	46	63	101
90A07	3.6	4.9	9.1	12	15	18	23	27	32	41	55	69	93	151
90A09	4.8	6.1	12	17	20	24	31	36	43	54	74	92	126	201
90A11	6.0	8.1	15	21	25	30	39	46	54	68	93	115	155	251
90A13	7.2	9.8	18	25	30	36	47	55	65	82	111	138	187	301
90A15	8.4	11	21	30	35	42	55	64	76	96	130	162	217	352
90A17	9.6	13	24	34	40	48	63	73	87	109	148	185	248	402
90A19	10	14	27	38	45	55	71	82	98	123	167	208	279	453
90A21	12	16	30	43	50	61	79	92	109	137	186	231	310	503
90A23	13	18	33	47	55	67	87	101	120	151	205	254	341	553
90A25	14	19	36	51	60	73	95	110	131	164	223	277	372	603
90A27	15	21	39	56	65	79	103	119	142	178	242	300	403	654

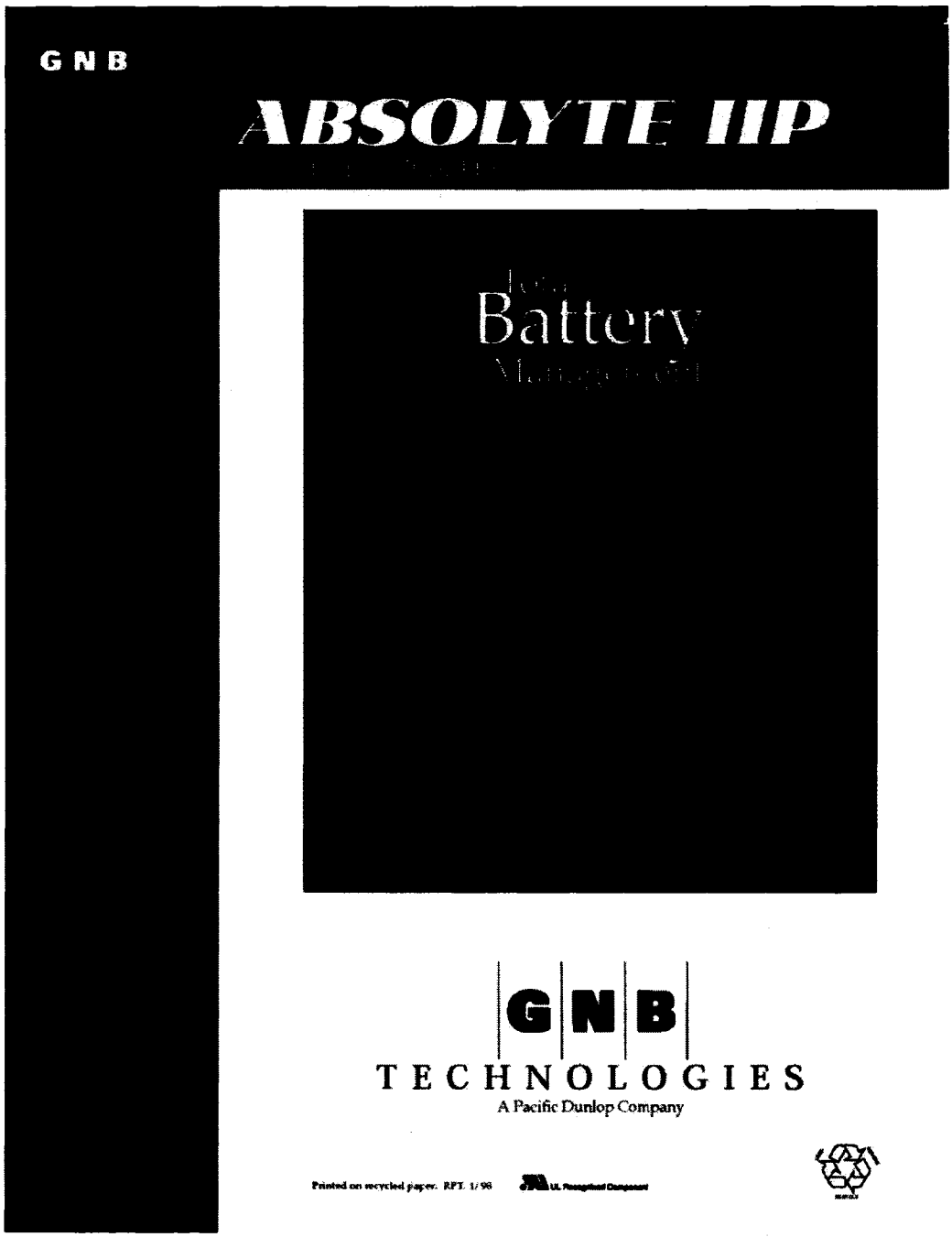

Appendix 6: Wales Village Power System Specifications

Wales Village Power System Specifications

General: 142 kW diesel genset, 75 kW diesel genset, 148 kW diesel genset, 2-AOC 15/50 wind turbines, 200 –130 Ah Ni-Cad batteries, 156 kVA rotary converter, 180 kW optional dump load.

Genset A

Manufacturer	Cummins
Model	LTA 10
Rated Power	142 kW
Rated Speed	1200 RPM

Genset B

Manufacturer	Allis-Chalmers
Model	3500
Rated Power	75 kW
Rated Speed	1800 RPM

Genset C

Manufacturer	Cummins
Model	LTA 10
Rated Power	148 kW
Rated Speed	1200 RPM

Wind turbines

Manufacturer	AOC
Model	15/50
Rated Power	50 kW
Rated Speed	11.3 m/s
Operating Frequency	60 Hz

Batteries

200 – Saft Ni-Cad	Sintered/plastic bonded electrode nickel cadmium batteries
Configuration	200 cells in series
Nominal voltage of string	240 V
Nominal capacity	130 Ah

Bi-directional rotary power converter/controller

Manufacturer	
Rated capacity	156 KVA
Rated power	100 kW
No load loss	5 kW
Operating Efficiency	92%

Optional dump load

Type of load	Resistive
Rated capacity	180 kW
Rated power	100 kW

Contact:
Mari Shirazi, National Renewable Energy Laboratory, Mari_Shirazi@nrel.gov

Appendix 7: Details of Wales Village Power System Components in HOMER

HOMER Input Summary

File name: Wales Village1.hmr
File version: 2.2 beta
Author: Ashish

AC Load: Primary Load 1

Data source: Synthetic
Daily noise: 15%
Hourly noise: 20%
Scaled annual average: 1,638 kWh/d
Scaled peak load: 139 kW
Load factor: 0.492

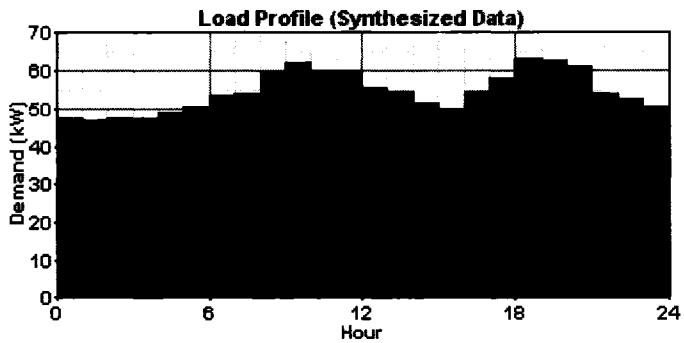

AC Wind Turbine: AOC 15/50

Quantity	Capital ($)	Replacement ($)	O&M ($/yr)
2	110,000	88,000	500

Quantities to consider: 0, 2
Lifetime: 20 yr
Hub height: 0.556 m

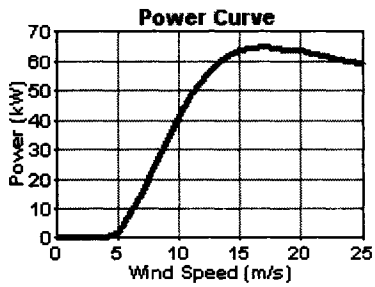

Wind Resource
Data source: Synthetic

Month	Wind Speed (m/s)
Jan	7.2
Feb	8.7
Mar	7.0
Apr	7.9
May	6.4
Jun	8.9
Jul	11.1
Aug	8.1
Sep	8.1
Oct	9.8
Nov	9.4
Dec	8.5

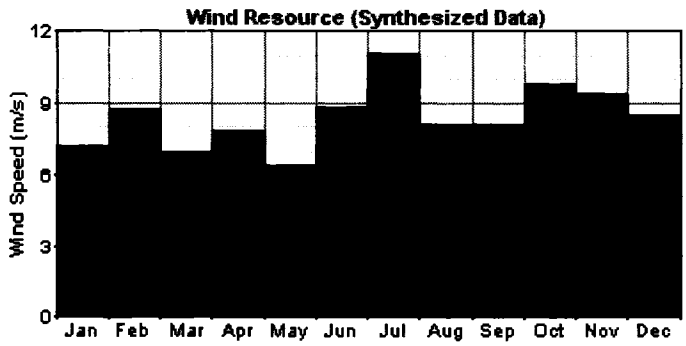

Weibull k:	2.00
Autocorrelation factor:	0.850
Diurnal pattern strength:	0.500
Hour of peak wind speed:	6
Scaled annual average:	8.42 m/s
Anemometer height:	10 m
Altitude:	0 m
Wind shear profile:	Logarithmic
Surface roughness length:	0.01 m

AC Generator: Generator 2

Size (kW)	Capital ($)	Replacement ($)	O&M ($/hr)
142.000	34,000	34,000	1.000

Sizes to consider:	0, 142 kW
Lifetime:	30,000 hrs
Min. load ratio:	30%
Heat recovery ratio:	0%
Fuel used:	Copy of Diesel
Fuel curve intercept:	0.091 L/hr/kW
Fuel curve slope:	0.147 L/hr/kW

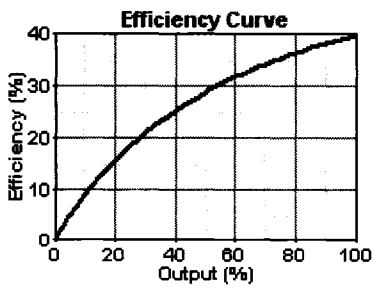

AC Generator: Generator 3

Size (kW)	Capital ($)	Replacement ($)	O&M ($/hr)
148.000	34,800	34,800	1.000

Sizes to consider: 0, 148 kW
Lifetime: 15,000 hrs
Min. load ratio: 30%
Heat recovery ratio: 0%
Fuel used: Copy of Diesel
Fuel curve intercept: 0.08 L/hr/kW
Fuel curve slope: 0.25 L/hr/kW

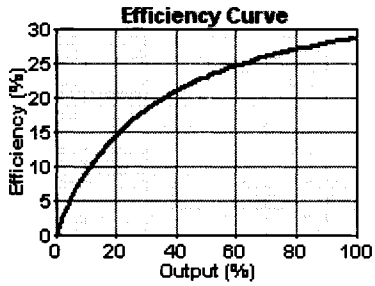

Fuel: Copy of Diesel

Price: $ 0.794/L
Lower heating value: 47.2 MJ/kg
Density: 800 kg/m3
Carbon content: 88.0%
Sulfur content: 0.330%

Battery: Saft SPH130

Quantity	Capital ($)	Replacement ($)	O&M ($/yr)
1	14,000	14,000	200.00

Quantities to consider: 0, 1
Voltage: 240 V
Nominal capacity: 130 Ah
Lifetime throughput: 631,691 kWh

Converter

Size (kW)	Capital ($)	Replacement ($)	O&M ($/yr)
40.000	55,000	44,000	1,200

Sizes to consider: 0, 40 kW
Lifetime: 30 yr
Inverter efficiency: 90%
Inverter can parallel with AC generator: Yes
Rectifier relative capacity: 100%
Rectifier efficiency: 90%

Economics

Annual real interest rate: 7%
Project lifetime: 20 yr
Capacity shortage penalty: $ 3/kWh
System fixed capital cost: $ 36,000
System fixed O&M cost: $ 1,000/yr

Generator control

Check load following: No
Check cycle charging: Yes
Setpoint state of charge: 80%
Allow systems with multiple generators: Yes
Allow multiple generators to operate simultaneously: Yes
Allow systems with generator capacity less than peak load: Yes

Emissions

Carbon dioxide penalty: $ 0/t
Carbon monoxide penalty: $ 0/t
Unburned hydrocarbons penalty: $ 0/t
Particulate matter penalty: $ 0/t
Sulfur dioxide penalty: $ 0/t
Nitrogen oxides penalty: $ 0/t

Constraints

Maximum annual capacity shortage:	0%
Minimum renewable fraction:	0%
Operating reserve as percentage of hourly load:	0%
Operating reserve as percentage of peak load:	0%
Operating reserve as percentage of solar power output:	0%
Operating reserve as percentage of wind power output:	0%

Appendix 8: Lime Village Power System Specifications

Lime Village Power System Specifications

General: 35 kW diesel genset, 21 kW diesel genset, 12 kW photovoltaic
95-530 Ah lead-acid batteries, 30 kVA bi-directional power converter

Genset A

Engine	John Deere (manufactured by Yanmar)
Model	Model 4020TS106
Number of cylinders	4
Engine type	In-line, 4-cycle
Aspiration	Turbocharged
Net rated power, prime	24.3 kW
Generator	Marathon
Model	283PSL1506
Rated power	23KW @105 degree C rise

Genset B

Engine	
Model	
Number of cylinders	4
Engine type	In-line, 4-cycle
Aspiration	Natural
Net rated power, prime	~35 kW
Generator	
Model	
Rated power	

Photovoltaic Array

75-Siemens M55 panels	
Configuration	15 panels in series X 5 strings in parallel
Rated capacity	4 kW
105-BP Solar BP275UL panels (1 spare)	
Configuration	15 panels in series X 7 strings in parallel
Rated capacity	8 kW
Total rated capacity	12 kW

Batteries	
95-GNB Absolyte IIP, 6-90A13	Valve regulated, absorbent glass mat, lead-calcium battery
Configuration	95 cells in series
Nominal voltage of string	190 V
Nominal capacity (8-hour rate)	530 Ah

Bi-directional power converter/controller	
AES Static Power Pack	
Rated capacity	30 kVA
AC Bus	3-phase, 120/208 V, 60 Hz
DC Bus	192 V
PV controller	PWM
Interface	Touch screen
Data acquisition	
Data summary	Summation data since last reset (see Table 2)
Error log	
Variable averaging period	1 minute to 24 hour
Data columns	40
Data rows	150
Description	The SPP maintains 150 records (40 columns each) in its internal memory. The site computer runs Telix terminal software to monitor the SPP, as well as to automatically retrieve the data log. This is facilitated by a script, which is always running under Telix. Currently, the SPP is recording 15 minute averages and the site computer is retrieving the data once per day. The download frequency can be increased by implementing a different script, which is currently on the site computer (see Table 1).

Table 1: Data Log Column Description

LOG	Log entry number
TIME	Time
DATE	Date (DD/MM/YY)
DP1%	Diesel power, phase 1, % of rated power
DP2%	Diesel power, phase 2, % of rated power

DP3%	Diesel power, phase 3, % of rated power
DP1KW	Diesel power, phase 1, kW
DP2KW	Diesel power, phase 2, kW
DP3KW	Diesel power, phase 3, kW
DV1	Diesel voltage, phase 1
DV2	Diesel voltage, phase 2
DV3	Diesel voltage, phase 3
DPF1	Diesel power factor, phase 1
DPF2	Diesel power factor, phase 2
DPF3	Diesel power factor, phase 3
DFREQ	Diesel frequency
IP1%	Inverter power, phase 1, % of rated power
IP2%	Inverter power, phase 2, % of rated power
IP3%	Inverter power, phase 3, % of rated power
IP1KW	Inverter power, phase 1, kW
IP2KW	Inverter power, phase 2, kW
IP3KW	Inverter power, phase 3, kW
IV1	Inverter voltage, phase 1
IV2	Inverter voltage, phase 2
IV3	Inverter voltage, phase 3
IPF1	Inverter power factor, phase 1
IPF2	Inverter power factor, phase 2
IPF3	Inverter power factor, phase 3
IFREQ	Inverter frequency
VPC	Volts per battery cell (total battery bank divided by # of banks, in realtime)nominal voltage divided by 96 (AES, Len Wright, , also Mark Hensley 781-874-0223, and email
BA	Battery amps
TVPC	Temperature-compensated volts per cell (total voltage div
BT	Battery temperature(a computation has
AMBT	Ambient temperature (currently measuring genset room temperature)
SA	Solar amps
WA	Wind amps (does not apply)(can be reprogrammed)
SRAD	Solar radiation
WSP	Wind speed (does not apply) (can be reprogrammed)
ONA	Genset A On/Off
ONB	Genset A On/Off

Data Summary Description(total power exported and imported to inverter)
Genset and site kwh are only available using pulsing kilowatt hour meters, and able to collect fuel flow data from various brands of meters)

Inverted energy (need to confirm with AES)	KWh
Charged energy(need to confirm with AES)	KWh
Energy delivered to village	KWh (kwh to village)
Diesel A run hours	H
Diesel B run hours	H
Diesel A fuel consumed	L (not connected right now)(need to upgrade)
Diesel B fuel consumed	L (not connected right now)
Diesel A energy generated	KWh
Diesel B energy generated	KWh

Other meters

Village load meter	Stand alone metering , with CT' connected to inverter to count pulsed by phase, not totally accurate, calibrated, tells #pulses per kWh, 19 pulses, is 20 kWh off. Need 19.5 pulses, Replace or Recalibrate, Get AES on the line, a very good quality meter, There is an issue AES needs to resolve, This is fixable and data is currently being logged into the inverter, see data summary description
Station Service power	Meter exists (must purchase modem option)
Turtle receiver into site computer	Turtle system dials into the system to get info get upload from PC, log files from PC

Configuration:
Site computer has a harddrive, TELEX program interfaces with the PLC in the inverter. The site PC is then theoretically accessible via PC anywhere, however we have not been able to maintain a reliable telephone connection, that is why we are planning to add the satelite link to the internet.
As of this moment, a check by the onsite operator, who has limited computer skills indicates that the automatic script which activates Telex has failed. A new script has been provided a new script, however it is unlikely that the powerplant operator will be able to install the new program fix without assistance.

Contact List:

Dennis Meiners Alaska Energy Authority 907-269-4698 (3004fax), dmeiners@aidea.org
Ernie Baumgartner McGrath Light and Power 907-524-3009
Joe Bobby Powerplant operator Lime Village 907-526-5236
Lime Village Powerplant 907-526-5128 (907-526-5004)
AES Inverters Mark Hensley 781-874-0223 (fax, 781-874-8323), email, mark.hensley@aesltd.com.au
Brendan Taylor, Northern Power Systems, 802-496-2955

Appendix 9: Details of Lime Village Power System Components in HOMER

HOMER Input Summary

File name: Lime Village Project1_IEEE accepted paper.hmr
File version: 2.2 beta
Author: Ashish

AC Load: Primary Load 1

Data source: Synthetic
Daily noise: 15%
Hourly noise: 20%
Scaled annual average: 244 kWh/d
Scaled peak load: 23.3 kW
Load factor: 0.437

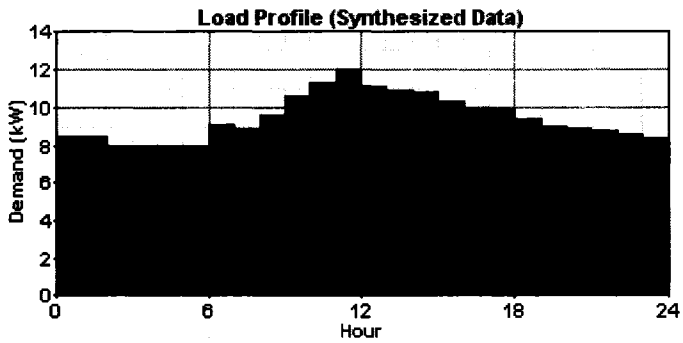

PV

Size (kW)	Capital ($)	Replacement ($)	O&M ($/yr)
12.000	54,195	25,000	125

Sizes to consider: 0, 12 kW
Lifetime: 20 yr
Derating factor: 90%
Tracking system: No Tracking
Slope: 15 deg
Azimuth: 15 deg
Ground reflectance: 0%

Solar Resource

Latitude: 61 degrees 36 minutes North

Longitude: 0 degrees 0 minutes East

Time zone: GMT +0:00

Data source: Synthetic

Month	Clearness Index	Average Radiation (kWh/m2/day)
Jan	1.364	1.020
Feb	1.086	2.220
Mar	0.954	4.230
Apr	0.736	5.500
May	0.491	4.960
Jun	0.389	4.420
Jul	0.400	4.290
Aug	0.442	3.730
Sep	0.683	3.720
Oct	1.035	2.820
Nov	1.839	1.870
Dec	1.647	0.720

Scaled annual average: 2.06 kWh/m2/d

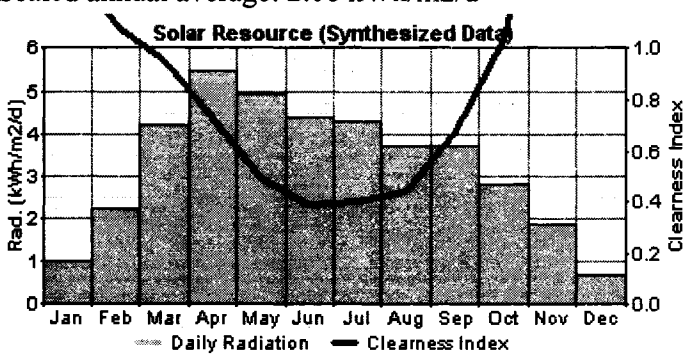

AC Generator: Generator 1

Size (kW)	Capital ($)	Replacement ($)	O&M ($/hr)
21.000	18,500	12,771	0.625

Sizes to consider: 0, 21 kW
Lifetime: 30,000 hrs
Min. load ratio: 30%
Heat recovery ratio: 0%
Fuel used: Copy of Copy of Diesel
Fuel curve intercept: 0.082 L/hr/kW
Fuel curve slope: 0.168 L/hr/kW

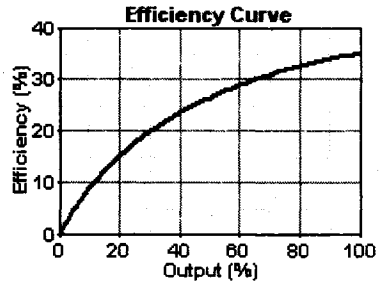

AC Generator: Generator 2

Size (kW)	Capital ($)	Replacement ($)	O&M ($/hr)
35.000	28,000	17,000	0.625

Sizes to consider: 0, 35 kW
Lifetime: 30,000 hrs
Min. load ratio: 30%
Heat recovery ratio: 0%
Fuel used: Diesel
Fuel curve intercept: 0.08 L/hr/kW
Fuel curve slope: 0.25 L/hr/kW

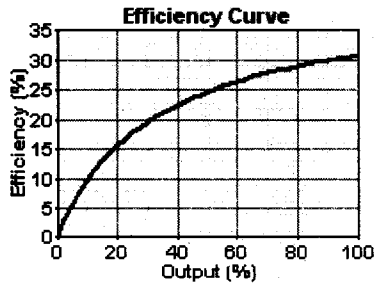

Fuel: Diesel

Price: $ 1.05/L
Lower heating value: 43.2 MJ/kg
Density: 820 kg/m3
Carbon content: 88.0%
Sulfur content: 0.330%

Fuel: Copy of Copy of Diesel

Price: $ 1.05/L
Lower heating value: 48.5 MJ/kg
Density: 840 kg/m3
Carbon content: 88.0%
Sulfur content: 0.330%

Battery: Surrette 4KS25P

Quantity	Capital ($)	Replacement ($)	O&M ($/yr)
13	34,288	23,000	100.00

Quantities to consider: 0, 13
Voltage: 4 V
Nominal capacity: 1,900 Ah
Lifetime throughput: 10,569 kWh

Converter

Size (kW)	Capital ($)	Replacement ($)	O&M ($/yr)
30.000	34,000	10,000	200

Sizes to consider:	0, 30 kW
Lifetime:	10 yr
Inverter efficiency:	95%
Inverter can parallel with AC generator:	Yes
Rectifier relative capacity:	100%
Rectifier efficiency:	95%

Economics

Annual real interest rate:	7%
Project lifetime:	20 yr
Capacity shortage penalty:	$ 3/kWh
System fixed capital cost:	$ 20,000
System fixed O&M cost:	$ 1,000/yr

Generator control

Check load following:	No
Check cycle charging:	Yes
Setpoint state of charge:	80%

Allow systems with multiple generators:	Yes
Allow multiple generators to operate simultaneously:	Yes
Allow systems with generator capacity less than peak load:	Yes

Emissions

Carbon dioxide penalty:	$ 0/t
Carbon monoxide penalty:	$ 0/t
Unburned hydrocarbons penalty:	$ 0/t
Particulate matter penalty:	$ 0/t
Sulfur dioxide penalty:	$ 0/t
Nitrogen oxides penalty:	$ 0/t

Constraints

Maximum annual capacity shortage: 0%
Minimum renewable fraction: 0%

Operating reserve as percentage of hourly load: 0%
Operating reserve as percentage of peak load: 0%
Operating reserve as percentage of solar power output: 0%
Operating reserve as percentage of wind power output: 0%